

FINITE ELEMENT ANALYSIS OF HEAT TRANSFER IN THE  
HUMAN HEAD

SARFARAZ KAMANGAR

DISSERTATION SUBMITTED IN FULFILLMENT OF THE  
REQUIREMENTS FOR THE DEGREE OF MASTER OF  
ENGINEERING SCIENCE

FACULTY OF ENGINEERING

UNIVERSITY OF MALAYA

KUALA LUMPUR

2013

**UNIVERSITI MALAYA**

**ORIGINAL LITERARY WORK DECLARATION**

Name of Candidate: **Sarfaraz Kamangar** C/Passport No

Registration/Matric No **KGA100072**

Name of Degree: **Master of Engineering Science**

Title of Project Paper/Research Report/Dissertation/Thesis ("this Work"):

**Finite Element Analysis of Heat Transfer in the Human head**

Field of Study: **Heat Transfer**

I do solemnly and sincerely declare that:

- (1) I am the sole author/writer of this Work;
- (2) This Work is original;
- (3) Any use of any work in which copyright exists was done by way of fair dealing and for permitted purposes and any excerpt or extract from, or reference to or reproduction of any copyright work has been disclosed expressly and sufficiently and the title of the Work and its authorship have been acknowledged in this Work;
- (4) I do not have any actual knowledge nor do I ought reasonably to know that the making of this work constitutes an infringement of any copyright work;
- (5) I hereby assign all and every rights in the copyright to this Work to the University of Malaya ("UM"), who henceforth shall be owner of the copyright in this Work and that any reproduction or use in any form or by any means whatsoever is prohibited without the written consent of UM having been first had and obtained;
- (6) I am fully aware that if in the course of making this Work I have infringed any copyright whether intentionally or otherwise, I may be subject to legal action or any other action as may be determined by UM.

Candidate's Signature

Date

Subscribed and solemnly declared before,

Witness's Signature

Date

Name:

Designation:

## ABSTRACT

Heat transfer in human body is an important issue that dictates the wellbeing of any person from health point of view. The heat is generated inside the body that has to be dissipated to outside environment based on the requirement of the body heat. The transfer of heat is controlled by a self-controlled thermoregulatory system of human body. In the current study, an investigation of heat transfer in human head is carried out by using finite element method. The 3-D geometry of human head was modeled with the help of 8 noded brick elements. Only a section of the head is modeled to take advantage of the symmetrical geometry of the head. The head is modeled with different tissues namely, skin, fat, bone and brain having varying physical and geometrical properties. The current work is focused to simulate the effect of various physical and geometrical parameters such as ambient temperature, heat transfer coefficient and variation in the thickness of different tissue layers of human head. Apart from this, the transient behavior of heat transfer in human head is investigated for situation when the person enters into a well heated car that has been parked in open sunlight. The temperature elevation of the car parked in sunlight was measured using the infrared camera. The cooling of head under severe fever condition is also investigated. It is found that the deep brain temperature remains almost constant for a wide range of environmental temperature whereas the skin temperature increases with the increase in ambient temperature but decreases with increase in the heat transfer coefficient. The effect of increased value of combined heat transfer coefficient is to reduce the temperature level in the human head. It is observed that the effect of combined heat transfer coefficient is more prominent on the outer layers of head than the brain area. It is observed that the skin temperature decreased when skin layer thickness is increased.

It is found that the fat layer thickness plays the dominant role as compared to skin layer thickness in controlling the skin temperature when all other parameters are kept constant. It is observed that the temperature at most of the places of human face increases exponentially with respect to time for a person entering the car parked in sunlight for long time. The maximum temperature was found on the skin surface which is directly exposed to hot conditions. For a severe fever condition, the head can be cooled by employing an ice helmet on the section of the head that can bring down the temperature under acceptable limit after 300 seconds of cooling.

University of Malaya

## ABSTRAK

Pemindahan haba dalam badan manusia merupakan satu isu penting yang menentukan kesejahteraan mana-mana orang dari sudut kesihatan pandangan. Haba yang dihasilkan dalam badan yang perlu dilesapkan kepada persekitaran luar berdasarkan keperluan haba badan. Pemindahan haba dikawal oleh sistem kawalan diri penyejukan badan manusia. Dalam kajian semasa, penyiasatan pemindahan haba dalam kepala manusia dijalankan dengan menggunakan kaedah unsur terhingga. Geometri 3-D kepala manusia telah dimodelkan dengan bantuan daripada 8 elemen bata noded. Hanya satu bahagian kepala dimodelkan untuk mengambil kesempatan daripada geometri simetri kepala. Kepala dimodelkan dengan tisu yang berbeza iaitu, kulit, lemak, tulang dan otak mempunyai pelbagai ciri-ciri fizikal dan geometri. Kerja semasa memberi tumpuan untuk mensimulasikan kesan parameter fizikal dan geometri pelbagai seperti suhu ambien, pekali pemindahan haba dan perubahan dalam ketebalan lapisan tisu yang berlainan kepala manusia. Selain daripada ini, tingkah laku fana pemindahan haba dalam kepala manusia disiasat bagi keadaan apabila seseorang itu masuk ke dalam kereta yang juga dipanaskan yang telah diletakkan dalam cahaya matahari terbuka. Ketinggian suhu kereta yang diletakkan di cahaya matahari telah diukur dengan menggunakan kamera inframerah. Penyejukan kepala bawah keadaan demam teruk juga disiasat. Ia didapati bahawa suhu otak yang mendalam kekal hampir malar untuk pelbagai suhu alam sekitar manakala suhu kulit meningkat dengan peningkatan dalam suhu ambien tetapi berkurangan dengan peningkatan dalam pekali pemindahan haba. Kesan nilai meningkat pekali pemindahan haba gabungan adalah untuk mengurangkan tahap suhu di dalam kepala manusia. Adalah diperhatikan bahawa kesan pekali

pemindahan haba gabungan adalah lebih penting pada lapisan luar kepala daripada kawasan otak. Adalah diperhatikan bahawa suhu kulit menurun apabila ketebalan lapisan kulit meningkat. Ia mendapati bahawa ketebalan lapisan lemak memainkan peranan dominan berbanding ketebalan lapisan kulit dalam mengawal suhu kulit apabila semua parameter lain dimalarkan. Adalah diperhatikan bahawa suhu di kebanyakan tempat muka manusia meningkat mendadak terhadap masa bagi seseorang memasuki kereta yang diletakkan di bawah cahaya matahari untuk masa yang lama. Suhu maksimum ditemui pada permukaan kulit yang secara langsung terdedah kepada keadaan panas. Bagi keadaan demam teruk, kepala boleh disejukkan dengan menggunakan topi keledar ais pada bahagian kepala yang boleh menurunkan suhu di bawah had diterima selepas 300 saat penyejukan.

## ACKNOWLEDGEMENT

Firstly, I would like to express my sincerest gratitude to my supervisors Dr. Irfan Anjum Badaruddin and Dr. Ahmad Badaruddin Badry for their excellent guidance and constant encouragement throughout this work.

I would like to thank my parents and family, for their affection and continuous encouragement during the course.

I would be thankful to all those friends who helped me directly or indirectly.

University of Malaya

## Table of Content

ABSTRACT.....	ii
ABSTRAK.....	iv
ACKNOWLEDGEMENT.....	vi
TABLE OF CONTENT.....	vii
LIST OF FIGURES.....	ix
LIST OF TABLES.....	xii
NOMENICLATURE.....	xiii
Chapter 1.....	1
1.1 Background.....	1
1.2 Applications of heat transfer in human body.....	3
1.3 Mathematical modeling and simulation studies.....	3
1.4 Heat transfer in human body.....	4
1.5 Problem statement.....	4
1.6 Objectives and Scope of the studies.....	5
1.7 Summery.....	5
Chapter 2.....	6
2.1 Introduction.....	6
2.2 Heat transfer in human body.....	7
2.2.1 Mathematical and Simulation models.....	7
2.2.2 Human Body Segments.....	18
2.2.2a Human Hand.....	18
2.2.2b Human Eye.....	21
2.2.2c Human Head.....	24
2.2.2d Human Leg.....	26
2.2.2e Human Tongue.....	27

2.2.3	Experimental Analysis.....	27
2.3	Summery.....	34
Chapter 3	.....	35
3.1	Introduction.....	35
3.2	Finite element method (FEM).....	35
3.3	FEA Model development.....	39
3.4	Summery.....	39
Chapter 4	.....	46
4.1	Effect of ambient temperature.....	46
4.2	Effect of heat transfer coefficient.....	55
4.3	Effect of variation of thickness of different tissue layers.....	62
4.3.1	Effect of skin layer thickness.....	63
4.3.2	Effect of Fat layer thickness.....	66
4.3.3	Effect of Bone layer thickness.....	69
4.4	Effect of hair on heat transfer.....	71
4.5	Investigation of high temperature environment.....	76
4.6	Effect of cooling helmet during hyperthermia.....	83
Chapter 5	.....	91
5.1	Conclusion.....	91
References	.....	94

## LIST OF FIGURES

Fig. 3.1	The geometric model of human head	40
Fig. 3.2	Human head model with hair	41
Fig. 3.3	Human head model with cooling jacket	42
Fig. 3.4	Human head meshed model	43
Fig. 3.5	Human head meshed model with hair	43
Fig. 3.6	Human head meshed model with cooling jacket	44
Fig. 3.7	FLIR thermal imager.	45
Fig. 4.1	Temperature variation in human heat at different values of $T_a$ a) $0^{\circ}\text{C}$ b) $10^{\circ}\text{C}$ c) $20^{\circ}\text{C}$ d) $30^{\circ}\text{C}$ e) $40^{\circ}\text{C}$ f) temperature from innermost to outer layer of head	48
Fig. 4.2	Thermal gradient at $26^{\circ}\text{C}$ a) x direction b) y direction c) z direction d) Total Gradient	50
Fig. 4.3	Thermal flux at $26^{\circ}\text{C}$ a) x direction b) y direction c) z direction d) Total flux	51
Fig. 4.4	Nodal temperature at $2^{\circ}\text{C}$ b) total thermal gradient at $2^{\circ}\text{C}$ c) total thermal flux at $2^{\circ}\text{C}$	52
Fig. 4.5	Nodal temperature at $12^{\circ}\text{C}$ b) total thermal gradient at $12^{\circ}\text{C}$ c) total thermal flux at $12^{\circ}\text{C}$	53
Fig. 4.6	Nodal temperature at $24^{\circ}\text{C}$ b) total thermal gradient at $24^{\circ}\text{C}$ c) total thermal flux at $24^{\circ}\text{C}$ .	54
Fig. 4.7	Nodal temperature at $36^{\circ}\text{C}$ b) total thermal gradient at $36^{\circ}\text{C}$ c) total thermal flux at $36^{\circ}\text{C}$ .	55
Fig. 4.8	Temperature variation in human heat at different values of $h_{cv}$ a) $9\text{ W/m}^2\cdot^{\circ}\text{C}$ b) $10\text{ W/m}^2\cdot^{\circ}\text{C}$ c) $11\text{ W/m}^2\cdot^{\circ}\text{C}$ d) $12\text{ W/m}^2\cdot^{\circ}\text{C}$ e) $13\text{ W/m}^2\cdot^{\circ}\text{C}$ f) temperature from innermost to outer layer of head.	56
Fig. 4.9	convective and radiative heat transfer coefficient at $8.25\text{W/m}^2\cdot^{\circ}\text{C}$ a) Nodal temperature b) total thermal gradient c) total thermal flux.	57
Fig. 4.10	convective and radiative heat transfer coefficient at $9.5\text{W/m}^2\cdot^{\circ}\text{C}$ a) Nodal temperature b) total thermal gradient c) total thermal flux	59
Fig. 4.11	convective and radiative heat transfer coefficient at $10.5\text{W/m}^2\cdot^{\circ}\text{C}$ a) Nodal temperature b) total thermal gradient c) total thermal	60

		flux	
Fig. 4.12	convective and radiative heat transfer coefficient at $11.5\text{W/m}^2\text{ }^0\text{C}$	a) Nodal temperature b) total thermal gradient c) total thermal flux	60
Fig. 4.13	convective and radiative heat transfer coefficient at $12.5\text{W/m}^2\text{ }^0\text{C}$	a) Nodal temperature b) total thermal gradient c) total thermal flux	61
Fig. 4.14	Effect of combined heat transfer coefficient on temperature variation across human head		62
Fig. 4.15	a) nodal temperature b) thermal gradient c) thermal flux for skin layer thickness of 0.1 cm		64
Fig. 4.16	a) nodal temperature b) thermal gradient c) thermal flux for skin layer thickness of 0.3 cm		64
Fig. 4.17	a) nodal temperature b) thermal gradient c) thermal flux for skin layer thickness of 0.4cm		65
Fig. 4.18	a) nodal temperature b) thermal gradient c) thermal flux, fat layer thickness of 0.05cm		67
Fig. 4.19	a) nodal temperature b) thermal gradient c) thermal flux, fat layer thickness of 0.25cm		67
Fig. 4.20	a) nodal temperature b) thermal gradient c) thermal flux, fat layer thickness of 0.35cm		68
Fig. 4.21	a) nodal temperature b) thermal gradient c) thermal flux, bone layer thickness of 0.4 cm		69
Fig. 4.22	a) nodal temperature b) thermal gradient c) thermal flux, bone layer thickness of 0.9 cm		69
Fig. 4.23	a) nodal temperature b) thermal gradient c) thermal flux, bone layer thickness of 1.4 cm		70
Fig. 4.24	a) nodal temperature b) thermal gradient c) thermal flux, bone layer thickness of 1.9 cm		70
Fig. 4.25	Human head model with hair a) nodal temperature at $30^0\text{C}$ b) thermal gradient at $30^0\text{C}$ b) thermal flux at $30^0\text{C}$		73
Fig. 4.26	Variation of temperature for ambient a) $20^0\text{C}$ b) $25^0\text{C}$ c) $35^0\text{C}$ d) $40^0\text{C}$		75
Fig. 4.27	Temperature variations across the radial direction in human head with hair		76
Fig. 4.28	Temperatures recorded at 11am a) Steering b) Dashboard c) driver seat d) back right seat		78

Fig.	4.29	Temperatures recorded at 1pm a) Steering b) Dashboard c) driver seat d) back right seat	79
Fig.	4.30a	Temperature variation during hours of the day	80
Fig.	4.30b	Temperature at face after 60 seconds inside the car	80
Fig.	4.31	Temperature variation in above bone with time	82
Fig.	4.32	Temperature variation in below bone with time	82
Fig.	4.33	Human head wrapped with cooling helmet	84
Fig.	4.34	Temperature distribution after 3 second	85
Fig.	4.35	Temperature distribution after 30 second	85
Fig.	4.36	Temperature distribution after 60 second	86
Fig.	4.37	Temperature distribution after 300 second	87
Fig.	4.38	Temperature distribution after 600 second	87
Fig.	4.39	Temperature distribution after 1200 seconds	88
Fig.	4.40	Temperature distribution after 1800 seconds	88
Fig.	4.41a	Temperature variation with time at various points above fat layer Head	89
Fig.	4.41b	Temperature variation with time at various points below fat layer in Head	90

## LIST OF TABLES

Table 3.1	Physical properties of tissues used in thermal modeling of a human head.....	41
Table 3.2	The number elements and respective nodes for various cases studied.....	46

University of Malaya

## NOMENICLATURE

$k$	thermal conductivity
$\rho$	density
$r$	radius
$C_p$	specific heat
$Q$	metabolic rate
$T$	temperature
$[K]$	stiffness matrix
$\{T\}$	solution variable
$\{F\}$	force vector
$N$	total number of nodes
$T_a$	Ambient temperature
$h_{cv}$	convective heat transfer coefficient

## CHAPTER 1

### INTRODUCTION

#### 1.1 Background

The heat transfer in human body is an important and vibrant field, which helps in analyzing the human heat stress in various atmospheric conditions. The two systems namely the active and passive systems constitute the interactive thermoregulatory set up of human body. The former controls the human body temperature at certain level and also predicts regulatory responses such as shivering, vasomotion and sweating. The latter simulates heat transfer with the surroundings. The human body behaves as heat engine and acts as open system thermodynamically. The bio- heat produced by the various chemical reactions taking place in the human body which interns provides energy for the system of the body. In order to maintain healthy body function the human body must maintain a constant internal temperature. Hence the regulation of the internal heat with the surroundings would assist in this process. However the various metabolic activities (oxidation of food elements) in the human body also assist to maintain the required body temperature. Heat generated in the human body by metabolism is dissipated to the surroundings of the human body by conduction, convection, radiation, evaporation of the moisture from skin and through respiration.

Conduction is the heat transfer through interaction of the heat at the atomic level. The heat generated within human body core can be conducted to adjacent tissue and reaches to body skin surface. It can be then conducted to clothing or convicted through air that is in direct contact with the skin. Similarly the convection is mode of heat transfer in which the heat transferred through the motion of molecules of liquids or gases across the heated surface. The human body surrounded by the air, sweeps away

the air molecule in the vicinity of the skin. The rate of convection is higher if the movement of air is greater. Although conduction and convection continuously remove heat, when the skin temperature is higher than the surrounding temperature, however the amount of heat dissipated to the surroundings is not significant when compared to the overall heat dissipation from the human body. The radiation heat transfer constitutes the significant amount of heat dissipated to the surroundings by emitting the heat in the form of mainly infrared rays. The nude human body may dissipate up to 60% of its excess heat by means of radiation. But it may also gain radiant heat from warmer surrounding objects. But the major amount of heat loss from the human body takes place through evaporation process whereby the body activates sweat glands to increase moisture level on the surface of human body. The rate of evaporative heat loss is directly related to vapor pressure, and the moisture present on the skin. The most significant amount of heat loss occurs during the period of increased physical activity of human body.

The bio heat models of human body and its influence interaction with the surroundings has been studied in the last few decades. The first bio heat model was developed by A. C. Burton in the year 1934. He considered the human body as a single homogeneous cylinder with uniform metabolic heat generation. In the year 1948 Penne's developed a significant thermal model on the effect of blood flow on the tissue temperature. Wissler, in 1961, used the idea of Penne's and developed the steady state, multi element, human thermal model. He divided the human body in to six homogeneous cylindrical elements representing the head, trunk, two arms, two legs, which were connected by circulating blood. In 1971, Stolwijk presented a six element model that run on an early digital computer and each element was subdivided into four nodes representing central core, muscle, fat and skin. Gagge et al. in 1970 also

developed two noded simple model for predicting the thermal stress due to surrounding atmosphere.

## **1.2 Applications of heat transfer in human body**

Mathematical modeling for the thermal response of the human body under

Various personal and environmental conditions is needed in various applications such as

- To predict the human body behavior under various life threatening conditions,
- To design energy efficient HVAC systems for buildings,
- It can be used also in the car industry, in textile industries,
- In aerospace, medicine, and military applications,
- Mathematical modeling has been used in the analysis of hyperthermia in treating tumor, cryosurgery, laser eye surgery and many other applications in medicines.

## **1.3 Mathematical modeling and simulation studies**

The solutions to the various engineering and physical problems are achieved either by experimental analysis or through mathematical modeling and simulations. The innumerable advantages of mathematical modeling and simulation over experimental analysis have made the former one of the popular tool to solve many engineering and science related problems. The most major hurdle in experimental analysis is the requirement of the experimental set up which needs a huge investment and time consuming process which leads to the various complications in the research. As for as the time is concerned, the experimental analysis requires epoch, on the other hand the time required for the simulation study is substantially low. The important factor in the simulation process is the achievement of the end results within lesser time compared to the experimental analysis. It also discusses the various causes and provides alternative

ways to arrive at the required accuracy of the analysis. The exposure to the hazardous atmosphere encountered in the experimental analysis can be avoided.

#### **1.4 Heat transfer in human body**

The bio heat produced from the various chemical and physiological reactions taking place in the human body has to regularly dissipate to the surrounding atmosphere in order to maintain the required body temperature and thermal comfort. This heat is distributed all over the body by blood circulation, and is conducted to the surface. Due to the temperature difference heat is transferred to the surroundings by means of convection, radiation and evaporation. Little amount of heat is also dissipated through respiration process. If the body organs has to function properly then the temperature of the internal body organs must be maintain at specific temperature especially for the brain which controls all the mechanism.

#### **1.5 Problem statement**

The heat transfer in human head is a complicated process. The head is the main part of the human body which acts as the control mechanism for all other body functions. Thus it is important to know the various factors involved in the human head during the various physiological and metabolic activities. Many researchers have addressed the various problems in the human body heat transfer to explain all the phenomenon taking place in the whole human body. The simpler models were developed to simulate the heat transfer processes from the whole body. But as of the research work published related to the human head heat transfer has been addressed by very few researchers. The present study emphasizes the study of various parameters which govern the heat transfer from human head. Further an attempted has made to predict the various factors which can be considered to regulate the heat generation and regulation in the human head

responses to the thermal conditions. It is very important to know the behavior of human head under different environmental conditions. Thus the present study focuses on the heat transfer in human head at various environmental conditions.

### **1.6 Objectives and scope of the studies**

The current study is focused to investigate the thermal behavior of human head. The study consider takes into account the normal environmental conditions which could be prevailing in the most parts of the world and the dimensions of head are considered to be a normal human head dimension. The objectives of the current study are as follows

- To investigate the thermal behavior of human head under different environmental conditions
- To study the effect of variation in thickness of different tissue layers
- To investigate the effect of heat accumulated in parked car to human head
- To investigate the effect of cooling helmet during hyperthermia.

### **1.7 Summery**

The heat transfer in human body is an important subject, which helps in understanding the human health conditions. The heat produced inside the body by metabolism is lost to the environment through conduction, convection, radiation.

The heat transfer modeling is required which has number of application such as thermal comfort, medicine, aerospace etc. The thermoregulation of human body is a complex process, there for in this study the thermal response of human head in mild environment is considered.

## CHAPTER 2

### LITERATURE REVIEW

#### 2.1 Introduction

The heat transfer in human body is important subject as stated before which helps in understanding the human health at various environmental conditions. Since last 50 years research is going on this subject. There are lots of research papers present on this subject. The purpose of this chapter is to provide some of the related information regarding the research being carried out pertaining to heat transfer in human head, by various researchers across the world.

In the year 1934, A. C. Burton [1] proposed the first model of human body; in this model he represented the human body as a single homogeneous cylinder with uniform metabolic heat generation. He suggested that the steady state temperature profile is parabolic in agreement with the experimental observations of Bazett and McGlone [2].

Pennes [3] developed a significant milestone in the field of human thermal model in the year 1948, he investigated the effect of blood flow on tissue temperature, he advanced the notion that heat transfer between the blood and tissue in small vessels and adjacent tissue is proportional to the product of the perfusion rate and the difference between the blood and tissue temperatures. He assumed that uniform perfusion rate without accounting for blood flow direction, neglecting the important anatomical features of the circulatory network system such as counter current arrangement of the system, and choosing only the venous blood stream as the fluid stream equilibrated with the tissue.

In the year 1971 Stolwijk [4] presented a mathematical model of physiological regulation of man. In this model human body is divided into six segments, and each segment was further divided into four nodes. A total of 25 nodes were used to represent the thermal characteristics of body. The twenty fifth nodes represent the central blood. The model predicted with reasonable accuracy of thermal responses to loads of ambient temperature and heat production in human body.

## **2.2 Heat transfer in human body**

### **2.2.1 Mathematical and simulation models**

Ferreira and Yanagihara [5] have developed a mathematical model of human thermal system. The 15 elliptical cylinders were used to represent the human body segments. The model considered 3D heat conduction, heat transfer between blood and tissue, heat transfer between large arteries and veins. The differential equations were solved by finite-volume method. They demonstrated the substantial of simulation with the experiments.

Yildirim and Ozerdem [6] have developed three dimensional transient model of human body. The model is multi segmented, multi layers represents human body with spatial sub divisions which simulates heat transfer phenomenon within the body and at its surface. They assumed the body is exposed to a combination of convection, evaporation and radiation which are taken into account as boundary conditions. The finite difference solution method is used to solve the bio heat equation in radial and tangential direction, in order to find out the temperature distribution of human body. They found that numerical results of the model are good agreement with the experimental data.

Kilic et al. [7] studied thermal comfort with steady state energy balance method, in first section of simulation of study; they calculated the body core temperature and required skin temperature and sweat rates by using the equations of thermoregulatory controls mechanisms. The variations of body core temperature with activity level was calculated, in the second section of simulation they investigated the heat loss from the body by convection, radiation, evaporation and respiration and ratio of the each heat loss mechanisms to total heat loss are calculated, They showed that as ambient temperature increases the sensible heat loss decreases whereas the latent heat loss increases from the body. At the low ambient temperature, especially radiative heat loss in the sensible heat loss mechanisms has high values.

Muhsin and Gokhan [8] employed the combined computational model of virtual thermal manikin and a room, to determine heat and mass transfer between thermal manikin and environment. They calculated fluid flow, temperature and moisture distribution, heat transfer between human body and ambient, radiation and convection heat transfer rates and skin temperature. They found that the natural convection coefficients for whole body fell within the mid-range of previously published data. They suggested that the method used for calculating regional heat transfer coefficients are valid, and can be used for different postures of thermal manikin.

Sorensen and Voigt [9] presented a detailed geometry of surface of a seated female identical to thermal manikin. The geometry was used in CFD calculations that were compared to the measurements of heat transfer and flow around the manikin. The radiative heat transfer coefficient and natural convection flow were calculated, and the results were in good agreements with previously published data.

Huizenga et al. [10] developed a model of human thermal regulation based on stolwijk model. The model included several significant improvements over stolwijk model, such as increase in number of segments, including blood flow counter current, addition of clothing layer, physiological mechanisms, metabolic heat production are considered in detailed. They suggested that model is capable of predicting human physiological responses in transient and non-uniform thermal environments.

Murakami et al. [11] investigated the wind effect on human body under various wind conditions by using CFD. At first human body has placed in a stagnant environment, secondly in weak wind of velocity 0.25m/s and wind velocity attacking human body has increased to 2.5m/s. lastly two human bodies has arranged standing in a row. They concluded that the effect of wind on human body depends not only on velocity, but also on turbulence intensity, and also by direction of approaching wind. The convective heat transfer coefficient over human body surface under weak wind (0.25m/s), are 2-3 times larger than stagnant environment. An interactive wind effect was observed in case of two human bodies. The blocking effect of windward body on leeward one is well observed. They extended their work [12] to investigate the combined numerical simulation of airflow, radiation and moisture transport for predicting the heat transfer from human body. They used low Reynolds number type k- $\epsilon$  model in CFD. A two node Gagge's model was adopted to simulate metabolic heat production in human body. The results shown were very close to the actual human body in similar situations.

Sevilgen and Kilic [13] studied three dimensional steady state numerical analysis of room heated by two panel radiators. A virtual manikin with real dimension and physiological shapes was added to model of the room. The heat interaction between

human body surface and room environment, air flow, temperature, humidity and local heat transfer characteristics of manikin was computed numerically under different environments. The results show that energy consumption can be significantly reduced while increasing the thermal comfort by using better insulated outer wall and materials and windows.

Kang et al. [14] presented a 61 node thermoregulation model that is coupled with thermal environment model for occupied space with no air conditioning. With the model air temperature, humidity, as well as ET and WBGT indices can be obtained for thermal environmental assessment. Transient body and skin temperature together with sensible and evaporative heat loss can be calculated. They noticed that root mean square deviations (RMSDs) of the predicted results from model are less than standard deviations (SDs) of the corresponding experimental data.

Miyanaga et al. [15] developed a simplified human body model for evaluating a radiant cooled space by combining cylindrical and rectangular parts. The radiative and convective heat transfer, the effective radiation area and the projection area factor of the model was determined. The results obtained were good in agreement with real subjects. Finally human body model was applied to analysis of thermal environment in radiant cooled space. They found that analyzed values mean surface temperature agreed well with real subjects under various different thermal radiant conditions. They suggested that the model is applicable for simulation of thermal response of real subjects.

Zolfaghari and Maerfat [16] developed thermoregulatory bio-heat model to investigate the heat transfer in human skin. The model was constructed by combining penne's equation with Gagge's model. In the model human skin is subdivided into three layers

(epidermis, dermis and subcutaneous). The bio-heat equation is solved and time dependent temperature of skin tissue was obtained. They verified results of model by comparing with published analytical and experimental data. In other study [17], they presented a new predictive thermal response index TRESP on the basis of study presented by Ring and de Dear [18]. The TREPS index was verified by extensive comparisons with published analytical and experimental data which presented a good agreement under both transient and steady state conditions. Their results showed that new index can accurately predict the thermal response with an average error of 0.19 and 0.28 under steady and transient conditions respectively.

Al-Othmani et al. [19] developed a modified human body bio-heat model presented in Salloum et.al [37] to predict the circumferential skin temperature variation of nude and clothed body segments under various non-uniform radiative environments. The nude and clothed body model was integrated to predict heat and mass diffusion.

Min et al. [20] presented a mathematical model to simulate heat and moisture transfer through fabrics. The radiation heat transfer between surface and surface diffusion along fabric was included in the model. The results show that contribution of radiation and conduction through air was 20% of total heat flux and surface diffusion does not play a significant role in total moisture transfer. They concluded that microclimate plays very important role in heat and mass transfer from skin to the environment.

A dynamic model of human thermoregulation for predicting human thermal responses in wide range of environmental conditions was presented by Fiala et al. [21]. In this model, importance is given to heat exchange with environment, local variation of

surface convection, radiation exchange, evaporation and moisture collection at skin. Other thermal effects are also modeled: impact of activity level, and change of effective body area with posture. Differential equations were solved by stable and accurate hybrid numerical scheme. The model prediction was compared with analytical solutions of cylindrical and spherical segments shows good agreements and stable numerical behavior for large time steps.

Atmaca et al. [22] investigated the effect of radiant temperature on local different body segments, and to analyze the interior surface temperature for different wall and ceiling construction with their effect on thermal comfort. Modified Gagge 2 node model was used to simulate the segment wise thermal interaction between human body and environment. The sol-air temperature approach is used to calculate the interior surface temperature of walls and ceiling. They suggested that body segments close to the hot surfaces are more affected than others, and un-insulated walls and ceiling exposed to solar radiation reach high levels, all of which causes thermal discomfort for occupants.

Kaynakli et al. [23] presented a computational model of human thermoregulatory system based on heat balance equation combined with empirical equations of defining sweat rate and skin temperature. They divided human body into 16 segments to determine sensible and latent heat loss. Their result shows that heat losses from coverless segments were more than other segments of human body. When clothing resistances increases, the required ambient temperature decreases. The presented results are in good agreement with available experimental data.

Tanabe et al. [24] developed a numerical simulation method for predicting the effective radiation area and the projected area of human body for any posture. They compared the present method to confirm with the measured values for the effective radiation area factor and projected area factor for both standing and sitting postures. They found that the predicted values agree well with the experiments. The author extended their work [25] and developed a 65-node thermoregulatory model based on stolwijk model for evaluating thermal comfort. The model has 16 segments, each consisting of four layers of core, muscle, fat and skin. This model was combined with radiation exchange model and computational fluid dynamic model. The comprehensive simulation was described in the paper.

Foda et al. [26] compared the predictions of skin temperature and local and overall thermal sensation from different models of human thermoregulatory system. In this paper, recently measured data from the literature were tested against one of the study presented by Al-Othmani et al. [19], the University of California, Berkeley (UCB) thermoregulation model and a multi-segmental (MS) Pierce model. The local and overall thermal sensation was predicted for different room conditions obtained from experiments. The overall thermal sensation was further predicted using three other models. Their results show MS-Pierce model has best predictability in steady state and showed very good performance with the study of Al-Othmani et al. [19].

A numerical method for simulating 3D bio-heat transfer equations with different heating style was developed by Karaa, et al. [27]. This method was intended for temperature predication and parameter measurement. A mathematical model based on classic Pennes heat transfer was examined in biological bodies. A finite difference method was used to discretized the governing equation. They suggested that the

numerical method can be used to predict the evolution of temperature within the tissue during bio-heat transfer process.

Thermodynamic analysis of human heat and mass transfer based on the 2<sup>nd</sup> law of thermodynamics was presented by Prek [28-29]. The two node human thermal model was used, and this model was improved to establish the exergy consumption within the human body as a result of heat and mass transfer. He showed that human body's exergy consumption for selected human parameters exhibits minimal value at curtained combination of environmental parameters. And also shows that there is a correlation between exergy consumption and thermal sensation. The author extended his work [30] to present the human-indoor environmental interaction based on exergy analysis. The exergy destruction was estimated as consequences of human body-environment interaction. The two node human thermal model was extended to calculate exergy destruction. The analysis showed the impact of specific environmental parameters on exergy destruction. This approach enables the definition of a combination of indoor parameters that ensures minimal human exergy destruction with regard to physiological parameters.

Mady et al. [31] presented the modeling exergy behavior of human body aiming at establishing relationship between exergy destruction rate and exergy efficiency with ageing and environmental conditions. A detailed model of human thermal system was used to analyze exergy destruction rate for each part of the body and exergy efficiency as a function of ageing and environmental conditions. They concluded that exergy destroyed and exergy and exergy efficiency decrease over lifespan and the human body is more efficient and destroys less exergy in the lower humidities and higher temperature.

Wu, X. et al. [32] derived a human body exergy consumption formula according to Gagge's two node thermal models. They compared the values of calculated human body exergy consumption from the formula and shukuya's formula and observed that human body exergy consumption reaches minimum value by either of this formula in same thermal conditions. Thermal sensation was found to be slightly cool under minimum exergy consumption and optimal performance.

Nilsson, H. O. [33] presented a construction of new numerical thermal manikin by using the measured data of thermal manikin as well as subjective results of experiments. He visualized the simulated as well as measured results in new clothing independent comfort zone diagram. The results shows a good agreement between the equation used in the simulation and real life measurements in the different environments

An integrated model for simulating interactive thermal processes in human – clothing system was studied by Yi et al. [34]. They modified stowijk's model by considering sweat accumulation on the skin surface and this was used to simulate the physiological responses. This human model was coupled with the moisture model which takes into consideration the adsorption of water vapor. They found that the result was in good agreement with the previous published data.

Afrin et al. [35] presented a generalized dual phase lag mode for living biological tissue based on non-equilibrium heat transfer between energy carrier (arterial, venous blood and tissue). They calculated the phase lag time for heat flux and temperature gradient. They noticed that phase lag time for heat flux and temperature gradient depends only on properties of artery, venous and tissue, blood perfusion rate

and convective heat transfer rate. They found that if the properties of blood and tissue are same then the phase lag time for heat flux and temperature gradient is identical, otherwise it is different for the different properties of blood and tissue.

Dongmei, P. et al. [36] developed a four node thermoregulation model to predict the thermoregulatory responses of a sleeping person. This model was compared with the experimental data present in literature. The results showed that the four node thermoregulation model can be used to predict the thermoregulatory responses of a sleeping person with the acceptable accuracy.

A new transient bio-heat model of the human body and its integration to clothing model was developed by Salloum, M. et al. [37]. They used an exact anatomical data of the human body which calculated the blood flow rates and their variations based on physiological data. The model was capable of predicting the transient physiological responses such as skin, core temperature. The human body model was combined with the existing clothing model based on heat and mass diffusion through the clothing layers. The results were found to be good agreement with the published experimental data.

A transient thermal model of human body-clothing- environment system was presented by Wan and Fan [38]. This model was integrated with the human thermoregulation and heat and mass transfer through clothing. They also included ventilation induced by body motion, liquid sweat movement and coupling effect of heat and moisture transfer. They compared the results of the model with experimental data and convicted that the model has captured the main mechanisms involved in the human–clothing–environment system.

A mathematical model was presented by Min, K. et al. [39] to simulate heat and mass transfer from skin to environment through fabrics. In this model, radiation heat transfer between the surfaces and surface diffusion along the fibers is included. The results show approximately 20% of radiation and conduction contributes each for total heat flux. They concluded that surface diffusion does not play a significant role, whereas a microclimate plays a very important role in heat and moisture transfer from the skin to environment.

Study of heat and mass transfer within multi-layer clothing assemblies consisting of different types of battings was presented by Wu and Fan [40]. The finite volume method was used to solve the model. The numerical results were validated with the experimental measurements which show good agreements and then applied to evaluate the positions of different types of batting affect. They found that placing hygroscopic wool batting close to body and non-hygroscopic polyesters away from the body could reduce the moisture accumulation within and the total heat loss through assemblies.

Xu, et al. [41] developed a multi segmented mathematical model for predicting shivering and thermoregulatory responses during long term cold exposures. They included new knowledge of shivering thermogenesis, including the control and maximal limit of its intensity, inhibition due to low core temperature, and prediction of endurance time. The model was validated against three different cold conditions. They observed that the prediction of the core and mean skin temperature, shivering response were in good agreements with the observations.

Zhang et al. [42] developed a human thermal model by considering the physiological differences between individuals. A model was developed to translate the descriptive data about an individual to a set of physiological parameters. These parameters may be include into thermal model of human thermoregulation and comfort. Then the model is used to predict the thermal responses of an individual. A thermal simulation of this model was also presented.

### **2.2.2 Human body segments**

#### **2.2.2a) Human hand**

Pardasani and Adlakha [43] developed a finite element model using coaxial circular sector element of dermal regions of human limb to investigate the distribution of heat in the radial and angular direction. The model included the significant variation of physical and physiological parameters, like blood mass flow rate, metabolic heat generation and thermal conductivity. A computer program was developed to simulate the entire problem. The results obtained were in good agreement with the physiological fact.

Agrawal et al. [44] developed a three dimensional steady state model of human limb, to investigate the flow in dermal regions of tapered limb. The model included the importance of biophysical parameters like blood mass flow rate, thermal conductivity and rate of metabolic generation. The finite element method was employed using elliptical hexahedral elements.

A steady state heat transfer model of human upper limb was developed by Ferreira and Yanagihara [45]. In his study the impact of blood flow through superficial veins and subcutaneous vascular structure in palm of hand over heat transfer between the limb and environment was evaluated. The detailed circulatory network composed of vessels with

diameter larger than 1mm was included. The model was validated with comparing its results from exposures to hot, neutral and cold environments to experimental data present in literature. They demonstrated that under neutral and hot environments temperature variation in arm and forearm are very small, while opposite was observed during cold exposure.

Trobec and Depolli [46] developed a mathematical model and computer simulation program based on digitized slice data. Heat transfer in non-homogenous tissue was modeled with bio-heat equation. The metabolism was modeled by Q10 rule, while heat exchange between blood and tissue was modeled as a function of local temperature and regional blood flow. They explained variations of steady state temperature in one of the study presented by Bazett and McGlone [2] measurements by computer simulation, believing that anatomical positions of his probes varied. They constructed positions by searching simulated positions which shows good agreements with measured values. They showed that fluctuation of measured temperature should not be smoothed out of the natural consequence of a complex interplay between the position of the measuring probes, anatomical position of the main arteries, dimensions of the forearm, blood flow, in homogeneity of tissues, and environmental temperature.

A coupled thermo fluid model to simulate blood flow and heat transfer in human finger was developed by He et al. [47]. The finite element model was developed to analyze the blood perfusion and heat transport in finger based on transport theory in porous media. The systemic blood circulation in upper limb was modeled based on one dimensional flow in elastic tube. The blood pressure and blood velocity were calculated, than temperature in large vessels and tissue of the finger were computed by numerically solving energy equation in porous media. The calculated blood flow in tissue has good

agreements with anatomical structure and measurements. They suggested that the model can predict peripheral blood flow, temperature variation and mass transport.

Gan [48] investigated the physiological interaction between fabric and human body via skin and effect on blood flow which in turn influence skin temperature. They examined skin blood flow by using different fiber blending, different characteristic of same fiber, and different moisture levels of same fiber type. The temperature and blood flow of skin of forearm was recorded by laser-Doppler flow meter with two probes. They concluded that a significant impact on both skin temperature and blood flow by fabric. The fabric surface characteristic play important role during transient heat exchange, and higher the moisture level longer the duration of impact.

Upreti and Jeje [49] presented a noninvasive technique to determine the peripheral rate of heat generation and blood flow in human limb from its recorded skin temperature. The technique involves an analysis based on calculus-of-variation, and features the well-known circadian cycle of mammalian body temperature. The technique was tested using a set of reported skin surface temperature data. The predicted rates of blood flow and heat generation were found to agree with their basal values. They suggested that the framework of variation of calculus and periodic optimal control algorithm developed which can be applied to different body parts to predict the blood flow and heat generation rates based on suitable heat transfer models.

Zhang et al. [50] investigated the variation of temperature in hand and blood flow after cold water stimulation by using the infrared thermography and ultrasound Doppler flowmetry. They also developed an image processing algorithm to measure temperature in various part of hand. Their results showed that the oscillation of temperature by local

cold stimuli is due to neuroregulation during rewarming. They also developed autonomic nervous system regulation model based on the physiology and bio-heat transfer. The results calculated from this model were in good agreement with the experimental results.

### **2.2.2b) Human eye**

Scott [51] developed a mathematical model of human eye based on bio-heat transfer equation. The temperature distribution in intraocular region was calculated by using Galerkin finite element method. A sensitivity analysis was performed to evaluate the effects of parameter values on the computed results. They found that a significant temperature changes in the anterior region, because of thermal conductivity of lens and choroidal blood flow rate. In addition the temperature distribution was observed to be sensitive to variations in the ambient temperature and the blood temperature.

A thermal model of human eye exposed to laser irradiation to simulate intraocular temperature distribution was presented by Amara [52]. The differential equation describing the system and includes the laser source, and boundary condition equations. The integral formulation is treated by finite element method to lead a discrete algebraic system which was solved by numerical method. They observed that, the more laser wavelength the more effect on eye hazardous. Since this is related to production of higher temperature that can lead to denaturation of ocular tissue.

Chua et al. [53] developed a mathematical model to predict temperature distribution in human eye exposed to laser source. They used Pennes equation to develop a model by using finite volume method. Their model showed good agreement with the experimental models, and also studied the ageing of eye, variation in thermal conductivity of lens,

laser power-off periods on its temperature distribution when subjected to a laser source. They found that lens has highest change in temperature as a person ages due to physical change of the eye and as the thermal conductivity of the lens increased.

Avtar, R. and Srivastava, R. [54] developed a mathematical model for the natural convection flow of aqueous humor in the anterior chamber of human eye. They obtained the expressions for temperature and velocity profile in the interior chamber as well as for stream functions. The results showed that increasing convection heat transfer coefficient lower the fluid temperature while increasing the thermal conductivity raises the temperature.

Ng and Ooi [55], has developed a 2D finite element model of human eye, to simulate thermal steady state conditions based on properties and parameters. The results obtained are verified with experimental and computational results by previous studies. Results show discrepancy of only 0.33% when compared to images from infrared (IR) screening and a difference of only 0.127% compared to another finite element model. The sensitivity analysis also proved good agreements with results by previous studies. They extended their research to present the 3D FEM model of human eye, to simulate temperature distribution during normal and electromagnetic conditions [56]. An average power absorption density of  $15,151\text{Wm}^{-3}$  and  $22,145\text{Wm}^{-3}$  for 750MHz and 1500 MHz radiation was found, while investigating on electromagnetic radiation. A peak temperature of  $38.18^{\circ}\text{C}$  was predicted for the 750MHz radiation while  $41.19^{\circ}\text{C}$  was computed for the 1500MHz radiation. These temperatures are in reasonable agreement with the simulated results computed by another report in the past. In another study [58], they reported the effect of aqueous humor flow on temperature distribution inside the human eye. They found that the presence of aqueous humor generally increases the

temperature at interior region while posterior sections are not affected. They also found that aqueous humor distort the temperature profile. Ng et al. [57] presented a comparison between the ocular temperature predicted by both the two dimensional and three dimensional human eye models. They found that a central ocular temperature for three dimensional model is higher than the two dimensional model. They also suggested that for initial investigation, use of two dimensional model may be sufficient for comparing the temperatures of various points inside the human eye.

A model of human eye has developed to investigate the effect of eye tumor on ocular temperature distribution by Ooi et al. [59]. The tumor is modeled to be a homogeneous tissue region that has high metabolic heat generation and blood perfusion rate. The governing equations were solved by numerically using boundary element method. The results obtained in this model demonstrated that presence of tumor cause increase in temperature inside the eye. And on the corneal surface, both increase in temperature and a slight thermal asymmetry are found.

Narasimhan et al. [60] investigated transient temperature evolution and thermal effect in different regions of human eye subjected to laser surgery. They developed a two dimensional model of human eye solving discretized form of bio heat transfer using finite volume formulation. It was showed that evolution of temperature during laser heating could reach higher than that required for irreversible cell damage. This is because the time scale for spatial diffusion is much larger than that of actual laser surgery. This excess temperature due to heat diffusion could damage adjoining cells. They proposed a method to maintain retinal pigmented epithelium temperature close to the required  $60^{\circ}\text{C}$  by pulsating the laser source between suitable maximum and minimum heat flux values. Further the author extended their work in Narasimhan et al.

[61] to investigate the transient simulation of retinal laser irradiation for square array consists of  $3 \times 3$  uniformly distributed spot under sequential and simultaneous mode. Finite volume formulation was used to Pennes bio-heat transfer model to generate temperature distribution in the eye.

A bio-heat transfer model of human eye by using b-splines as shape function for finite element method was developed by Kunter, and Seker [62]. This model was applied to calculate the steady temperature distribution in human eye. They evaluated human eye firstly in two dimension and verified simulated results with the results presented in the literature. To get accurate representation of actual human eye three dimensional model was simulated. They showed FEM with web-spline method is given more accurate results than the standard FEM. They also suggested that the 3D web-spline model has provided better accuracy than the 2D web-spline model and is able to give a more precise interpretation of the temperature inside the human eye.

### **2.2.2c) Human head**

The effect of physiological parameters on the temperature distribution of layered head with external convection was presented by Ley and Bayazitoglu [63]. They studied the arterial blood pressure, partial pressure of oxygen, partial pressure of carbon dioxide and cerebral metabolic rate of oxygen consumption. They showed how these parameters affect the brain temperature in special conditions like brain edema, hypoxia, hypercapnia, or hypotension. They concluded that change in cerebral blood volume will affect on the head temperature distribution. And also observed that varying physiological parameters so that cerebral blood flow is increased, the penetration depth is reduced and vice versa.

An analytical model of temperature distribution in human head was reported by Sukstanskii and Yablonskiy [64]. Their model predicts the changes in brain temperature as a function of internal and external parameters: temperature of arterial blood flow, oxygen extraction fraction, ambient temperature, and heat exchange with the environment. They suggested that the model can be used for predicting temperature responses to extreme conditions such as heavy exercise or exposure to heat or cold and estimating the temperature changes in brain during selective head cooling. In another work [65], they studied the brain cooling by external head cooling device by using analytical model of temperature distribution in the brain. They obtained analytical expressions which predict the brain temperature under the influence of input parameters. They showed that mild hypothermia can be achieved in neonates only if the two conditions are meeting, the sufficient low cerebral blood flow and sufficient high heat transfer coefficient describing the heat exchange between the head surface and a cooling device.

Khanday and Saxena [66] have obtained a theoretical finite element model of human head to analyze thermoregulation in different tissue layers. The domain has been discretized into four sub domain depending upon physiological and allied properties of the region. The partial differential equation for determining temperature in living tissue has been solved by finite element method. The model predicts that change in temperature as a function of internal and external parameters namely blood temperature, blood flow rate, ambient temperature and heat exchange with the environment. They suggested that the model can be used to predict temperature response in extreme cold conditions. And also suggested that, it will be helpful for estimating changes in brain temperature during selective head cooling as practice during surgery.

A computer model which describes the heat transfer in human head during scalp cooling was developed by Janssen et al. [67]. The model consists of simplified head and cooling cap. The heat transfer in head was described by using well known Pennes's bioheat equation. They determined the effect on scalp temperature and perfusion during cooling. Their results showed that temperature of the scalp skin lowered from 34.4°C to 18.3°C. A parameter study was also done, by varying thermal properties and head anatomy. They found that perfusion coefficient and thermal resistance of both fat and hair affect temperature and perfusion.

#### **2.2.2d) Human leg**

Xiao et al. [68] investigated the bio heat transfer problem of human knee for both disease diagnostics and therapeutically. They simulated temperature distribution of skin surface under different metabolic production and blood perfusion, and also evaluated hyperthermia based on heating from outside and hyperthermia based on heating in vessels. Heating from outside produces obvious effect on shallow treatment, but less effect on deep treatment. In the interventional hyperthermia, the one based on heating in artery is more effective than that in vein. A 3d computer model of the human knee for the simulation of topical cooling by using gel-packs or cryo-cuffs was developed by Trobec, R. et al. [69] The heat transfer in a knee was modeled by diffusion equations, and solved by explicit finite difference method. In the two different simulations they found that cooling process is more intensive with cryo-cuffs at a constant temperature, whereas in gel packed cooling of inner knee reaches their lowest temperature in 40min. they found good agreements of simulated values with the measured values.

### **2.2.2e) Human tongue**

Kai [70] has investigated heat transfer mechanism of tongue based on experimental and theoretical research. The relationship between tongue temperature and blood perfusion was obtained from animals and subordinate on human tongue. Also a one dimensional heat transfer equation and analytical solution was obtained by simplifying tongue as fin cube. They concluded that temperature of tongue surface increases with blood perfusion. Theoretical predictions are good agreements with experimental data measured by infrared on human tongue. They suggested that this method of modeling and calculation can be used for temperature predictions of other organisms.

### **2.2.3 Experimental Analysis**

Lichtenbelt et al. [71] has tested a multi-mathematical model of human thermoregulation for its capability to predict individual physiological responses. They compared predictions of a person with measured individual responses of subjects under mild cold conditions. The data was obtained from 20 subjects, rectal, and skin temperature, metabolic rate were measured for 1 h at 22<sup>0</sup> C followed by 3 h at 15<sup>0</sup> C. In conclusion, this study shows that on group level predictions of skin temperatures can be improved when adopting individualized body characteristics and measured MR, but the predictions on an individual level were not improved. Ishigaki, et al. [72] has estimated experimentally convective heat transfer coefficient of human body. They used heat flow meters to calculate thermally equivalent sphere and cylinder to human body. They obtained convective heat transfer coefficient experimental formulae in natural, forced and mixed convection. They found that diameters of 12.9 and 12.2cm sphere and cylindrical are the thermally equivalent to human body. Dear et al. [73] has presented convective and radiative heat transfer coefficient for individual human body segments.

In this study, a thermal manikin with 16 body segments used to generate convective and radiative and convective heat transfer coefficients. The test was conducted for both standing and sitting postures with a range of wind speeds from still air to 5.0m/s. they observed that whole body estimates of radiative and convective heat transfer coefficients in both still and moving air fell within the mid-range of estimates of already published data. They also observed that hands, feet, and peripheral limbs had higher convective heat transfer than the central torso region. Wind direction had little effect on convective heat transfer from individual body segments.

Kurazumi et al. [74] has studied the convective heat transfer area of human body. In their experimental study, the total body surface area of six healthy subjects was measured. They also measured the non-convective area and floor and chair contact area for various body postures. The effective thermal convective area for nine postures standing sitting in a chair, seiza sitting, cross leg sitting, sitting sideways, sitting with both knee erect, sitting with leg out, and lateral and supine positions was measured. They observed that for all body positions the effective thermal convective area factor was greater than effective thermal radiation area factor, but smaller than the total body surface area. They extended their research [76] to investigate convective and radiative heat transfer coefficients, while focusing on convective heat transfer area of human body. In the experimental studies thermal sensors measuring total heat flux and radiative heat flux were employed. The mannequin was placed in different postures as follows: standing, chair sitting, cross leg sitting, leg out sitting, and supine. Radiative heat transfer coefficient was determined for each posture. New empirical formulas were proposed for convective heat transfer coefficient of the human body in different postures. They also presented in a different study [75] the convective heat transfer area, radiative heat transfer area and conductive heat transfer area for the subject in 9

postures. They found that posture was shown to have a noticeable effect on the heat transfer areas of the human body.

The interaction of surface heat and moisture transfer from human body under different environmental conditions and walking speeds was investigated by Qian and Fan [77]. In this experimental study a sweating/non-sweating fabric manikin was developed. They showed that surface thermal insulation is little affected by moisture transfer. The surface moisture vapor resistances measured under isothermal conditions tend to be greater than those measured under non-isothermal conditions, especially when the wind velocity is less than 2.0 m/s. The Lewis Relation holds under non-isothermal conditions, but does not hold under isothermal condition when the wind velocity is small. Huizenga et.al [78] has studied Skin and core temperature response of human body to partial- and whole-body heating and cooling in a controlled environmental chamber. Skin, and core temperature thermal sensation and comfort responses was collected for 19 local body part and for whole body. They observed that Core temperature increased in response to skin cooling and decreased in response to skin heating. Hand and finger temperatures fluctuated significantly when the body was near a neutral thermal state.

Sakoi et al. [79] have investigated thermal comfort skin temperature, and sensible heat losses for whole body as well as local areas in various asymmetric radiant fields. A series of human subject experiments and thermal manikin experiments were carried out by using radiation panels. They obtained comfort sensation, local discomfort at 25 locations, and local skin temperature in human subject, as well as local sensible heat losses in 20 segments in thermal manikin experiments. They found that Local sensible heat losses same as measured by using thermal manikin when local skin

temperatures as human subjects measured. They observed that local skin temperature and local sensible heat loss changed depending on the environmental thermal non-uniformity, even if the mean skin temperature and sensible heat loss remained almost the same. The relationship between the local skin temperature and local sensible heat loss cannot be depicted by a simple line; instead, it varies depending on the environmental thermal non-uniformity. Munir et al. [80] has evaluated the validity of original stolwijk model for predictions of skin temperature under transient conditions by comparing the results calculated by experiments from large number of subjects. The results showed that the original Stolwijk model accurately predicts both the absolute value and the tendency in the transient mean skin temperature. They suggested that stolwijk model is valid for predictions of transient skin temperature for average person under low activity conditions.

The relative humidity effect on skin temperature and skin wittedness for different operative temperature was investigated by Atmaca and Yigit [81]. Gagge's two node model was used to simulate individual segments rather than to whole body. Predicted results are compared with their experimental results, and literature data found to be with reasonable accuracy. An experimental study has been presented on the effect of local exposures on human responses by Zhang and Zhao [82]. They exposed 30 male subjects of their three body parts face, chest and back to local cooling airflow, whose temperature ranged from 22 to 28<sup>0</sup> C. The local thermal sensation of all body parts, overall thermal sensation and thermal acceptability on voting scale at regular interval was reported. Their results show that local exposure affected local thermal sensation of the unexposed body parts significantly, based on which a new influencing factor method was proposed. Cooling air temperature does not effect on the influencing factor and the weighting factor of each body parts. A predictive model was obtained which shows face

cooling could improve thermal acceptability more than chest or back cooling. Ono et.al [83] presented an experimental and numerical study on convective heat transfer coefficient for the human body in outdoor environment. A wind tunnel test and CFD analysis was performed to measure convective heat transfer coefficient in outdoor environment. They proposed a formula that can calculate the mean convective heat transfer coefficient for the human body. They also suggested that this formula is valid after comparing the results to the numerical simulation and evaluation.

Van Ooijen et al. [84] investigated the metabolic and temperature response to mild cold in summer and winter. 10 men and 10 women subjects aged 19-36 year participated in the experiment. The metabolic rate and body temperature were measured continuously for ambient temperature of 22<sup>0</sup>C. They found that the average metabolic response during cold exposure, measured as the increases in kJ/min over time was significantly higher in winter compared to summer. They concluded that higher metabolic response in winter compared to summer indicates cold adaptation. Jansky et al. [85] presented an experimental study on local peripheral cooling (immersion of legs up to the knees into 12<sup>0</sup>C water). Six male subjects participated in the experimental study. The recorded data shows the skin temperature decreased on some non-cooled areas of the body (fingers, palms and thigh) immediately after local cooling, but chest and forehead were not influenced. The data also indicates that change in skin temperature due to skin blood flow in body surface areas permanently fluctuates. The vasoconstrictor response is being controlled independently of the central temperature input.

Partial and whole body thermal sensation and comfort was studied by Arens et al. [86]. An experiment was carried out by exposing the subjects in uniform environment and was polled for their local and overall thermal sensation and comfort. They observed that

the sensation and comfort for the local body parts vary greatly. Hands and feet feels colder than other body parts in cool environment, Whereas head feels warmer than other body parts in warm environment. The local sensation (head) appears the warmest in warm environment, and coldest (heads and feet) appears coldest in cold environment. They extended their work in another experimental study [87] and determined skin temperature, core temperature, thermal sensation and thermal comfort for 19 local body parts by exposing the subjects in a warm and cool environment. Overshoot in sensation and comfort is stronger when local body parts are cooled or warmed than when the whole body experiences a step-change. They extended their work and developed a three part series of models for predicting the local thermal sensation [88], and local comfort of different parts of the body [89], and whole body sensation [90], was presented by Zhang et al. These models predicted the thermal responses for sedentary activity in different environmental conditions, (uniform, non-uniform, stable and transient).

Masayuki et al. [91] investigated convective heat transfer coefficient for each of the body part of clothed human body under different airflow conditions. This was then compared with the nude body. This process was done by measuring clothing surface temperature for both sitting and standing posture by using infrared-radiometer. They observed that convective heat transfer coefficient for clothed body was greater than the nude body. They also estimated the clothing insulation for each body parts. They found differences at body part level between standing and sitting postures.

Takada et al. [92] developed a thermal model to predict the thermal response of human body. They considered individual characteristics of human body temperature regulation. Based on the experimental data on four subjects they identified the coefficients in two node model. They show that the combination of six coefficients related to sweating and skin blood flow rate regulation in the two-node model which can be tuned for

individuals. In another work [93], the author studied the validity of two node model for predicting the steady state skin temperature by evaluating large number of experimental results. They showed that two node model can predict effectively the steady state temperature in the low activity conditions. They also suggested that the addition of shivering model represents the most significant improvement in the two node model.

Influence of clothing type on metabolic, thermal and subjective responses in cool environment was presented by Lee and Choi [94]. They investigated the effect of two different type of clothing (s- type, short sleeves and knee trousers, L-type, long sleeves and long trousers), on metabolic, thermal and subjective responses in cold environment. They concluded that energy expenditure of subjects was higher in S-type than in L-type. The increase rate of the EE in females was greater than in males,

Jin et al. [95] proposed a model for local and overall thermal sensation in non-uniform thermal environments. In total 179 tests were carried out in a controlled environmental chamber. During experiment, subjective responses for both local and overall thermal sensation were recorded. Results showed that local thermal sensation can be predicted by skin temperature to a high degree of accuracy for local ventilation conditions. A new approach for using pierce two node model for different body parts to predict the local skin temperature was presented by Foda and Siren [96]. In this study an experiment was carried out to measure local skin temperature at 24 site on the human body at three different indoor conditions (i.e. neutral, warm and cold). The results showed that the modified model predicts the local skin temperature with an average deviation of  $\pm 0.3^{\circ}\text{C}$ .

Choi and Loftness [97] conducted an experimental study to investigate the use of skin temperature to evaluate thermal sensation. They conducted an experiment with 26 volunteers in an experimental chamber from temperature 20<sup>0</sup>C and 30<sup>0</sup>C. They found that skin temperature changes rate were more consistent with thermal comfort conditions than with the actual levels of skin temperatures of participants. An investigation of change in thermal perception and thermoregulation that simultaneously take place due to temperature step in thermal transient was studied by Cheng et al [98]. An experiment was carried out in microclimate controlled room for two temperatures down step from 32/28 to 24<sup>0</sup>C and up step from 20<sup>0</sup>C to 24<sup>0</sup>C, and then the subjects were evaluated for change in thermal sensation and skin physiological properties. They suggested that thermoregulatory burden might be adequately controlled when the temperature step in thermal transition zone is limited to 4<sup>0</sup>C or lower.

### **2.3 Summery**

It is understood clearly from the literature that there is a substantial amount of research work have been carried out on human body by various researchers across the world. The researchers have considered the different environmental conditions and activity levels of human to simulate accurately the behavior of human body. Many researchers have considered different human body segments separately to simulate the thermal responses, because of the complex thermoregulatory behavior of human body as a whole. It is noted that there is not much of works particularly focusing on the heat transfer behavior of human head which is a vital part of human body. The wellbeing of head is directly related to proper functioning of the human body as a whole. Thus it is very important to consider the thermal behavior of human head in different environmental conditions as it is the most important part of the human body.

## **CHAPTER 3**

### **METHODOLOGY**

#### **3.1 Introduction**

Following the right type of methodology is an important decision to achieve the desired targets with sufficient accuracy and time. There are varied numbers of tools available to solve a given engineering problem. Among those various methods, finite element analysis has gained considerable importance in last few decades to tackle the difficult problems governed by complex phenomenon. Finite element analysis is particularly favorite method for scientist and engineers alike because of the various advantages offered by this method. Finite element analysis is an advanced technique to problems with domain having complex geometry. The development of finite element method has been started in the early 1900s. However it is believed that Courant is the first person to develop finite element method. In his paper, he used piecewise polynomial interpolation over triangular sub regions to investigate torsion problems. It was Clough [99] who popularized the term finite element in 1960s, and Zienkiewicz and Cheung [100] wrote a first finite element book. Since then investigators began to apply finite element to various other fields in engineering. Thus the current research is carried out by employing finite element analysis to heat transfer in human head.

#### **3.2 Finite Element Method (FEM)**

There are few basic steps involved in finite element method such as

- **Discretization of physical domain:** The first step involved is to divide the whole geometrical domain into a smaller set of segments known as elements. The elements can be a 1 dimensional element, 2-dimensional element or 3 dimensional element depending upon the geometry of the solution domain

considered. The elements are piecewise connected to each other by intermediate points which are known as nodes. The elements could be characterized by 1 node, 2 node, 3 node and so on based on number of points involved in a given element. The most popular elements are those having 2 node for 1 dimensional element, 3 or 4 node for 2-dimensional elements and 6 or 8 nodes of 3 dimensional elements. The choice of number of nodes depends on the accuracy required which generally increase with increased number of nodes but at the cost of increased number of equations to be solved which ultimately increases the time required for solution.

- Once the dimensionality of geometric domain and the type of element is decided then the next step is to assume a solution that may well describe the variation of solution variable inside a typical element. This step yields a set of shape functions for the element. The shape functions describe how the solution changes in the element. The variation of solution variable  $T$  inside the element can be conveniently represented as

$$\begin{aligned}
 T = & \frac{1}{8}(T_I(1-s)(1-t)(1-r) + T_J(1+s)(1-t)(1-r)) \\
 & + \frac{1}{8}(T_K(1+s)(1+t)(1-r) + T_L(1-s)(1+t)(1-r)) \\
 & + \frac{1}{8}(T_M(1-s)(1-t)(1+r) + T_N(1+s)(1-t)(1+r)) \\
 & + \frac{1}{8}(T_O(1+s)(1+t)(1+r) + T_P(1-s)(1+t)(1+r))
 \end{aligned}
 \tag{3.1}$$

$$T = N_I T_I + N_J T_J + N_K T_K + N_L T_L + N_M T_M + N_N T_N + N_O T_O + N_P T_P
 \tag{3.2}$$

The subscripts I, J, K..... represents the nodes of the element and s, t, r represents the local coordinates system in the x, y and z directions respectively.

The shape functions have the geometric information about the element embedded within themselves thus it describe the solution variable for instance temperature at any given point inside the element.

Using these shape function the governing equations such as complete heat conduction equation is subjected to an integration process by Galerkin method.

During integration, the higher order partial differential equations are converted into its weak form and multiplied with the shape function that yields an element stiffness matrix subjected to governed physical phenomenon. The resulting matrix form of equations can be conveniently represented as

$$[K]\{T\} = \{F\} \quad (3.3)$$

Where K is the stiffness matrix of dimension NxN, T and F are the solution variables and force vectors respectively of dimension Nx1

- Once the element stiffness matrix is available, the global stiffness matrix is compiled by taking the data of each element stiffness matrix combined with the information of the element connectivity position in the entire domain. The global stiffness will have the dimension of NxN where N indicates the total number of nodes available in the domain. The total number of equations to be solved are N and those are interconnected to each other thus requiring it to be solved simultaneously. Thus the emergence of computers and improvements in computational power of modern computer have made finite element analysis a very much affordable method which otherwise could have been limited to very simple problems with very few nodes.
- The next step is to specify the boundary conditions and modify that N number of equations to accommodate the boundary values.
- Once the boundary conditions are specified the next step is to solve the equations for desired solution variable.

- The last step would be to view the results of solution variable (temperature in heat transfer problem) and then calculate the secondary variables such as heat flux, thermal gradient etc. that depends on primary solution variable. For instance, the thermal gradient is calculated as

$$\frac{\partial T}{\partial r} = \frac{T_{m+1} - T_m}{r_{m+1} - r_m} \quad (3.4)$$

$$\frac{\partial T}{\partial z} = \frac{T_{m+1} - T_m}{z_{m+1} - z_m} \quad (3.5)$$

$$\frac{\partial T}{\partial \theta} = \frac{T_{m+1} - T_m}{\theta_{m+1} - \theta_m} \quad (3.6)$$

Where m indicates the node in r, z and  $\theta$  directions for gradient in those directions

The heat flux in r, z and  $\theta$  directions is calculated by

$$q_r = k \frac{\partial T}{\partial r} \quad (3.7)$$

$$q_z = k \frac{\partial T}{\partial z} \quad (3.8)$$

$$q_\theta = k \frac{\partial T}{\partial \theta} \quad (3.9)$$

The resultant heat flux is given by

$$q = (q_r^2 + q_z^2 + q_\theta^2)^{1/2} \quad (3.10)$$

There are numerous computer packages available to deal with the finite element analysis and the user do not have to worry about dealing with complex mathematical operations involved in achieving the solution for his/her problem under investigation. One such software is ANSYS which is very popular in handling the finite element analysis. It's a full-fledged package where the user can model the geometry as well as get the finite element solution using single package. It offers a comprehensive range of solutions for many physical phenomenon. It provides many varieties of elements with varied type of degrees of freedom to study the different physical problem. Due to its wide popularity and being user friendly, the current problem is solved by employing ANSYS.

### **3.3 FEA Model Development:**

The human head is generally approximated as a cylinder or a sphere having 4 different components such as brain, bone, fat and skin layers arranged from inner to outer surface of head. The dimensions of above mentioned layers may vary slightly from person to person based on the gender, race etc. A representative dimension and physical properties of these layers are available in the literature (A computer model of human thermoregulation for a wide range of environmental conditions: the passive system). The current model is assumed to be spherical in shape having dimensions and physical properties as given in table 3.1. The ANSYS preprocessor tool is used to develop the geometric model of the human head with different layers. The developed geometric model of the human head is shown in fig 3.1. It is to be noted that the lower most layer of human head is brain followed by bone layer that is followed by fat and then skin layers. The radius of different layers as indicated in table 3.1 shows its overall radius from the center point of brain. If one need to find the thickness of specific layers then the difference of that layer minus the presiding layer has to be taken into consideration. For instance, the thickness of bone layer is obtained by subtracting 8.60

(brain layer outer radii) from 10.05 which is the bone layer outer radii. In the same way, thickness of other layers can be obtained.

Table 3.1 Physical properties of tissues used in thermal modeling of a human head

Tissue layers	Radius r (cm)	Thermal conductivity k ( $\text{W m}^{-1} \text{K}^{-1}$ )	Density $\rho$ ( $\text{kg/m}^3$ )	Specific heat $C_p$ ( $\text{J kg}^{-1} \text{K}^{-1}$ )	Metabolic rate $Q$ ( $\text{W/m}^3$ )
Brain	8.60	0.49	1,080	3,850	13,400
Bone	10.05	1.16	1,500	1,591	0
Fat	10.20	0.16	850	2,300	58
skin	10.40	0.47	1,085	3,680	368
Hair	11.40	0.06578	-	-	-
Air	-	0.026	1.1774	1005.7	-

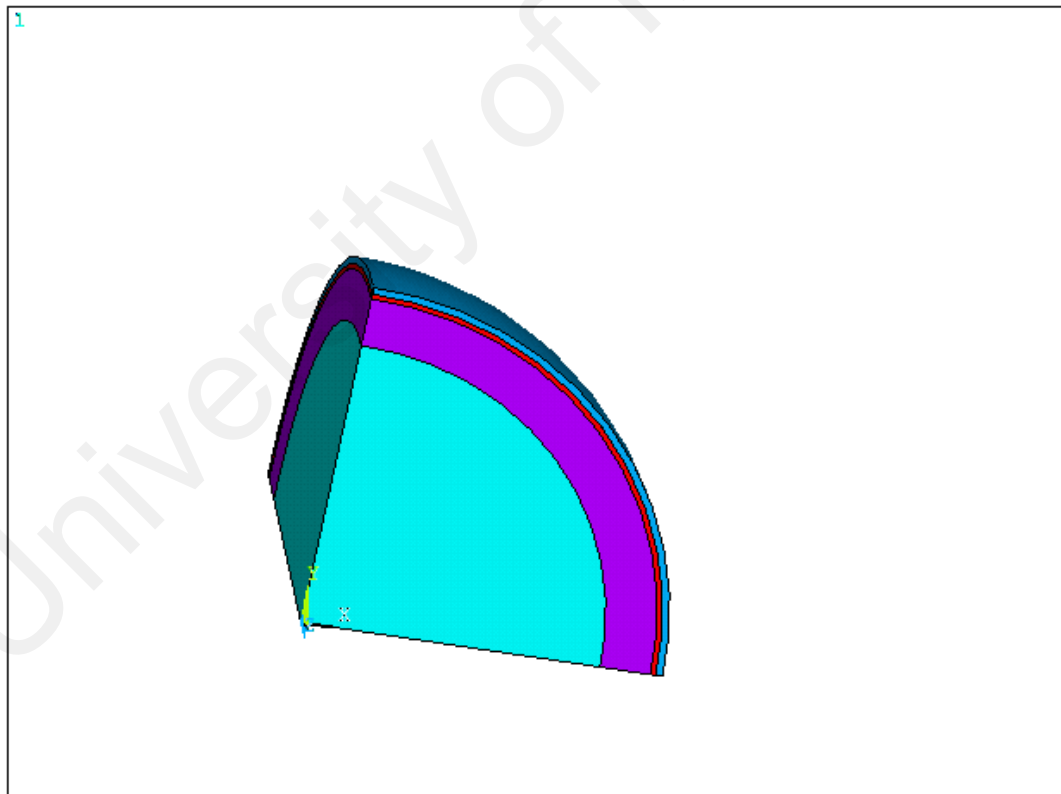


Figure 3.1: The geometric model of human head

Since the geometry is symmetrical in shape, only 1/8<sup>th</sup> part of the sphere is developed for the case of head without hair, to predict the heat transfer behavior. For the case of head with hair and head with cooling helmet, half of the head is developed to take advantage of symmetric section as shown in fig 3.2 and 3.3.

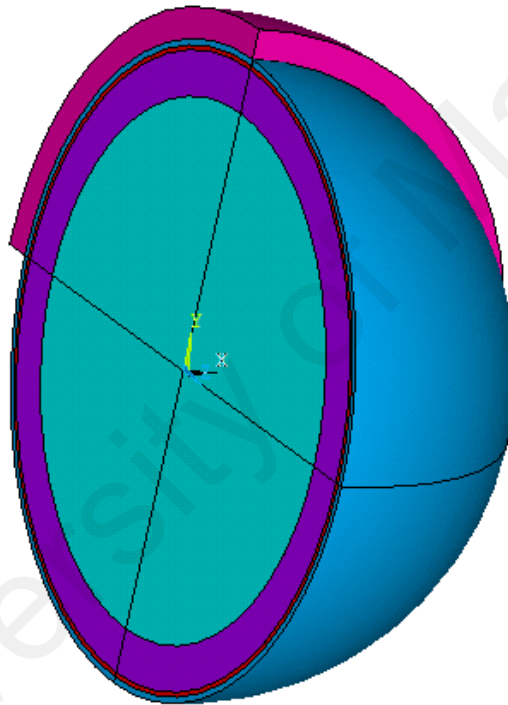


Figure 3.2: Human head model with hair

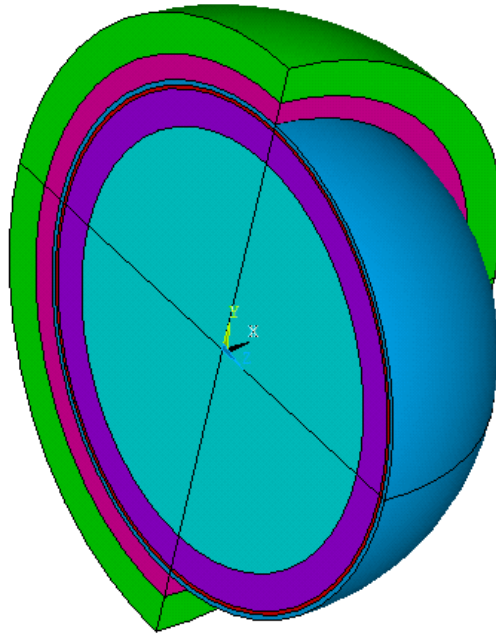


Figure 3.3: Human head model with cooling jacket

The developed model of the human head was meshed with 8 noded brick element. Sufficient number of elements is taken along the whole geometry and care was taken to mesh the domain with hexahedral elements which proves better accuracy than its counterpart tetrahedral elements. The meshed geometry for three cases is shown in figure 3.4 to 3.6. The brain has numerous blood vessels which helps in transferring heat from tissues to blood and blood to tissues depending upon the requirement. It would be very complex task to model such small vessels. Thus it was decided to model the effect of perfusion by convection rather than actually building the blood vessels. It is generally accepted that the blood temperature remains constant at  $36^{\circ}\text{C}$  and that of skin at  $36.8^{\circ}\text{C}$  under normal circumstances. Thus a convective heat transfer coefficient must exist between the blood vessels and the tissues of head that transfers heat between blood and the head tissues. A convective coefficient of  $235\text{ W/m}^2\text{C}$  between each node of the model and an imaginary node representing blood having a temperature of  $36^{\circ}\text{C}$  is applied which ultimately satisfied the temperature range of skin as mentioned above.

This value of convective coefficient ( $h$ ) is obtained by trial and error method until skin temperature is satisfied. Once the value of  $h$  is known then other geometrical and environmental parameters are varied.

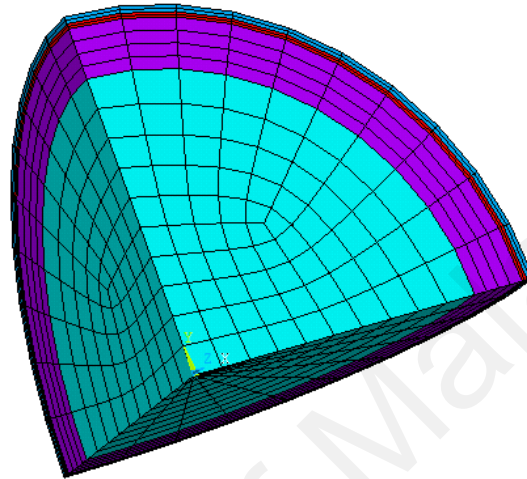


Figure 3.4: Human head meshed model

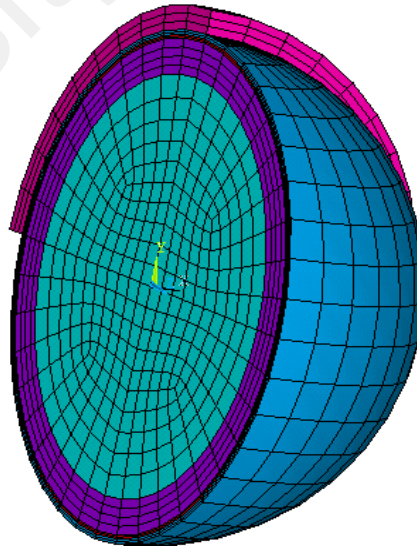


Figure 3.5: Human head meshed model with hair

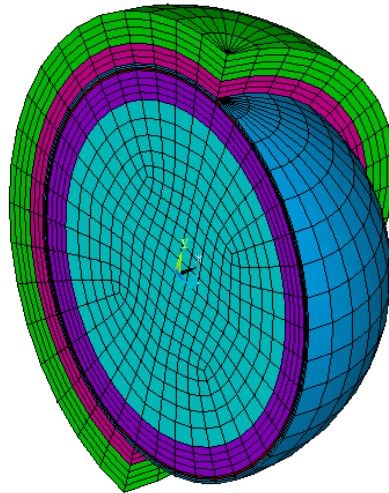


Figure 3.6: Human head meshed model with cooling jacket

Table 3.2 shows the number of elements and nodes into which the geometry was modeled for the different cases being considered.

Table 3.2: The number elements and respective nodes for various cases studied

Case	Head without hair	Head with hair	Head with helmet
No of Elements	1705	7215	8355
No of Nodes	2112	8670	10224

In order to simulate the extreme environmental temperature, the case of a parked car in sunlight during a typical day in Malaysia is considered. The temperature inside the car during the whole day was measured with the help of a FLIR infrared thermal imager. This imager can detect the temperature variations from  $-20^{\circ}\text{C}$  to about  $150^{\circ}\text{C}$  with an accuracy of  $0.1^{\circ}\text{C}$ . The car was parked in a sunny day having no shadows around it so that it can be directly exposed to sunshine throughout the day. The

temperature inside the car was measured at an interval of every 1 hour from morning 8 am until 5 pm in the evening with the help of thermal imager. This provided the data to judge the prevailing temperature inside the parked car. The minimum temperature is expected in the morning hours which comes around 22 deg C and maximum around 1 pm. The maximum value measured was around 75 deg C.



Figure 3.7: FLIR thermal imager

### 3.4 Summery

The current study is conducted by using finite element method. The human head is modeled in ANSYS commercially available software. The human head having different layers modeled with the physical properties. The human head is assumed to be a spherical in the current study. The geometry is spherical so only a small section of the head is developed. The modeled head is meshed with 8 noded brick element.

## CHAPTER 4

### RESULTS AND DISCUSSION

The simulated results are presented in terms of temperature variation across various layers of head. The investigation is carried out for reasonable range of environmental parameters such as ambient temperature and convective heat transfer coefficient between human head and outside environment. Apart from environmental parameters, the geometrical parameters of human head are also varied that provides an insight into the effect of thickness of different layers such as bone, fat and skin.

#### 4.1 Effect of ambient temperature

Figure 4.1a indicates the temperature variation in different layers of human head for the surrounding temperature  $0^{\circ}\text{C}$ . In this condition the outermost skin layer shows the lowest temperature of  $24.93^{\circ}\text{C}$  whereas a constant temperature is maintained in the brain tissue around  $36.98^{\circ}\text{C}$  when the environment temperature is  $0^{\circ}\text{C}$ . It can be seen from figure that due to lower environmental temperature, the conduction between fat and skin is more compared to bone and brain. It is also observed that there is a rapid decrease in temperature of fat layer from brain temperature. Figure 4.1a clearly shows that heat transfer takes place from the innermost layer (brain) to the outermost layer (skin).

Figure 4.1b shows the distribution of temperature in the different tissue layers of human head at surrounding temperature of  $10^{\circ}\text{C}$ . It is observed from this figure that a uniform decrease in the temperature takes place from the innermost layer to the outermost skin layer. It is also found that by comparing with the previous figure 4.1a, skin temperature increases with increases in surrounding temperature. A significant temperature variation

was found in the bone tissue from  $31^{\circ}\text{C}$  to  $34^{\circ}\text{C}$ . This figure also shows a constant temperature is maintain in the brain tissue when outside temperature increased to  $10^{\circ}\text{C}$ .

Figure 4.1c shows the temperature distribution in the different tissue layers of human head when the surrounding temperature was maintained at  $20^{\circ}\text{C}$ . The figure shows a uniform decrease in the temperature from  $37.03^{\circ}\text{C}$  to  $32.81^{\circ}\text{C}$  from the brain to the skin layer respectively. It is also observed that a large variation occurs from  $33.75^{\circ}\text{C}$  to  $35.62^{\circ}\text{C}$  in the bone layer. The skin shows the lowest temperature  $32.81^{\circ}\text{C}$ . It is observed that skin temperature increases with increases in surrounding temperature by comparing with the figure 4.1b. It is noted that the brain temperature is well within the normal range at  $20^{\circ}\text{C}$  outside temperature.

Figure 4.1d shows the variation of temperature in the different tissue layers of human head when the environmental temperature was maintained at  $30^{\circ}\text{C}$ . The figure shows a gradual decrease in the temperature from  $37.04^{\circ}\text{C}$  to  $35.01^{\circ}\text{C}$ , from the brain to the skin layer respectively. The brain layer temperature varies noticeably from  $36.14^{\circ}\text{C}$  to  $37.04^{\circ}\text{C}$ . The skin shows the lowest temperature  $35.01^{\circ}\text{C}$ .

Figure 4.1e depicts the temperature variation in the different tissue layers of human head for the environmental temperature maintained at  $40^{\circ}\text{C}$ . At this condition, the variation in brain layer is very small as the temperature across brain layer is found to be from  $37.0^{\circ}\text{C}$  to  $36.49^{\circ}\text{C}$ . It is found that the skin has a highest temperature around  $37.68^{\circ}\text{C}$ . This would cause severe uncomfortable feeling across the head.

Figure 4.1f illustrates the comparative distribution of temperature in the radial direction from inner most layer i.e. brain to the outer skin layer at different values of ambient temperature from  $0^{\circ}\text{C}$  to  $40^{\circ}\text{C}$ . It can be inferred that the variation of temperature is high at outer segment of head when environmental temperature is low as compared to the case of higher environmental temperature.

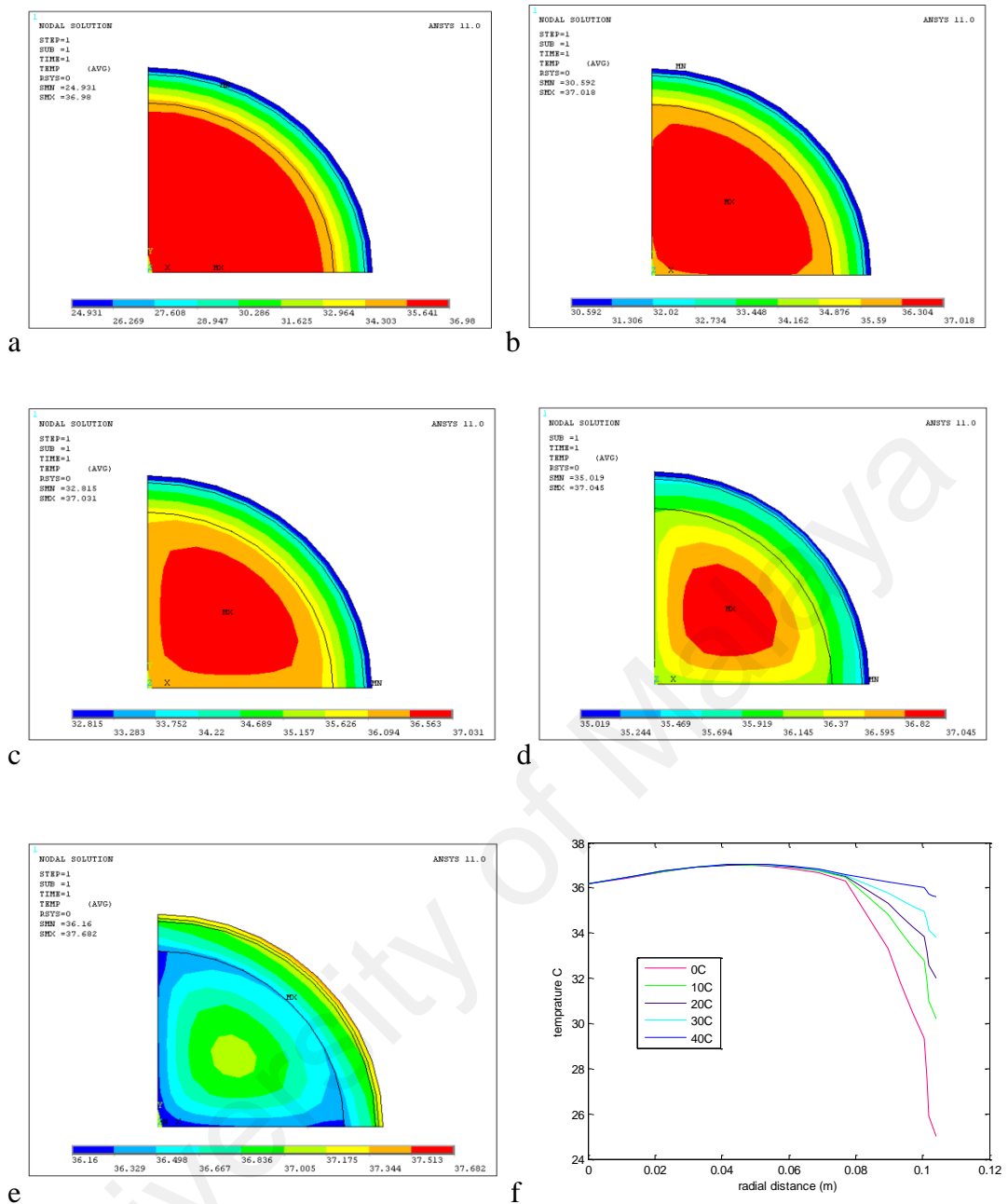


Figure 4.1: Temperature variation in human head at different values of  $T_a$

- a) 0°C b) 10°C c) 20°C d) 30°C e) 40°C f) temperature from innermost to outer layer of head

In any heat transfer phenomenon, thermal flux and thermal gradient gives an idea to judge the heat flow rate along with its movement in different directions. It is an important secondary parameter to study the behavior of heat transfer in objects. Since the range of temperature considered is large that would generate huge amount of data and corresponding figures that may be redundant. Thus a representative case of 26<sup>0</sup> C

ambient temperature is presented herewith to identify the thermal gradient and heat flux from the human head.

Figure 4.2 illustrates the thermal gradient in x, y, z direction along with the resultant of x, y, z components of gradient. The below figures 4.2 a, b and c describes the thermal gradients in x, y and z directions respectively. The inner blood temperature has been maintained at  $36^{\circ}\text{C}$  and blood perfusion was taken to be  $235 \text{ W/ m}^2 \text{ }^{\circ}\text{C}$ , whereas the surrounding temperature was kept at  $26^{\circ}\text{C}$ . It is clearly seen from the figure 4.2a that thermal gradient in the innermost section brain is  $443.34 \text{ }^{\circ}\text{C/m}$ , the highest compared to the other sections which shows the heat loss is more from the brain. And also observed that the thermal gradient in small area of fat is lowest, indicating the lowest heat loss taking place in the small area of fat layer in the x direction. The figure 4.2 b represents the thermal gradients in the y direction, which shows similar loss of the higher heat in the brain as in the figure 4.2 a and lowest heat loss in the fat layer in y direction. Similarly the figure 4.2 c shows the loss of heat in the z direction. As compared to other layers the heat loss is greater in the fat layer in z direction, and lowest in the central brain region.

The figure 4.2 d depicts the total gradient in the various tissue layers of the human head. There is significantly highest thermal gradient in the brain layer, which clearly shows the highest loss of heat transfer from the brain layer compared to the other tissue layers in the geometry. It is clearly seen that thermal gradient is gradually decreasing along the different layers up to skin layer. And also it is observed from the figure 4.2 d that a considerable loss of heat takes place in the fat layer. The bone tissue has a lower thermal gradient in the figure represents the less heat transfer.

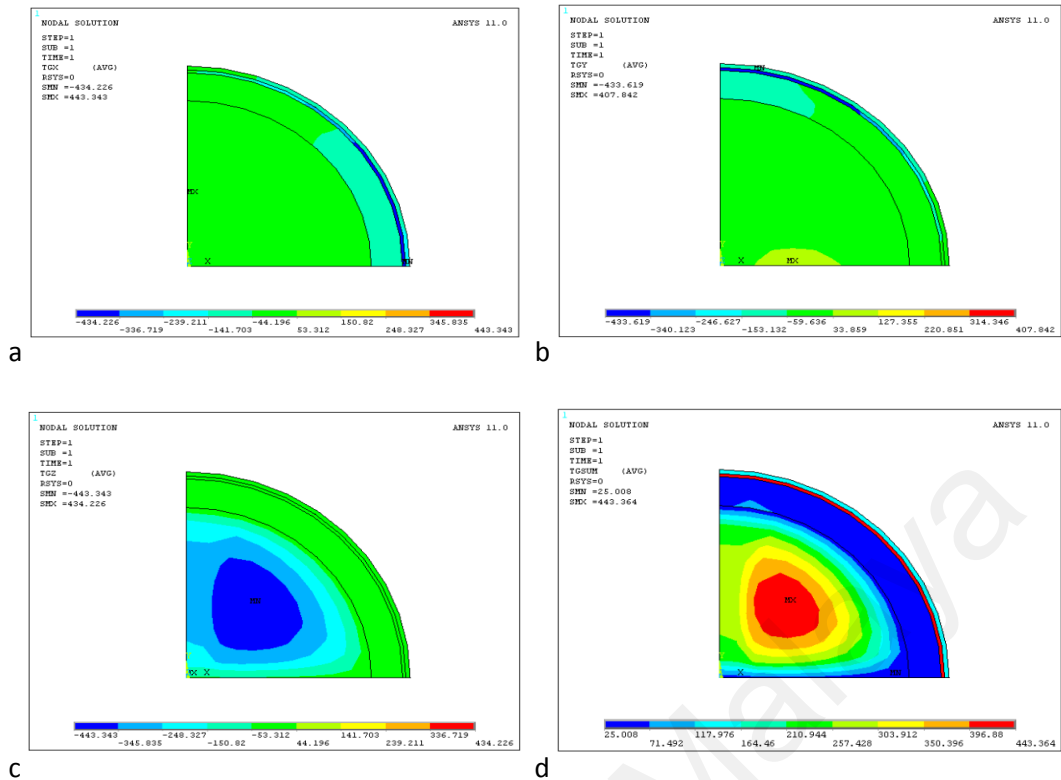


Figure 4.2: Thermal gradients at 26<sup>0</sup>C a) x direction b) y direction c) z direction d) total gradient

The figure 4.3a, b and c indicates the heat flux in the x, y and z-directions respectively. It is observed that the pattern of heat flux in x and y directions are somewhat similar whereas that of z direction is distinctively different. Even though the x direction heat flux is comparatively lowest but the heat flux in some portion of the brain can be noticed is more at the center of brain layer of the head compared to the heat flux in the other sections. It can be noticed that the resultant heat flux (figure 4.3 d) is lowest in the bone section as compared to other layers.

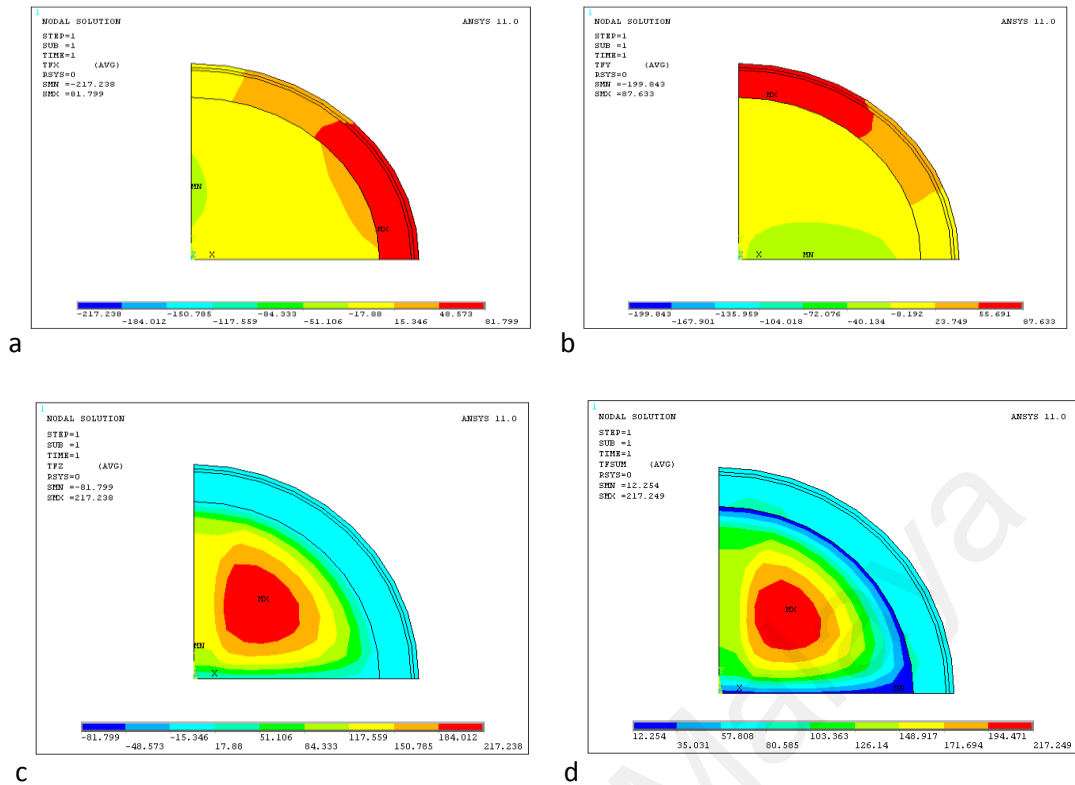


Figure 4.3 Thermal flux at 26°C a) x-direction b) y-direction c) z-direction d) total heat flux

In order to predict the heat transfer behavior as a function of ambient temperature, 4 other temperatures such as 2°C, 4°C, 24°C and 36°C are discussed in the following section. These temperatures are selected because it represents likely cases of environmental temperature covering a vast majority of habitual places of the world.

Figure 4.4 a, b and c represents the temperature, thermal gradient and heat flux respectively in the human head when ambient temperature is 2°C. It can be observed that the temperature of brain region is almost 36°C and that of skin is 25°C, 23°C. the skin temperature is increased marginally as compared to the case when ambient temperature is 0°C. The highest temperature gradient is found to be across the fat layer which can be attributed to its lowest thermal conductivity as compared to other layers of human head.

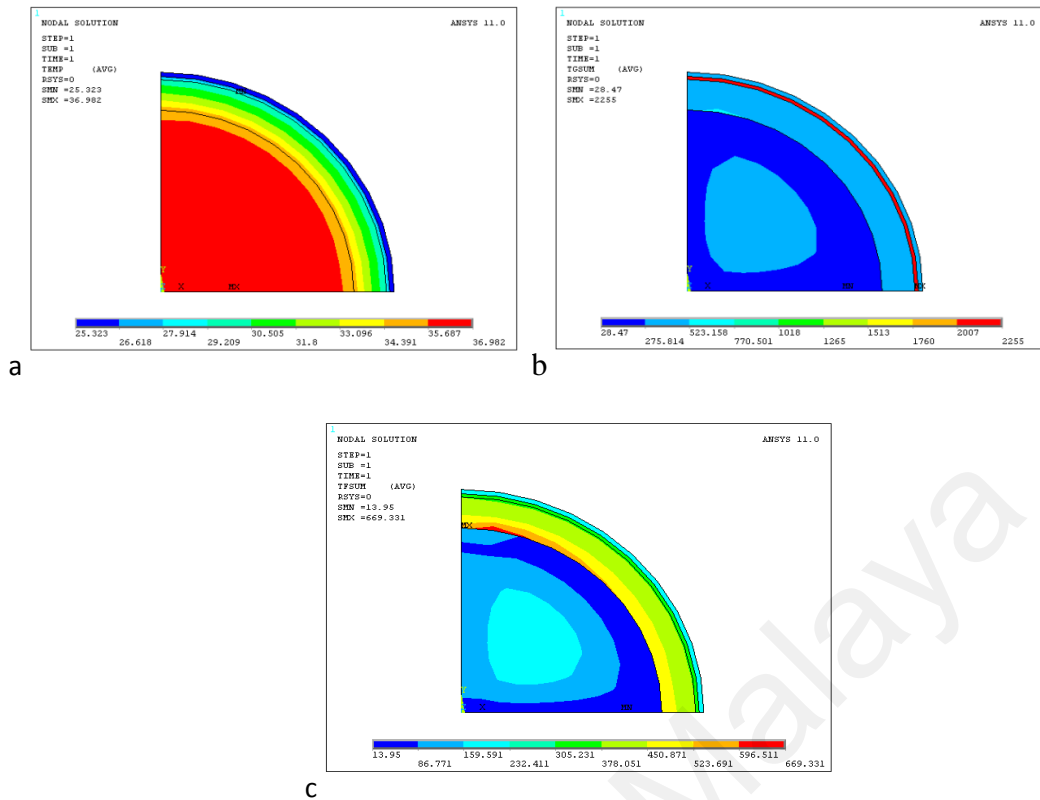


Figure 4.4: a) Nodal temperature at  $2^{\circ}\text{C}$  b) total thermal gradient at  $2^{\circ}\text{C}$  c) total thermal flux at  $2^{\circ}\text{C}$

Figure 4.5 a, b and c shows the variation of temperature, thermal gradient and heat flux respectively for the case of  $12^{\circ}\text{C}$  ambient temperature. The figure a shows a uniform decrease in the temperature from the brain to the skin layer. And also observed that a large variation from  $31^{\circ}\text{C}$  to  $35^{\circ}\text{C}$  in the bone layer. The skin shows the lowest temperature  $31^{\circ}\text{C}$ . The thermal gradient of skin is  $255^{\circ}\text{C}/\text{m}$ . The central region of brain has a thermal gradient around  $367^{\circ}\text{C}/\text{m}$ . It is noticed that the heat flux decreased by increasing the ambient temperature. This can be explained in a way that the heat transfer is directly related to temperature difference between two regions that acts as a driving force for heat to flow. Since the temperature difference between inside the head and outside environment decreases with increase in the ambient temperature that leads to reduction of the overall heat transfer rate reflected as reduced heat flux in figure 4.4 c.

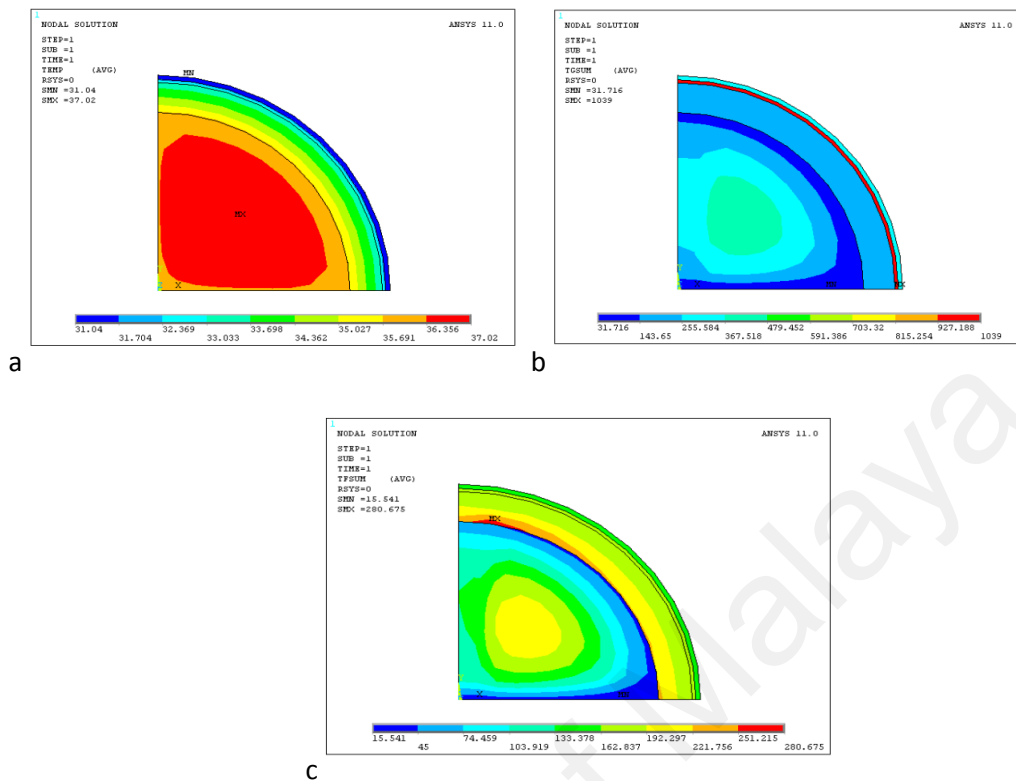


Figure 4.5: a) nodal temperature at 12<sup>0</sup>C b) total thermal gradient at 12<sup>0</sup>C c) total thermal flux at 12<sup>0</sup>C

The effect of further increase in ambient temperature to 24<sup>0</sup>C is shown in figure 4.6. It is observed that the skin temperature has increased to 33.69<sup>0</sup>C which is a normal temperature range for an acceptable thermal comfort level. The thermal gradient reduces to 50% as compared to the case of 12<sup>0</sup>C ambient temperature which represents 22% decrease in the heat flow rate. It may be noted that the heat flow from the body to outside environment is loss of body energy thus decrease in heat flow rate is desirable from body energy conservation point of view.

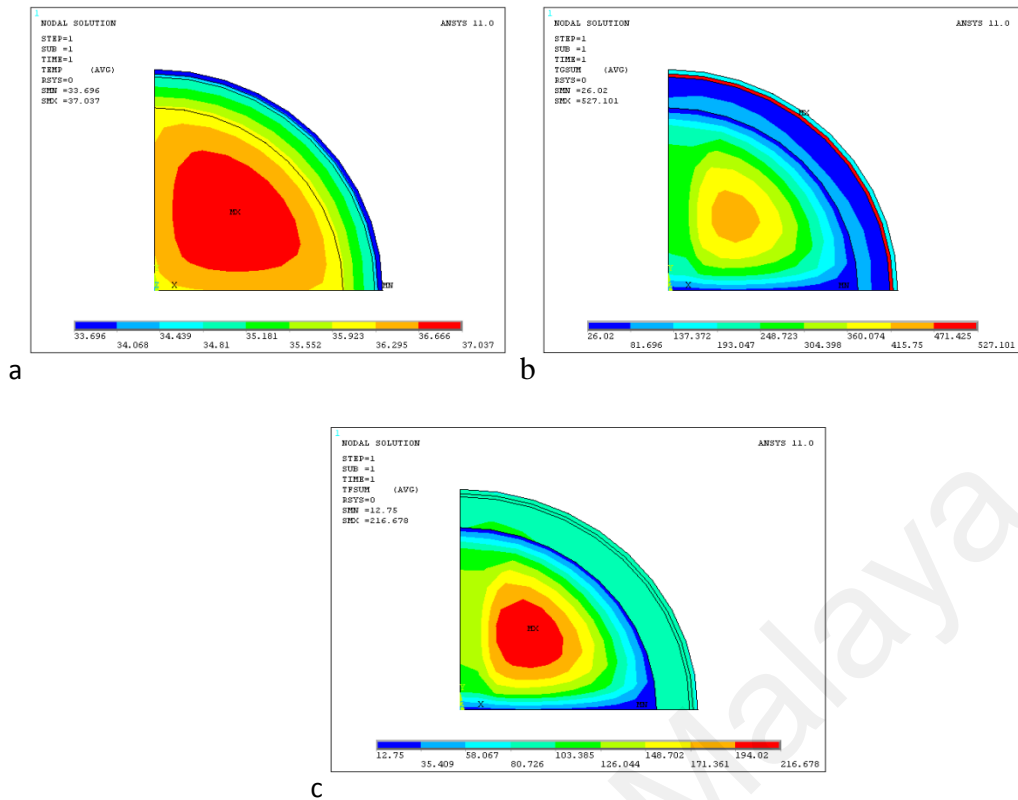


Figure 4.6: a) Nodal temperature at 24<sup>0</sup>C b) total thermal gradient at 24<sup>0</sup>C c) total thermal flux at 24<sup>0</sup>C

Increasing the ambient temperature to 36<sup>0</sup>C leads to skin temperature getting elevated to 36.16<sup>0</sup>C as shown in figure 4.7. This condition may lead to uncomfortable feeling for most of the human beings and it can result in the quick tiredness with slight activity level. It can be seen that the heat flow from the head to environment decreases but it may not be desirable at elevated skin temperature. As the human activity generates heat inside the human body including the head, it has to be dissipated at optimal rate to keep the body active without feeling tiredness. The increased skin temperature does not allow the heat to flow outside thus the brain has to reduce its activity level so that no further heat is generated that may cause damage to tissues.

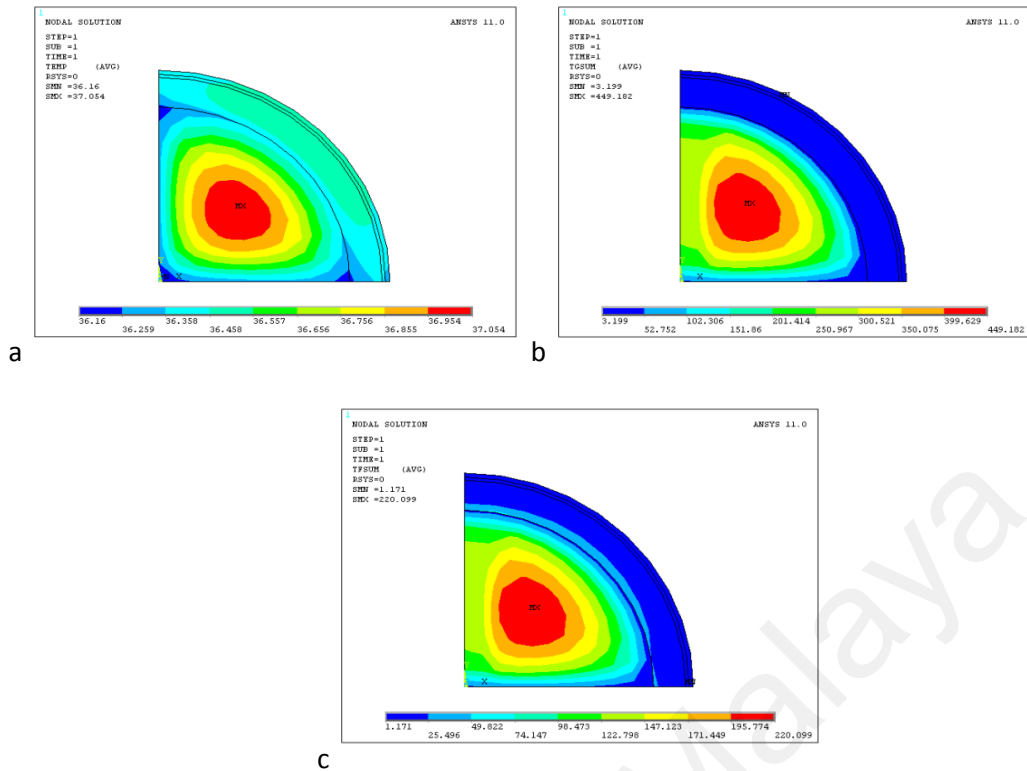


Figure 4.7: a) nodal temperature at  $36^{\circ}\text{C}$  b) total thermal gradient at  $36^{\circ}\text{C}$  c) total thermal flux at  $36^{\circ}\text{C}$

#### 4.2 Effect of heat transfer coefficients

Apart from ambient temperature  $T_a$ , the effect of combined heat transfer coefficient ( $h_{cr}$ ) due to convection and radiation is analyzed. In this case,  $T_a$  is maintained at  $25^{\circ}\text{C}$  and the value of  $h_{cr}$  is varied from 9 to  $13\text{ W/m}^2\text{ }^{\circ}\text{C}$ . Figure 4.8a shows the temperature distribution when the combined heat transfer coefficient is equal to  $9\text{ W/m}^2\text{ }^{\circ}\text{C}$ . It is seen that the temperature varies from minimum  $33.74^{\circ}\text{C}$  to maximum of  $37.03^{\circ}\text{C}$  in the various layers of the human head. It can be clearly seen from figure 4.8a that the inner most layer of brain has an area maintained at constant temperature around  $37^{\circ}\text{C}$  at the center and gradually decreases to the skin layer. The skin tissue has a lowest temperature around  $33.74^{\circ}\text{C}$ . A considerable variation also observed in the bone layer from  $34.84^{\circ}\text{C}$  to  $35.93^{\circ}\text{C}$ . The fat layer has a temperature  $34.10^{\circ}\text{C}$ . The lowest temperature is observed in the skin layer  $33.74^{\circ}\text{C}$ . The effect of increased value of combined heat transfer coefficient is to reduce the temperature level in the human head.

It is observed that the effect of  $h_{cr}$  is more prominent on the outer layers of head than the brain area. The maximum temperature which persists in the brain segment has changed negligibly when  $h_{cr}$  is increased from 9 to 13  $\text{W/m}^2\text{ }^\circ\text{C}$ . However, the outer skin temperature decreased by  $0.8\text{ }^\circ\text{C}$  due to change in combined heat transfer coefficient.

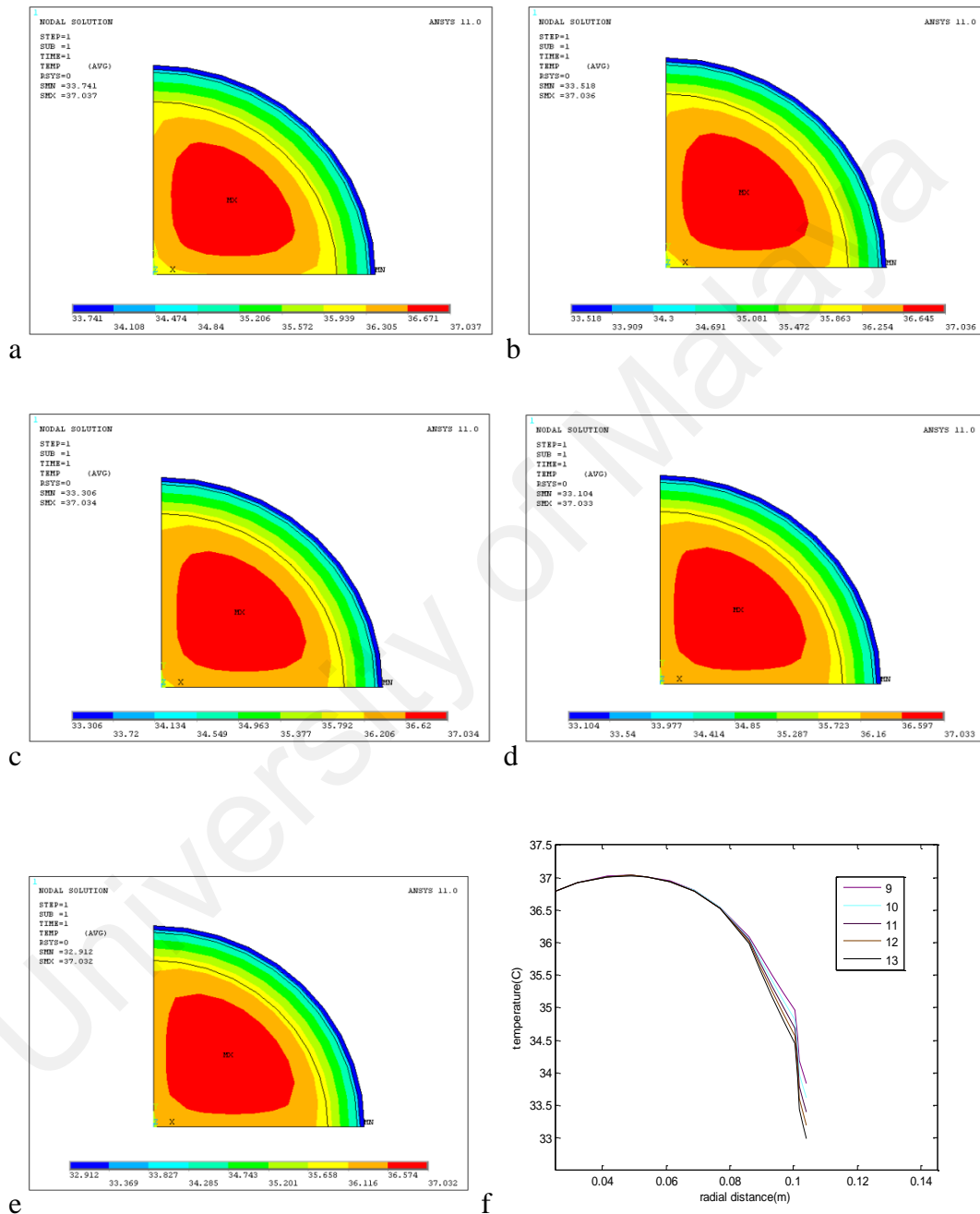


Figure 4.8: Temperature variation in human head at different values of  $h_{cr}$

a)  $9\text{ W/m}^2\text{ }^\circ\text{C}$  b)  $10\text{ W/m}^2\text{ }^\circ\text{C}$  c)  $11\text{ W/m}^2\text{ }^\circ\text{C}$  d)  $12\text{ W/m}^2\text{ }^\circ\text{C}$  e)  $13\text{ W/m}^2\text{ }^\circ\text{C}$  f) temperature from innermost to outer layer of head

The following section describes the temperature variation along with the thermal gradient and heat flux as a function of variation in heat transfer coefficient. It may be noted that the geometry of the head along with the thickness of brain, bone, fat and skin layer remains same as that of the previous case. The only exception is that the convective coefficient varies which can represent the effect of air velocity across the head. The ambient temperature was considered to be constant (i.e. 25°C). Figure 4.9 illustrates the behavior of heat transfer when combined convective coefficient is 8.25W/m<sup>2</sup> °C. It is seen that the skin temperature remains within the acceptable range and the maximum heat flux is found at a distance roughly 2 cm to 4 cm radius of the brain layer.

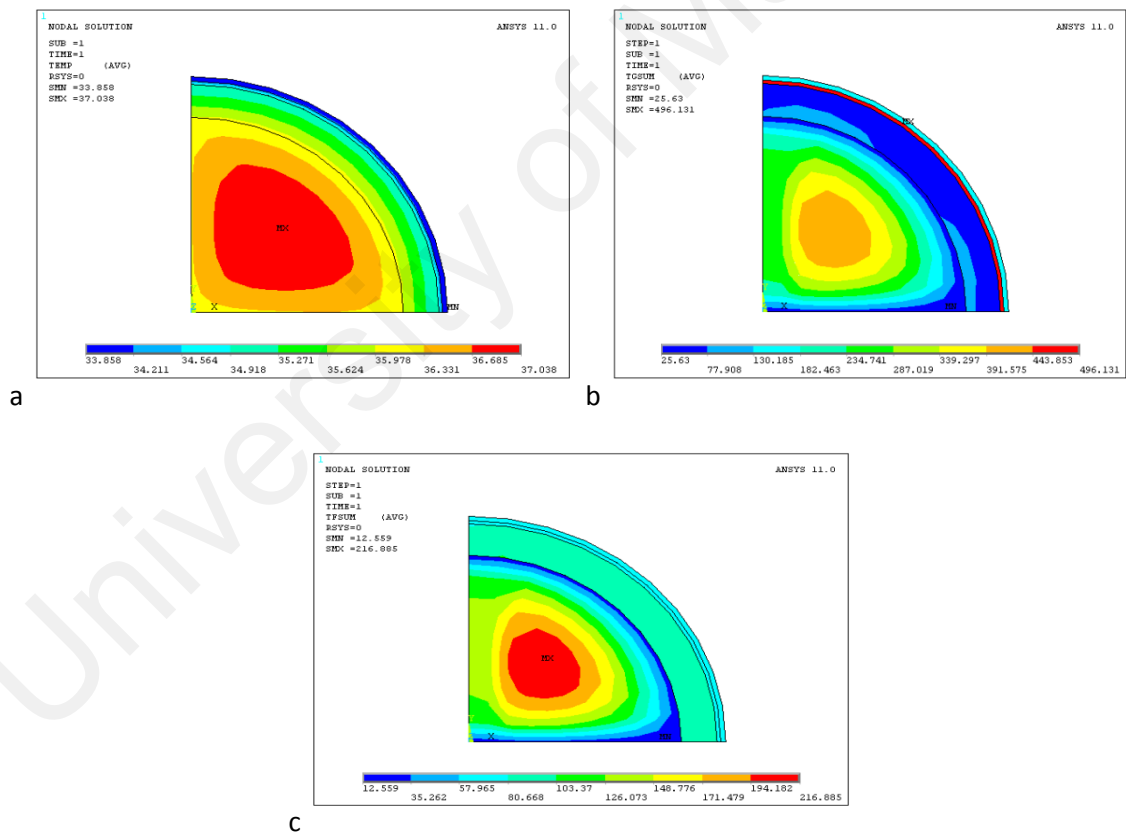


Figure 4.9: convective and radiative heat transfer coefficient at 8.25W/m<sup>2</sup> °C a) Nodal temperature b) total thermal gradient c) total thermal flux

The figure 4.10a shows the temperature distribution from  $33.62^{\circ}\text{C}$  to  $37.03^{\circ}\text{C}$  in the various layers of the human head for the combined (convective and radiative) heat transfer coefficients at  $9.5 \text{ W/m}^2\text{C}$ . It can be seen clearly from the figure 4.10a that the inner most layer brain has an elliptical region maintained at constant temperature around  $37^{\circ}\text{C}$  at the center and gradually decreases to the skin layer. The skin tissue has a lowest temperature around  $33.62^{\circ}\text{C}$ . A considerable variation also observed in the bone layer from  $34.0^{\circ}\text{C}$  to  $35.9^{\circ}\text{C}$ . The fat layer has a temperature  $34^{\circ}\text{C}$ . The lowest temperature is observed in the skin layer  $33.62^{\circ}\text{C}$ .

The figure 4.10b indicates the distribution of thermal gradient in the different layers of the human head for the combined (convective and radiative) heat transfer coefficient at  $9.5 \text{ W/m}^2\text{C}$ . It is clearly observed from the figure 4.10b that a circular region of the brain layer at the center has large thermal gradient around  $426.43^{\circ}\text{C/m}$ , which gradually decreases to the lowest at the end of the brain. The bone layer has lowest thermal gradient compared to the other layers. And a significant largest thermal gradient was observed in fat tissue, which shows the heat loss is more from the fat tissue compared to the other layers. By comparing with the previous figure 4.9b, a slight increase in the largest thermal gradient is found. The skin layer has thermal gradient around  $140.55^{\circ}\text{C/m}$ .

The figure 4.10c explains the distribution of thermal flux in the different layers of the human head for the combined (convective and radiative) heat transfer coefficient at  $9.5 \text{ W/m}^2\text{C}$ . It is clearly seen that the brain tissue at the center has the largest thermal flux (i.e  $216.48 \text{ W/m}^2$ ) and decreases uniformly to the lowest (i.e  $12.83 \text{ W/m}^2$ ) at the boundary of the brain layer. The brain tissue losses highest heat from the center to the end. The bone and fat and skin tissue maintained almost equal thermal flux around  $80.75 \text{ W/m}^2$ .

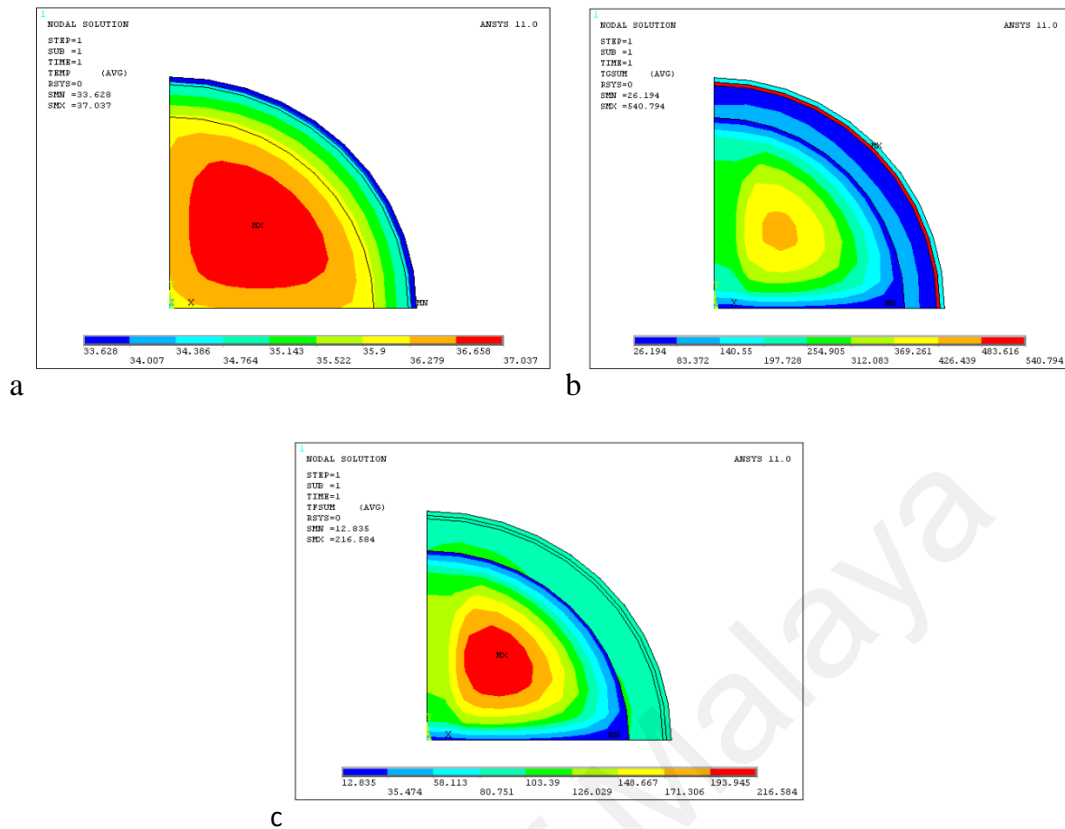
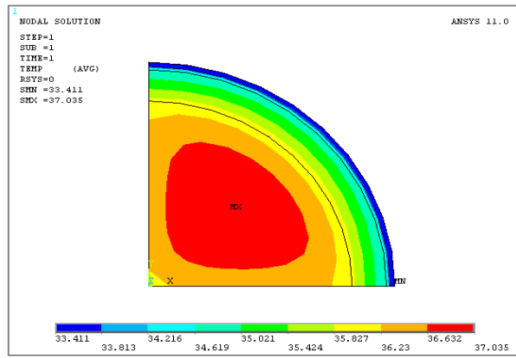
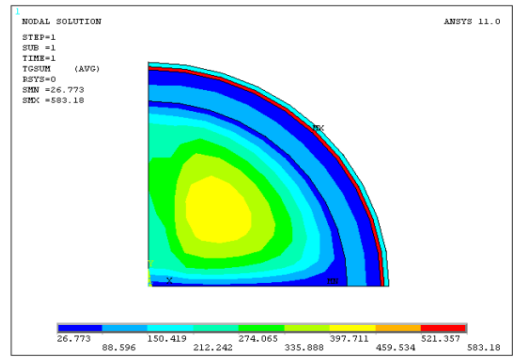


Figure 4.10: convective and radiative heat transfer coefficient at  $9.5\text{W/m}^2\text{ }^0\text{C}$  a) nodal temperature, b) total thermal gradient c) total thermal flux

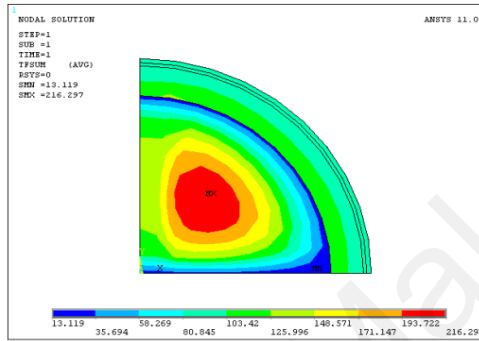
Figure 4.11 to figure 4.13 illustrate the effect of combined heat transfer coefficient when its value is varied from  $10.5\text{W/m}^2\text{ }^0\text{C}$ ,  $11.5\text{W/m}^2\text{ }^0\text{C}$  and  $12.5\text{W/m}^2\text{ }^0\text{C}$  respectively. It is worth mentioning that the higher the heat transfer coefficient the better would be the exchange of heat either from head to outside environment or vice-versa depending on the temperature difference between the head and the environment. It can be seen that the skin temperature decreases from  $33.41\text{ deg C}$  (fig4.11) to  $33\text{ deg C}$  when convective and radiative heat transfer coefficient is increased to  $12.5\text{W/m}^2\text{ }^0\text{C}$ . the maximum thermal gradient which is found across the fat layer increased from  $583.18^0\text{C/m}$  to  $661.73^0\text{C/m}$  that itself indicates the heat transfer rate should increase, since heat transfer rate is directly proportional to the thermal gradient across given section of an object.



a

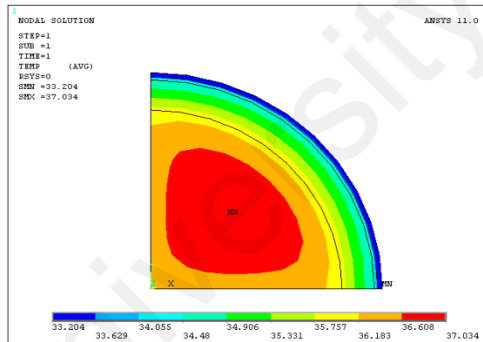


b

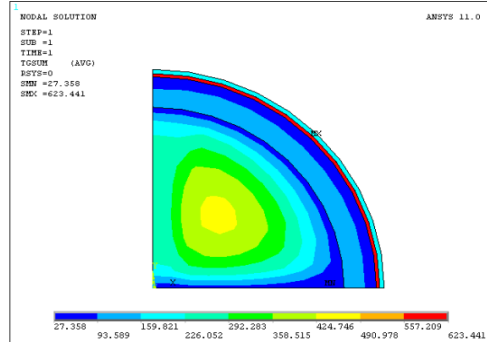


c

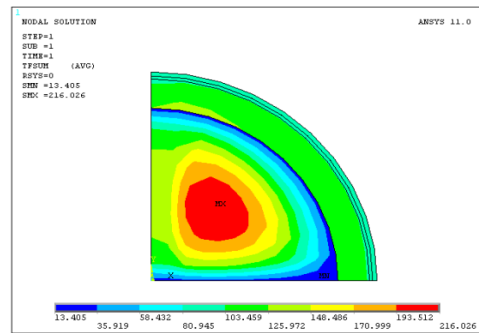
Figure 4.11: convective and radiative heat transfer coefficient at  $10.5 \text{ W/m}^2 \text{ } ^\circ\text{C}$ . a) nodal temperature b) total thermal gradient c) total thermal flux



a



b



c

Figure 4.12: convective and radiative heat transfer coefficient at  $11.5 \text{ W/m}^2 \text{ } ^\circ\text{C}$ . a) nodal temperature b) total thermal gradient c) total thermal flux

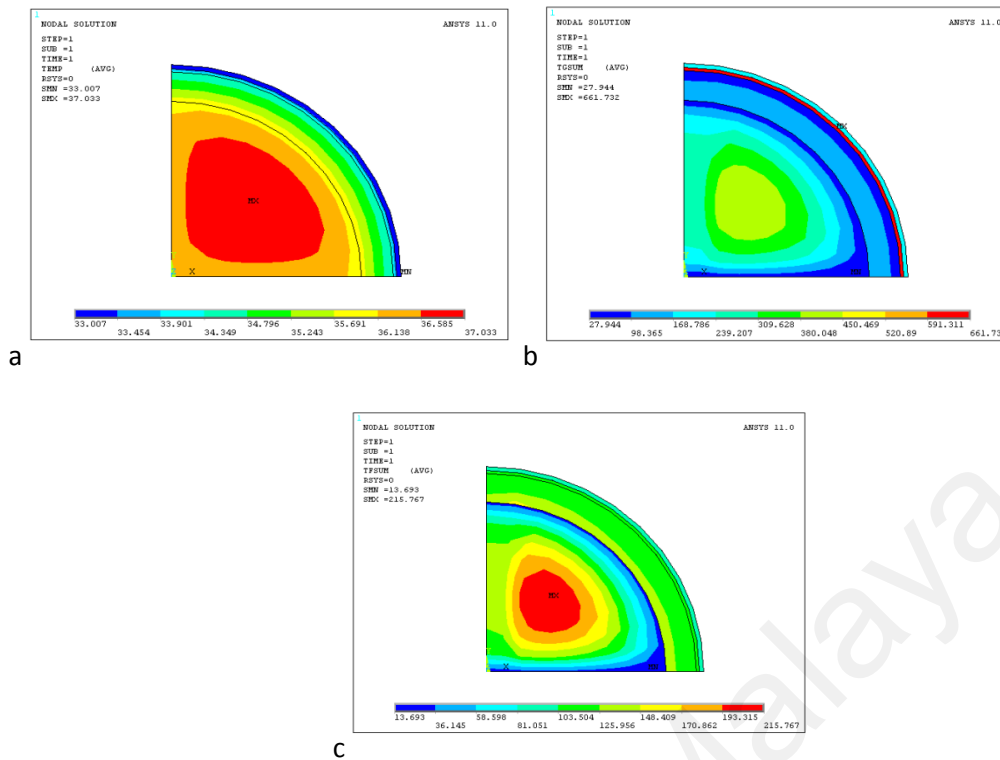


Figure 4.13: convective and radiative heat transfer coefficient at  $12.5 \text{ W/m}^2 \text{ } ^\circ\text{C}$ . a) nodal temperature, b) total thermal gradient c) total thermal flux

Figure 4.14 illustrates the change of temperature across different layers of human head as a function of combined convective and radiative heat transfer coefficient which is varied in the steps of  $8.25 \text{ W/m}^2 \text{ } ^\circ\text{C}$ ,  $9 \text{ W/m}^2 \text{ } ^\circ\text{C}$ ,  $9.5 \text{ W/m}^2 \text{ } ^\circ\text{C}$ ,  $10 \text{ W/m}^2 \text{ } ^\circ\text{C}$ ,  $10.5 \text{ W/m}^2 \text{ } ^\circ\text{C}$ ,  $11 \text{ W/m}^2 \text{ } ^\circ\text{C}$ ,  $11.5 \text{ W/m}^2 \text{ } ^\circ\text{C}$ ,  $12 \text{ W/m}^2 \text{ } ^\circ\text{C}$ ,  $12.5 \text{ W/m}^2 \text{ } ^\circ\text{C}$ , and  $13 \text{ W/m}^2 \text{ } ^\circ\text{C}$ . It can be clearly seen that as the heat transfer coefficient increases the skin temperature decreases where as there is a negligible change in temperature was observed in the brain layer. The bone and fat layers also shows the decrease in the temperature with the increase in the heat transfer coefficients. Thus it can be said that the increase in heat transfer coefficient which is strongly dependent on wind velocity is desirable to keep the skin temperature at acceptable range.

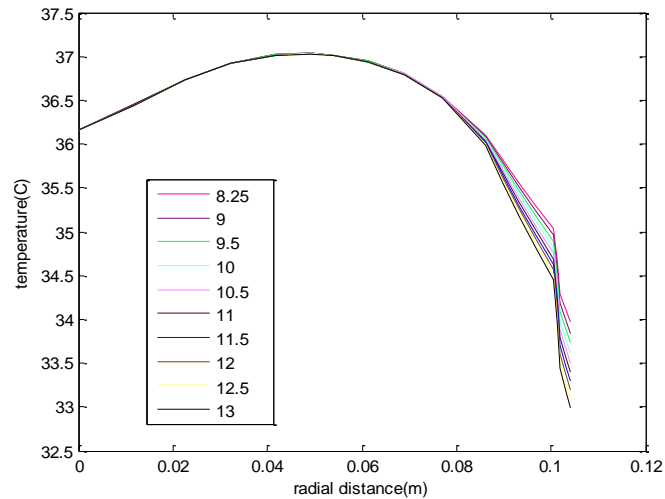


Figure 4.14: Effect of combined heat transfer coefficient on temperature variation across human head

### 4.3 Effect of variation of thickness of different tissue layers

The thickness of different layers of human head as given in table 1 is a representative case for a typical human head. It can be fairly assumed that the thickness of these layers may vary depending on the gender, race and environmental conditions of different places on the earth. The following section is aimed to study the effect of variation in these thicknesses of layers. The thickness of each layer is varied within a short acceptable range by keeping the other layers as constant thickness as given in table 1. It may be noted that the thickness of any given layer is the difference between the inner and outer radii of the layer from the center of head. The environmental parameters i.e.  $T_a$  and  $h_{cr}$  are maintained at  $30^{\circ}\text{C}$  and  $8.25 \text{ W/m}^2\text{ }^{\circ}\text{C}$  respectively.

#### 4.3.1 Effect of Skin layer thickness

The figure 4.15a shows the distribution of temperature in different layers of the human head from  $34.28^{\circ}\text{C}$  to  $37.10^{\circ}\text{C}$  when the thickness of the skin layer is reduced to 0.1cm. It can be observed from the figure that a constant temperature has been maintained at the center of the brain which uniformly decreases from the center to the skin. It is also observed that bone layer has the variation of temperature from  $34.59^{\circ}\text{C}$  to  $35.89^{\circ}\text{C}$ . And

lowest temperature was observed on skin tissue (i.e.  $34.28^{\circ}\text{C}$ ) and variation of temperature was found in the fat layer from  $34.59^{\circ}\text{C}$  to  $34.91^{\circ}\text{C}$ . The outer most layer skin has the lowest temperature around  $34.28^{\circ}\text{C}$ .

The figure 4.15b represents the distribution of thermal gradient in various layers of human head when the thickness of the skin layer is reduced to 0.1cm. It is found that a circular region at the center of the brain and the fat layer has a highest thermal gradient (i.e  $472.91^{\circ}\text{C/m}$ ) which shows the greatest heat transfer from these regions. And also observed that bone layer has the lowest (i.e.  $26.48^{\circ}\text{C/m}$ ) thermal gradient which indicates the lowest heat loss takes place in bone tissue layer. The thermal gradient of outer most skin layer has almost  $125.64^{\circ}\text{C/m}$ .

The figure 4.15c shows the distribution of thermal flux in various layers of human head when thickness of the skin layer is 0.1cm. It can be seen from the figure that a circular region at the center of the brain has concentrated with the largest thermal flux (i.e.  $231.72\text{ W/m}^2$ ) which gradually decreases to the lowest at the end of the brain layer (i.e.  $12.94\text{ W/m}^2$ ), and bone, fat and skin layers has equal thermal flux ( $61.56\text{ W/m}^2$ ) was observed.

It is observed that the skin temperature decreased from  $34.28\text{ Deg C}$  to  $33.87\text{ deg C}$  when skin layer thickness is increased from 0.1cm to 0.4 cm as shown in figure 4.15a to figure 4.17a.

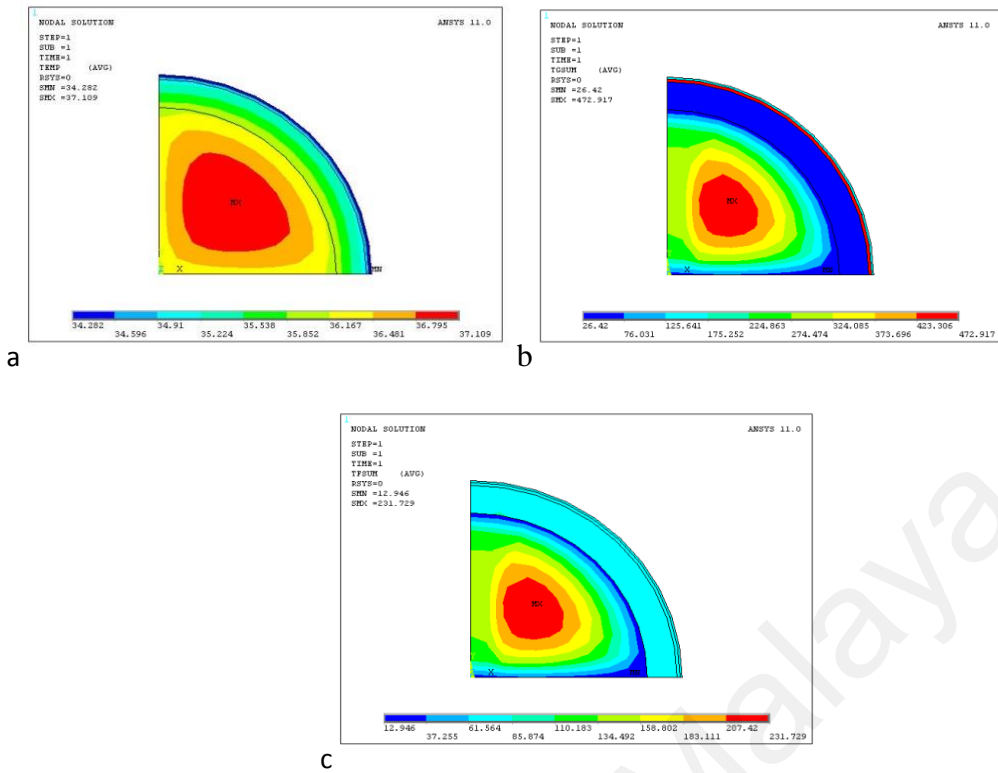


Figure 4.15: a) nodal temperature b) thermal gradient c) thermal flux for skin layer thickness of 0.1 cm

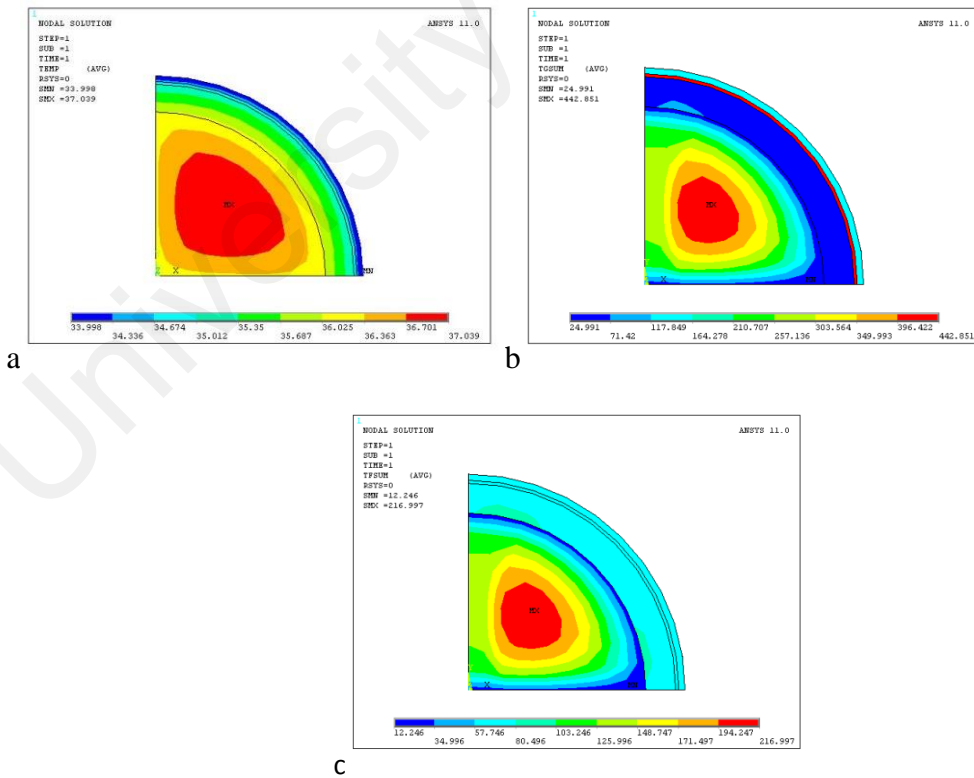


Figure 4.16: a) nodal temperature b) thermal gradient c) thermal flux, for skin layer thickness of 0.3 cm

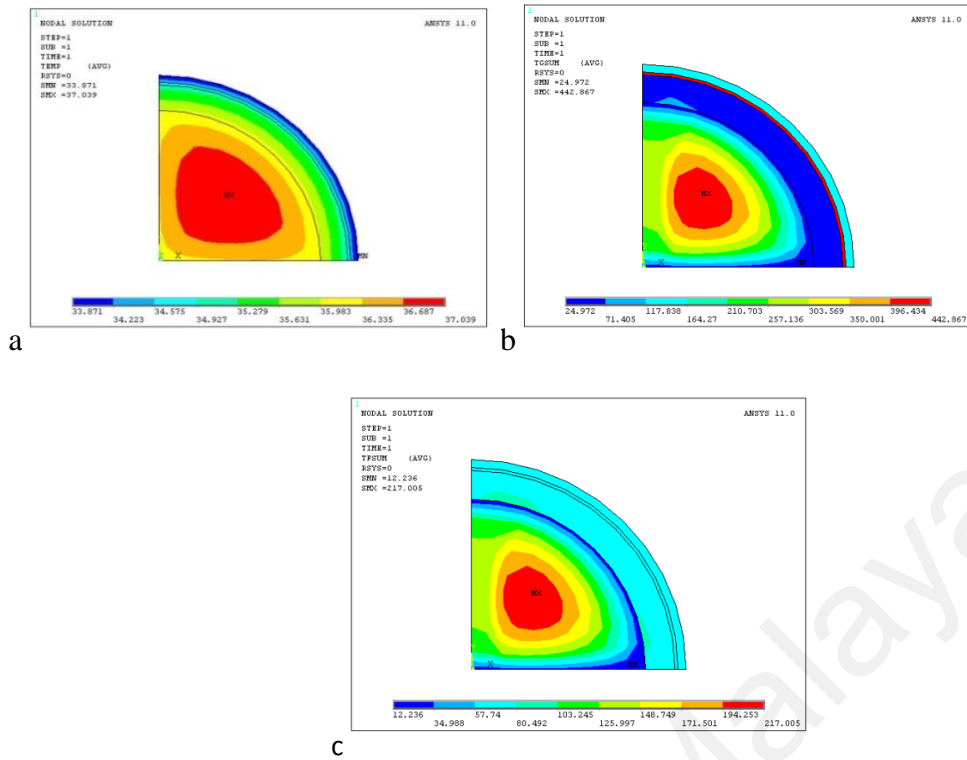


Figure 4.17: a) nodal temperature b) thermal gradient c) thermal flux for skin layer thickness of 0.4 cm

### 4.3.2 Effect of Fat layer thickness

The effect of fat layer thickness is illustrated in figures 4.17 to figure 4.19. The fat layer thickness is varied in steps of 0.05 cm, 0.25 cm and 0.35 cm. Figure 4.18a depicts the temperature distribution in various layers of the human head from  $34.50^{\circ}\text{C}$  to  $37.03^{\circ}\text{C}$  when the fat layer thickness is reduced from normal thickness 0.15cm to 0.05cm. It can be clearly seen from the figure that a constant temperature has been maintained at the center of the brain around  $37.03^{\circ}\text{C}$  which gradually decreases to the lowest at the skin layer (i.e.  $34.50^{\circ}\text{C}$ ). It is also observed that bone layer has temperature variation from  $34.78^{\circ}\text{C}$  to  $36.19^{\circ}\text{C}$ . And lowest temperature was observed on skin tissue (i.e.  $34.50^{\circ}\text{C}$ ).

The figure 4.18b represents the distribution of thermal gradient in various layers of human head when the fat layer thickness is reduced from normal thickness 0.15cm to

0.05cm. It is found that the region at the center of the brain and the fat layer has a highest thermal gradient (ie  $455.69\text{ }^{\circ}\text{C/m}$ ) which shows the greatest heat transfer from these regions. And also observed that bone layer has the lowest (ie  $25.14\text{ }^{\circ}\text{C/m}$ ) thermal gradient which indicates the lowest heat loss takes place in bone tissue layer. The skin layer has the thermal gradient around  $120.81\text{ }^{\circ}\text{C/m}$ .

The figure 4.18c shows the distribution of thermal flux in various layers of human head when the fat layer thickness is reduced from normal thickness 0.15cm to 0.05 cm. It can be seen from the figure clearly that the center of the brain has largest thermal flux (i.e.  $216.91\text{ W/m}^2$ ) which gradually decreases to the lowest at the end of the brain layer (i.e.  $12.31\text{ W/m}^2$ ). and also observed that bone layer has a thermal variation in some areas from  $57.78\text{ W/m}^2$  to  $80.51\text{ W/m}^2$ . The fat and skin layers have the almost equal thermal flux around (i.e.  $57.78\text{ W/m}^2$ ).

It is found from figure 4.18 to figure 4.20 that the skin temperature reduced by  $1.05\text{ }^{\circ}\text{C}$  when fat thickness is increased from 0.05 cm to 0.35 cm. Thus it can be said that the fat layer thickness plays a dominant role as compared to skin layer thickness in controlling the skin temperature when all other such as environmental, physical parameters are kept constant. This happens because fat has very low thermal conductivity that makes it to act as an insulator between inner and outer layers of human head.

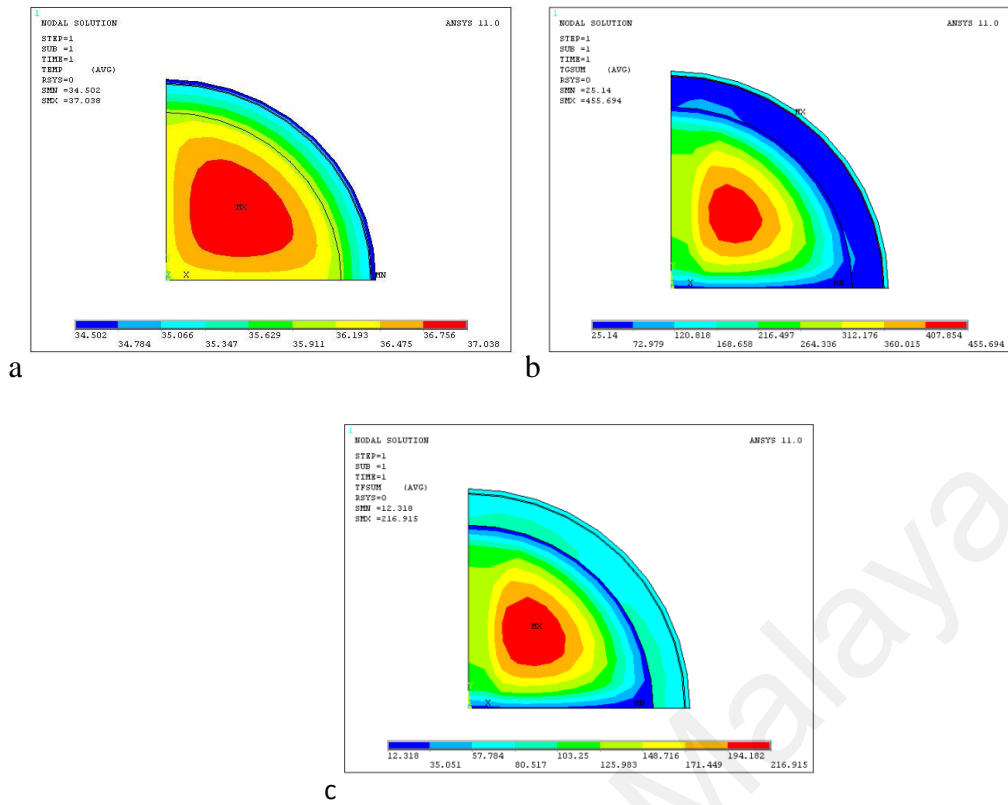


Figure 4.18: a) nodal temperature b) thermal gradient c) thermal flux, fat layer thickness of 0.05cm

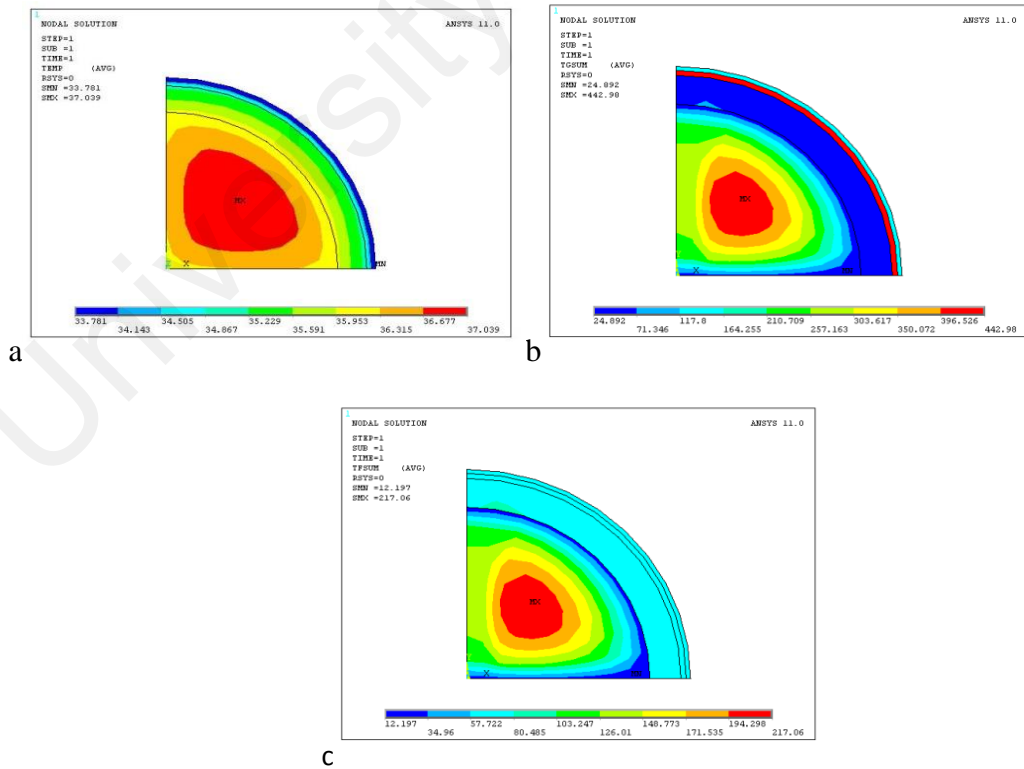


Figure 4.19: a) nodal temperature b) thermal gradient c) thermal flux, fat layer thickness of 0.25cm

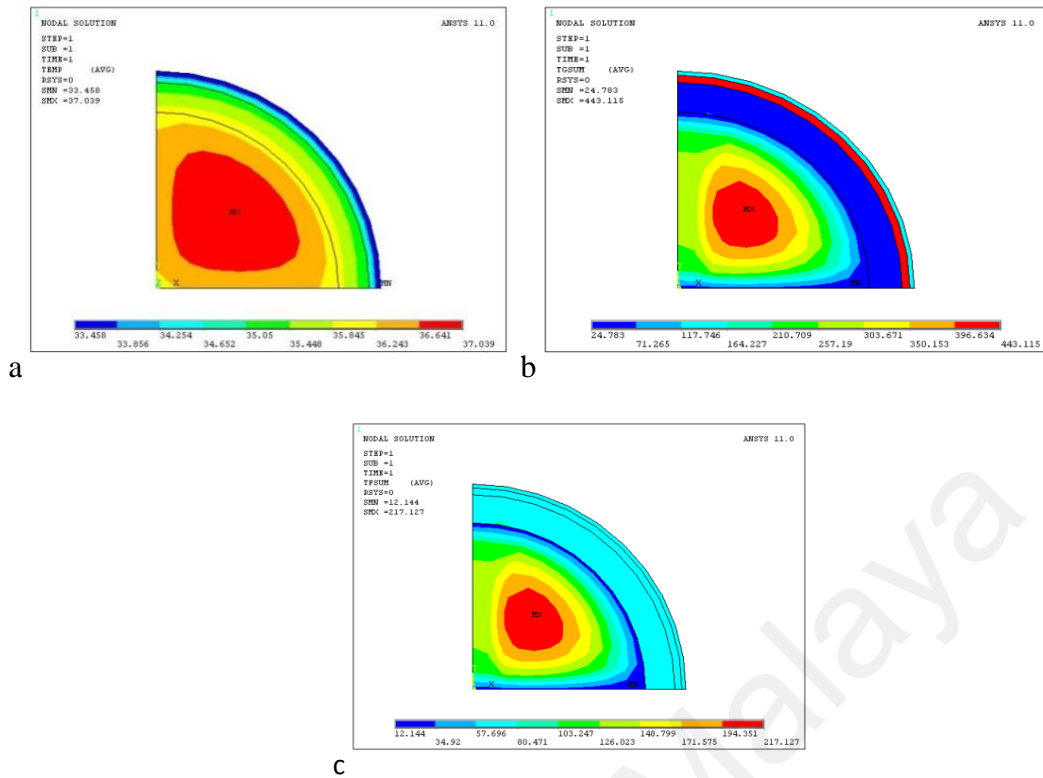


Figure 4.20: a) nodal temperature b) thermal gradient c) thermal flux, fat layer thickness of 0.35cm

### 4.3.3 Effect of bone layer thickness.

Figure 4.21 to figure 4.24 illustrate the impact of bone layer thickness on heat transfer behavior of human head. The bone layer thickness is varied in steps of 0.4 cm, 0.9 cm, 1.4 cm and 1.9 cm. it is to be noted that these dimension are obtained by selecting the bone radius as 9cm which when subtracted from brain radius of 8.6 cm results into 0.4 cm of bone thickness. Likewise, the other two bone layer radius is 9.5 cm and 10.5 cm respectively. Skin temperature decreased from  $34.76^{\circ}\text{C}$  to  $34.46^{\circ}\text{C}$  when bone thickness increased to 1.9cm. The thermal gradient increased from  $24.82^{\circ}\text{C/m}$  to  $25.36^{\circ}\text{C/m}$  when bone thickness is increased from 0.4 cm to 1.9 cm. the increase in bone thickness brings in similarity in heat flux profile of bone, fat and skin layer as shown in figure 4.24. The influence of bone thickness on skin temperature is lesser compared to that of fat layer thickness.

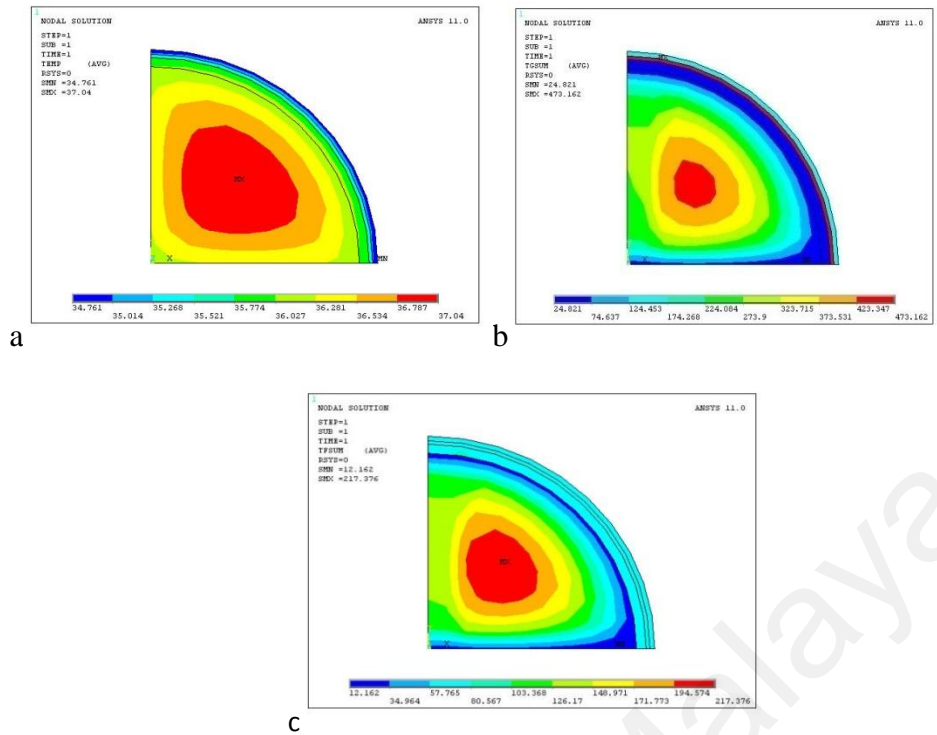


Figure 4.21: a) nodal temperature b) thermal gradient c) thermal flux, bone layer thickness of 0.4 cm

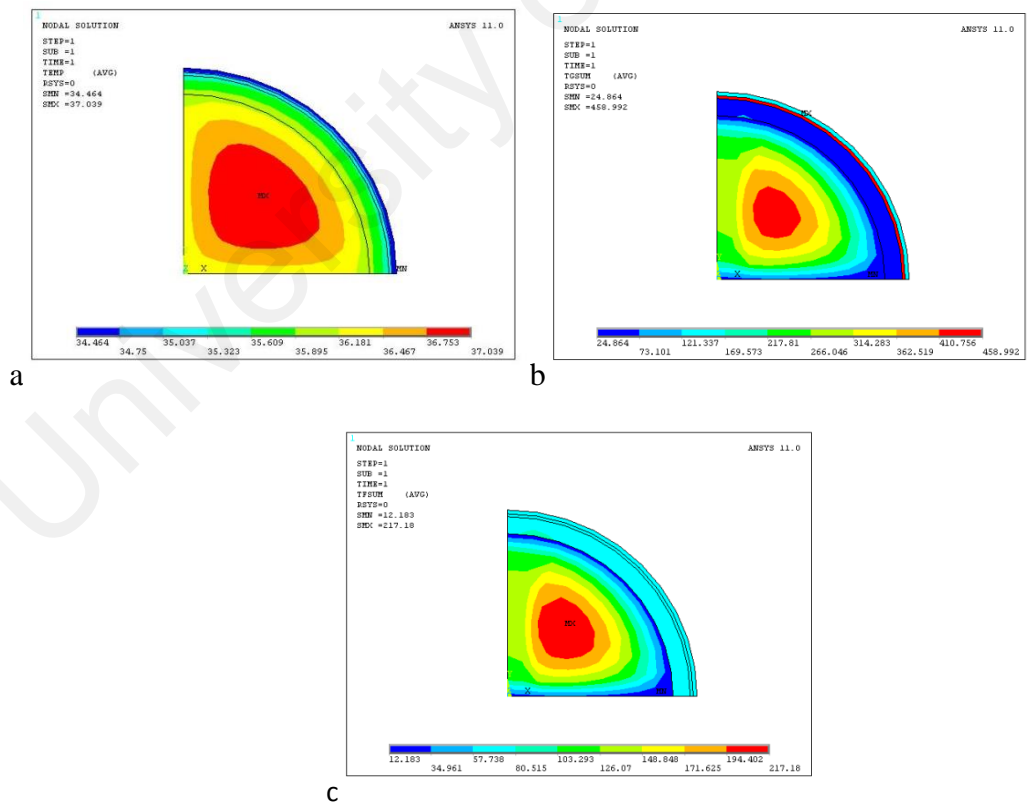


Figure 4.22: a) nodal temperature b) thermal gradient c) thermal flux, bone layer thickness of 0.9 cm

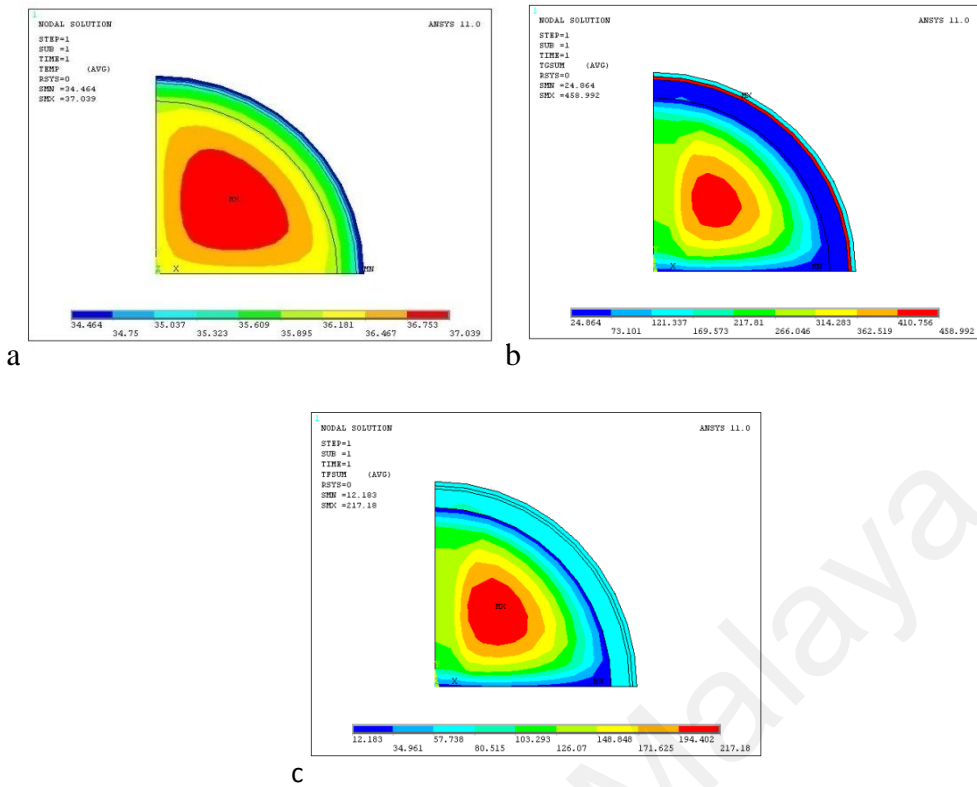


Figure 4.23: a) nodal temperature b) thermal gradient c) thermal flux, bone layer thickness of 1.4 cm

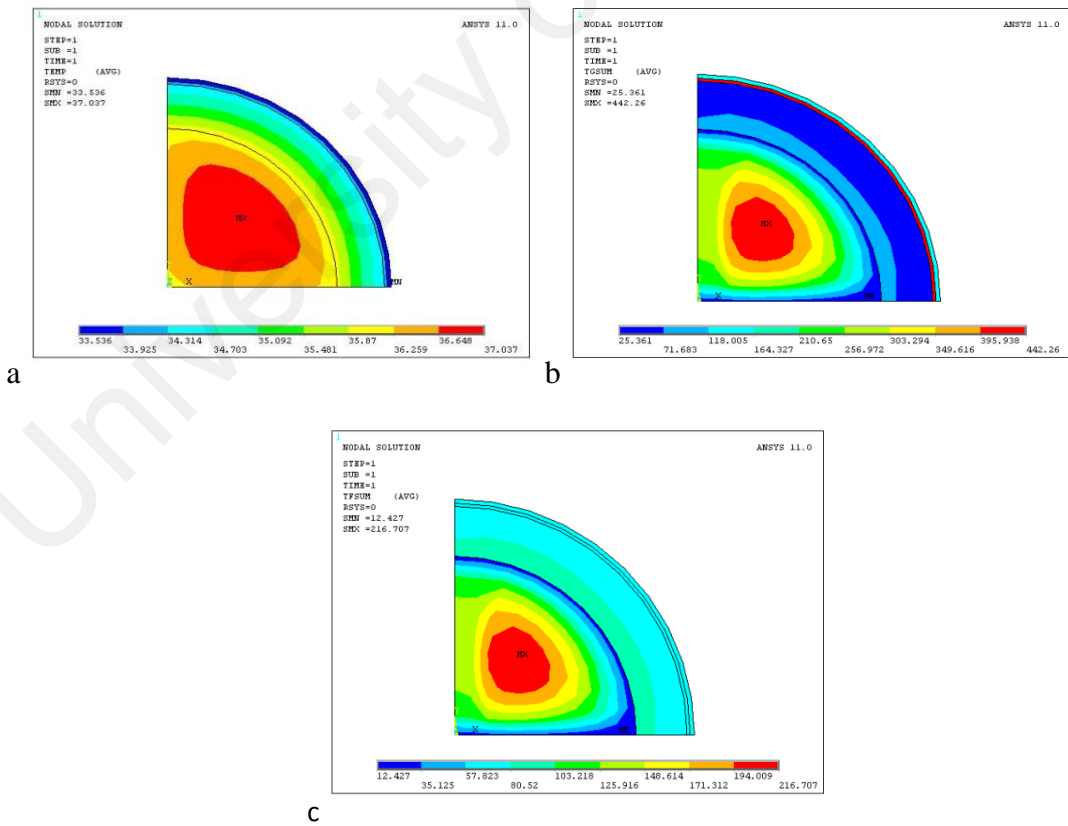


Figure 4.24: a) nodal temperature b) thermal gradient c) thermal flux, bone layer thickness of 1.9 cm

#### 4.4 Effect of hair on heat transfer

The presence of hair on human head may influence the heat transfer characteristics across human head. Thus an attempt is made to investigate the effect of hair on human head heat transfer behavior. Since the hair is generally symmetrically located above the forehead, a half section of head is modeled to evaluate the presence of hairs. Since hair are present infinite number with air gap in between themselves, an average thermal conductivity of hair and air is considered for this layer which comes out to be  $0.1 \text{ W/m}^{\circ\text{C}}$ . The length of hair is modeled as 1cm above the skin layer. The effect of hair is studied for 3 different values of ambient temperature such as  $20^{\circ\text{C}}$ ,  $25^{\circ\text{C}}$  and  $35^{\circ\text{C}}$ . The presence of hair alters the temperature contours across the human head as depicted in fig.4.25.

The figure 4.25a depicts the temperature distribution from  $37.44^{\circ\text{C}}$  to  $31.87^{\circ\text{C}}$  in different layers of the human head with the inclusion of hair for the surrounding temperature at  $30^{\circ\text{C}}$ . The heat transfer coefficient (convective and radiative) taken for this particular analysis is  $8.25 \text{ W/m}^2^{\circ\text{C}}$ , whereas the blood temperature is maintained at  $36^{\circ\text{C}}$ . The perfusion effect of blood was assumed to be  $235 \text{ W/m}^2^{\circ\text{C}}$ . Because of the heat generation factor the maximum temperature at the center of the head reaches slightly higher (i.e  $37.44^{\circ\text{C}}$ ) than the blood temperature. Due to the temperature gradient the temperature varies from the blood present in the innermost layer of the brain to the outermost skin layer. This is due to the effect of blood perfusion and convective and conductive heat transfer. It can be observed clearly from the figure 4.25a that the temperature gradually decreases along the different layers of the head indicating the uniform distribution along the inner to outer layer of the head. The brain has maintained a constant temperature in the innermost layer brain. It is evident from the figure that the heat transfer takes place gradually towards the outer surface of the head and from skin

surface to environment through hair indicating the flow of the heat from hottest region to the coolest region of the head thus obeying the basic heat transfer rules.

The figures 4.25 b describes the thermal gradients in the different layers of human head at the environmental temperature of  $30^{\circ}\text{C}$ . It is clearly seen from the figure that thermal gradient in the innermost section brain is  $662.2^{\circ}\text{C/m}$  the highest compared to the other sections which shows the heat loss is more from the brain and decreases gradually from the center to the end of the brain tissue to the lowest. And also observed that the thermal gradient in bone and only below the skin layer has lowest, indicating the lowest heat loss taking place in these areas. The skin layer has the thermal gradients around  $79.87^{\circ}\text{C/m}$ . The hair layers has the thermal gradient around  $298.2^{\circ}\text{C/m}$ , which shows the loss of heat takes place is more compared to the bone and skin layers in the model.

The figure 4.25c represents the thermal flux in the different tissue layers of human head when the surrounding temperature was  $30^{\circ}\text{C}$ . It can be seen from the figure clearly that an elliptical region of the brain tissue has a largest thermal flux (i.e.  $324.4\text{ W/m}^2$ ) at the deep center of the brain. The figure also shows that the maximum thermal flux from the center of the brain gradually decreases to the lowest at the end of the brain. The other layers bone, fat, skin and hair has the lowest thermal flux (i.e.  $8.21\text{ W/m}^2$ ), which means that the heat loss is lowest from these layers compared to the brain layer.

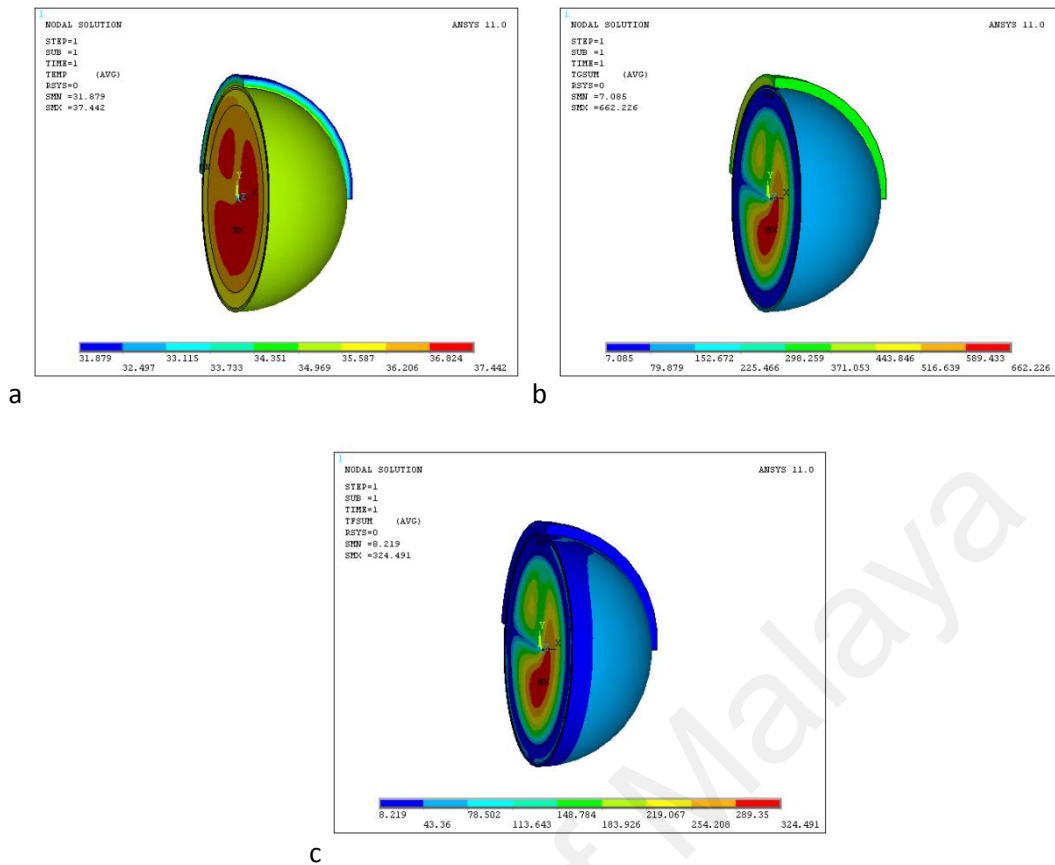


Figure 4.25: Human head model with hair a) nodal temperature at 30°C b) thermal gradient at 30°C c) thermal Flux at 30°C

Figure 4.26a, b, c and d shows the variation of temperature in the different layers of human head when the surrounding temperature was maintained at 20°C, 25°C, 35°C, and 40°C respectively. The 'figure 4.26a' depicts the variation of temperature in the different tissue layers of the human head model for the surrounding temperature was maintained at 20°C. It can be observed from the figure that the inner most brain layer has maintained a constant temperature in the cool environment which is required for the functioning of the internal organs. It is also seen that the temperature gradually decreases along the various layers from the brain to the hair layer. The figure also shows that skin has temperature around 31°C whereas the lowest temperature was seen in the hair layer with the variation in temperature from 24.6°C to 33.1°C. The bone layer also shows a variation of temperature almost 2°C.

Figure 4.26b' represents the variation of temperature in the different tissue layers of the human head model for the surrounding temperature maintained at 25<sup>0</sup>C. It can be seen clearly from the 'figure 4.26b' that a constant temperature was maintained in the brain layer when the ambient temperature increased 25<sup>0</sup>C. It is also observed that by comparing with the figure 4.25a, with increase in the ambient temperature skin temperature also increased. It is seen that the temperature is gradually decreases along the different tissue layers form brain to the hair layer. The 'figure 4.26b' also shows that skin has temperature around 33.3<sup>0</sup>C, whereas the lowest temperature was seen in the hair layer with the significant variation in temperature from 33.3<sup>0</sup>C to 28.2<sup>0</sup>C.

The 'figure 4.26c' depicts the distribution of temperature in various tissue layers of the human head model for the environmental temperature of 35<sup>0</sup>C. It can be seen clearly from the 'figure 4.26c' that the brain tissue has varying temperature across the layer as compared to almost constant temperature when ambient temperature is 25<sup>0</sup>C and 30<sup>0</sup>C . The temperature is gradually decreasing along the different tissue layers form the brain to the hair layer. The 'figure 4.26c' also shows that skin layer on face has temperature variation from 36.1<sup>0</sup>C to 36.7<sup>0</sup>C, whereas the lowest temperature was seen in the hair layer with the significant variation from 36.1<sup>0</sup>C to 35.4<sup>0</sup>C.

The 'figure 4.26d' indicates the variation of temperature in the different tissue layers of the human head model when the surrounding temperature was maintained at 40<sup>0</sup>C. It is also seen that the temperature is gradually increases along the different tissue layers form the brain to the hair layer. The 'figure d' also shows that skin has temperature around 37.5<sup>0</sup>C whereas the highest temperature was seen in the hair layer with the significant variation in temperature from 36.9<sup>0</sup>C to 39<sup>0</sup>C.

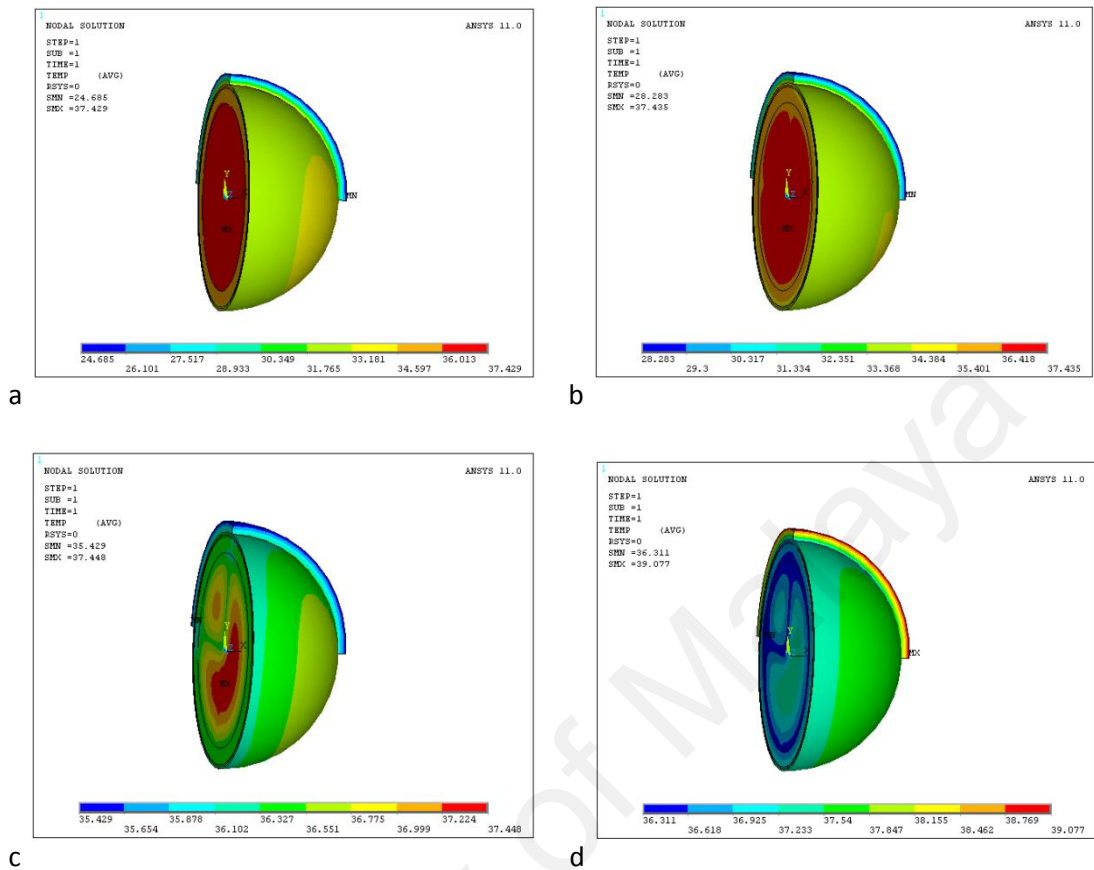


Figure 4.26: variation of temperature for ambient a) 20<sup>0</sup>C b) 25<sup>0</sup>C c) 35<sup>0</sup>C d) 40<sup>0</sup>C

Figure 4.27 illustrates the variation of temperature in radial direction of human head taking into account the effect of presence of hair. It is obvious from this figure that the temperature variation along the brain tissue is very small as compared to other layers. It is also observed that the brain temperature variation shows nonlinear behavior whereas the temperature varies linearly across other layers. Sharp variation of temperature is found across the hair layer. It is seen that the heat transfers from head to environment for ambient temperature less than 35<sup>0</sup>C and thereafter it starts reversing the process. This should force the brain to lower its activity level to reduce the heat generation inside the head thus making the human feel tired at higher ambient temperature.

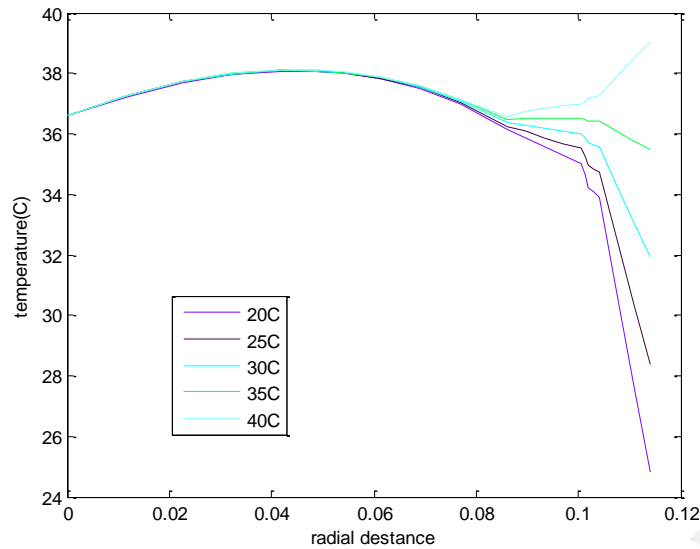


Figure 4.27: Temperature variation across the radial direction in human head with hair.

#### 4.5 Investigation of high temperature environment

It is known that the environment could pose some serious issues with respect to heat transfer in human body when the outside temperature reaches to a significantly higher temperature. These kinds of situations are found in numerous work places. One such situation is found in Malaysia and the car is parked in sunlight for few hours in day light. Malaysia is a country which falls within the equatorial region of the earth thus receives substantial sunlight and the weather is generally hot. It is one of the common problem in Malaysia that the inside space of car accumulates significant amount of heat when parked in sunshine thus elevating its temperature to more than 60<sup>0</sup>C on many occasions. Under such circumstances, the commuters start the air conditioner for few minutes to allow it to cool down to acceptable temperature before entering inside the car. The situation becomes worse when the person wants to drive the car immediately due to any urgency and it becomes even worse if the air conditioner is malfunctioning. Under such circumstances, if someone drives the car without allowing to cool then it

can pose severe problems to human body. In this study, an attempt is made to investigate the heat transfer into the human head when a person enters the car without allowing it to cool sufficiently. The simulation was carried out with inside temperature of car being elevated to 60<sup>0</sup>C. The study was carried out by experimentally determining the temperature of a car which was parked under sunlight for 9 hours from 8 am until 5 pm in the open area directly exposed to solar heat. An infrared thermal image camera was used to find the temperature at various locations such as driver seat, steering, back seat etc. Figures 4.28 to 4.30 show the temperature distribution inside the car space. It is obvious from these figures that the temperature at various locations can range from 30 deg C to 75 deg C depending upon the hour of the day. The temperature of car increases until around 2 pm and then starts declining. The maximum temperature observed at selected points was 75.1<sup>0</sup>C as shown in figure 4.29. The temperature at human face is measured after 60 seconds of sitting inside the car as illustrated in fig 4.30b. It is found that the skin temperature at face is raised to 36.7 deg C in just 1 minute of stay in the car. It be noted that the readings were taken for just 1 minute and further sitting in the car was avoided due to health reasons.

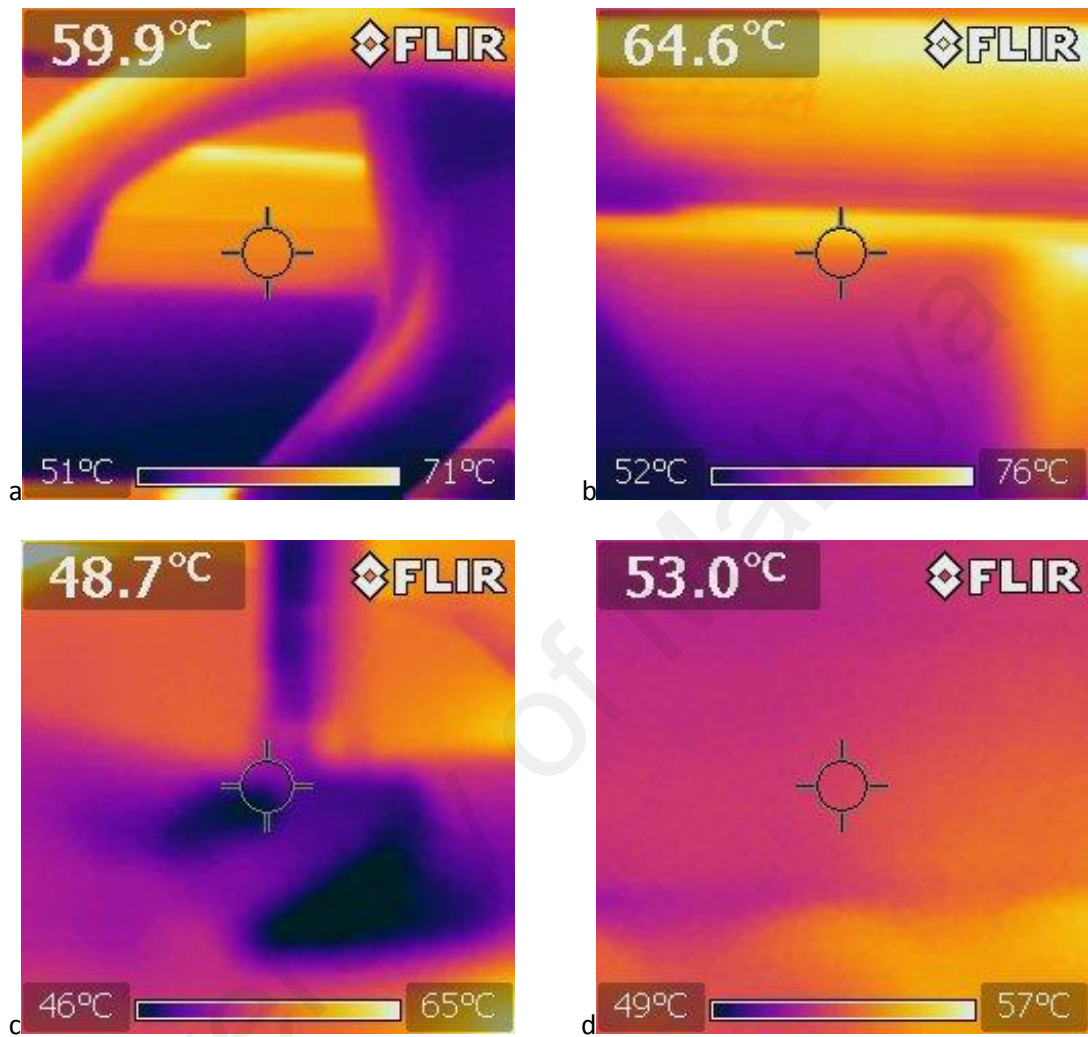


Figure 4.28: Temperatures recorded at 11 am a) Steering b) Dashboard c) driver seat d) back right seat

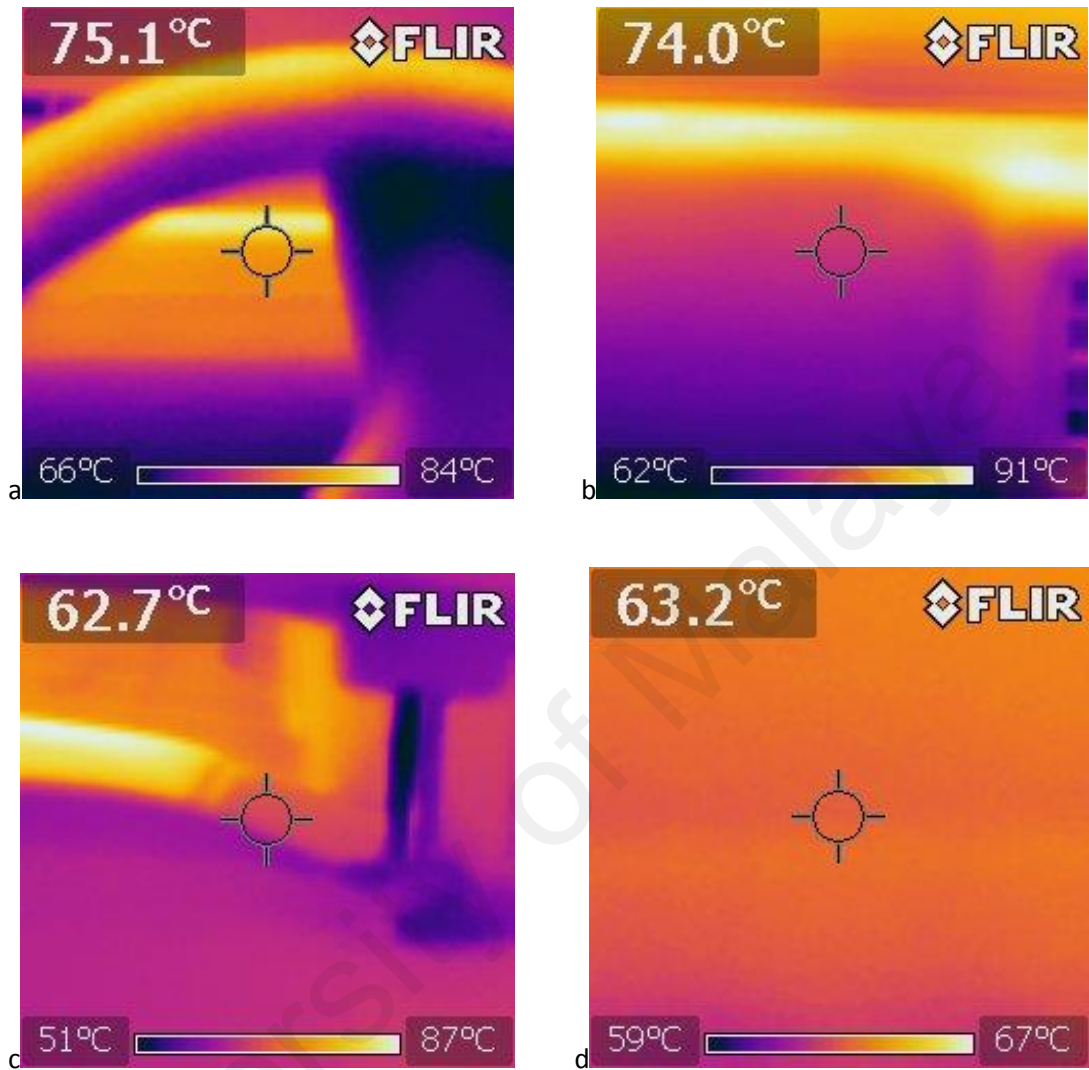


Figure 4.29: Temperatures recorded at 1pm a) Steering b) Dashboard c) driver seat d) back right seat

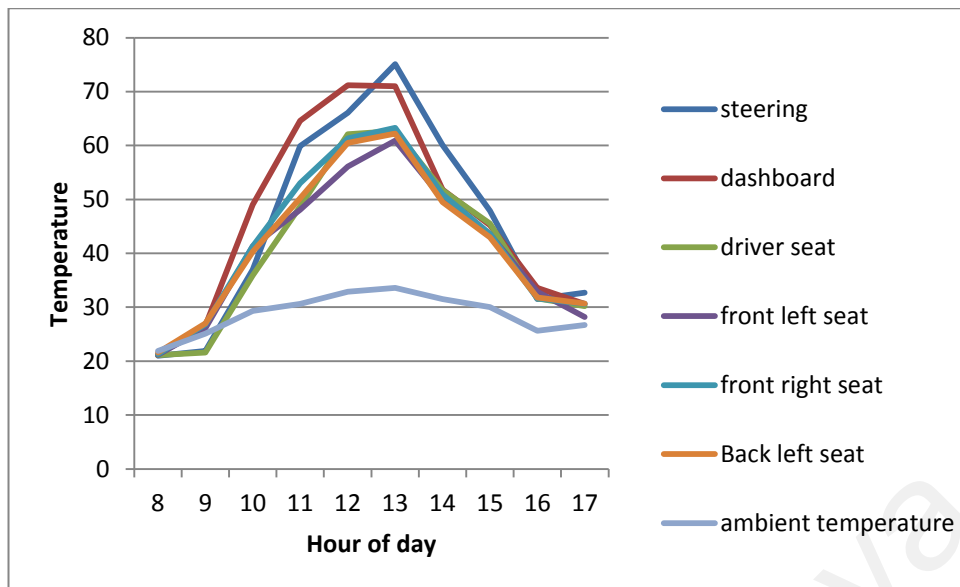


Figure 4.30a: Temperature variation during hours of the day

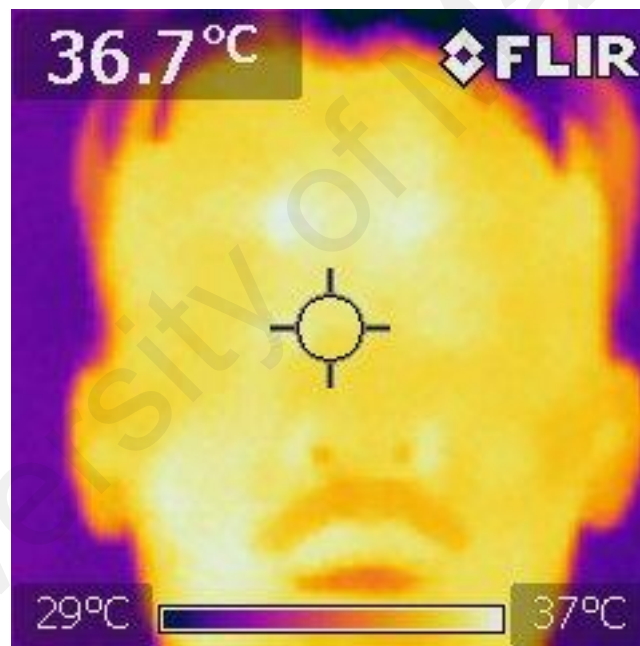


Figure 4.30 b: Temperature at face after 60 seconds inside the car

In the 2<sup>nd</sup> step, a simulation was carried out to investigate the transient behavior of human head when a person enters the car being elevated to 60 deg C. It was decided to simulate the heat transfer behavior of human head by taking 60 deg C as the prevailing temperature that closely resembles the temperature at the seats of the car. In this case the head dimensions are taken as that of a normal person given in table 1. The

simulation was carried out for 1800s that corresponds to 30 min. The initial conditions of temperature are obtained by setting the steady state analysis for normal environmental conditions corresponding to 30 deg C and then using this steady state solution as the initial condition for transient analysis. This ensures that the person enters the car with temperature distribution corresponding to 30 deg C environmental conditions.

Figure 4.31 and 4.32 shows the temperature variation across the different layers of head with respect to the change in time. The temperature was plotted at 7 locations in head such as top of the skin, skin-fat interface, centre of fat, fat-bone interface, bone-brain interface, just beneath the bone and at about 4.3 cm from the center of brain that represents the center point of bone and center of spherical head. It is observed that the temperature at most of the places increases exponentially with respect to time. The maximum temperature was found on the skin surface which is directly exposed to hot conditions. Its temperature rises to 41.75 deg C in 30 min that could produce some disastrous effects on the skin. The rise in temperature is very sharp for the first 10 minutes of entry into car and it reaches almost 40.5 deg C and then the subsequent rise in temperature is gradual. The rise of temperature below the bone layer is not as savior as that of above the bone layer. It can be attributed to the strong capability of bone to act as a barrier to heat flowing from outside environment thus protecting the brain tissue which is the most important part of the human body. Thus it can be said that the bone layer acts as a cushion to protect the brain tissue from structural as well as thermal loads. It is noticed that the deep brain temperature is not much affected due to exposure of such adverse environment as the deep brain temperature remains within the acceptable range for avoiding the damage to brain tissue.

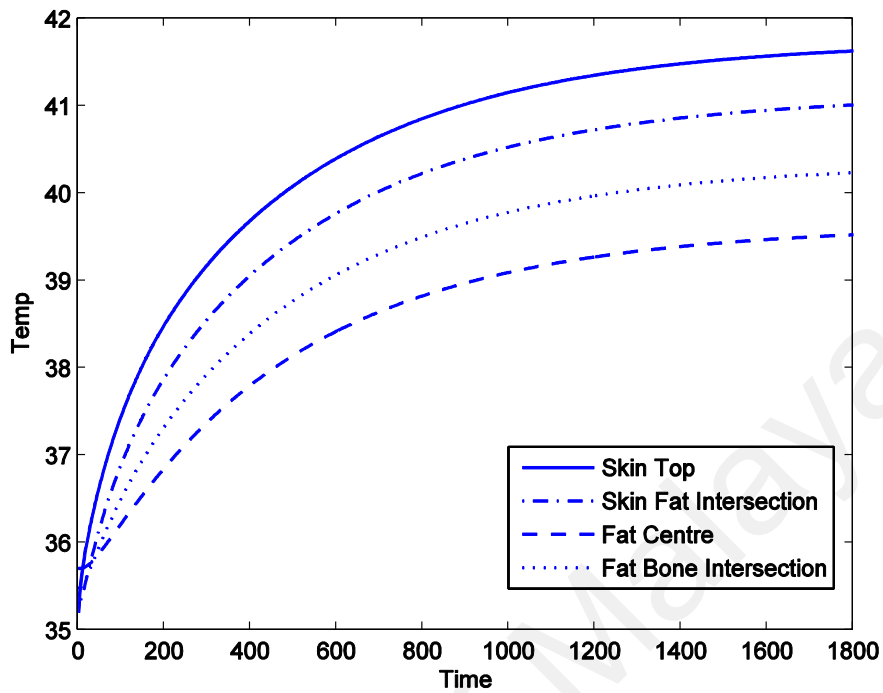


Figure 4.31: Temperature variation in above bone with time

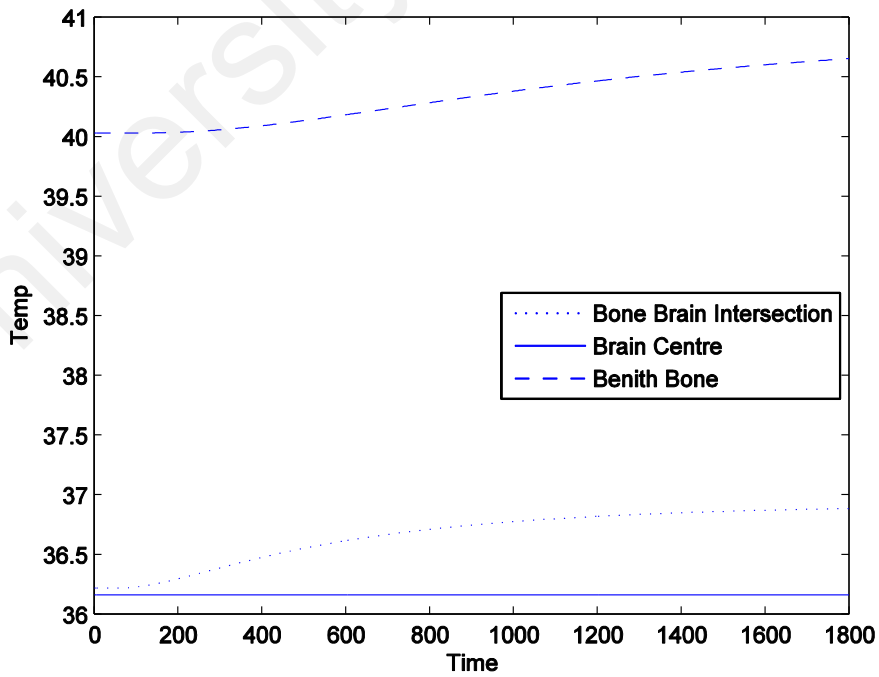


Figure 4.32: Temperature variation in below bone with time

#### **4.6 Effect cooling helmet during hyperthermia**

It is common to see that the human body is subjected to various types of bacterial and viral attacks that are counter attacked by the human body to protect itself. In this process, the body parts increase the activity level and thus generate lot of heat. The other situations where the body temperature could be elevated is those of hyperthermia condition. Hyperthermia is a condition in which the body temperature is elevated due to failed thermoregulation that occurs when a body produces or absorbs more heat than it dissipates. Extreme temperature elevation of body becomes a medical emergency requiring immediate treatment to prevent permanent damage to body organs or it may even lead to death. Some of the known causes of hyperthermia are heat stroke and adverse reactions to drugs. The former is an acute hyperthermia caused by exposure to excessive heat, or combination of heat and humidity, that overwhelms the heat-regulating mechanisms of the body causing uncontrollable elevation of body temperature. The latter is a relatively rare side effect of many drugs, particularly those that affect the central nervous system. Malignant hyperthermia is a rare complication of some types of general anesthesia. Under the condition of hyperthermia, it is extremely important to attend the patient immediately and start treatment. The far-away locations of medical center poses danger of putting the patient into immense risk since the temperature should be brought down immediately. The human head can be cooled by some of the conventional methods like putting the wet cloth on forehead to absorb the heat. This method though takes away little bit of heat but still not very effective when the temperature of head is elevated to dangerous level. Under such circumstances, other techniques are to be employed. The current study investigates the effect of using a helmet filled with coolant at low temperature wrapped across the human head. In this

study, it is assumed that the half of the head is wrapped with a helmet filled with ice. The helmet could be assumed to be similar to that of used for motor bike riding with only exception that it is filled with ice. The model of human head along with the helmet is shown in figure 4.33. The parrot color section (the upper most layer) shows the helmet above the hair layer which is shown in the light red color.

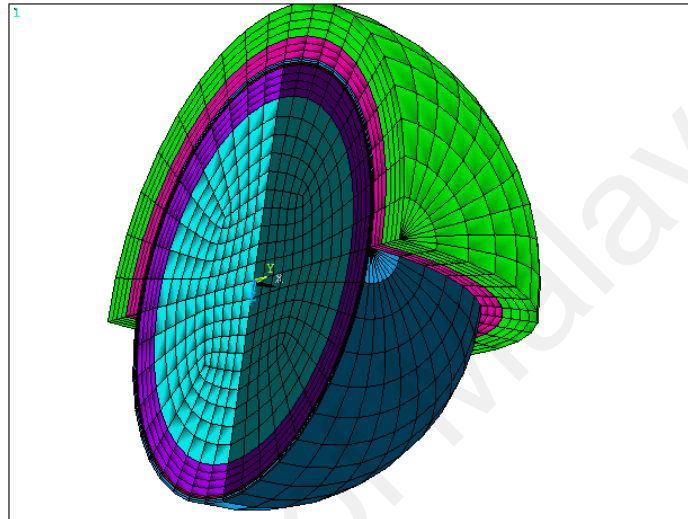


Figure 4.33: Human head wrapped with cooling helmet

The helmet is assumed to be made with a capacity to contain ice of 2 cm thick layer. The study is conducted to investigate the time required to bring the head temperature to acceptable range within a short period of time. The simulation is carried out to predict the transient behavior of helmet cooling technique. The head temperature is initially elevated to 40 deg C and then the helmet is brought into contact with the head.

Figure 4.34 shows the temperature after 3 second of helmet being brought into contact with head. It is obvious that a substantial portion of face is at maximum temperature of 39.75 deg C. Figure 4.35 shows the temperature variation after 30 seconds of cooling. It is seen that the head temperature drops to about 37.5 deg C after 10 seconds of cooling. It may be noted that the ice at 0 deg C has good potential to absorb the heat and the volume of ice contained in the helmet is substantial thus producing immediate effect on

the head temperature. Figure 4.36 shows the temperature variation after 60 seconds of cooling by helmet. It is seen that the temperature could be brought down to 36.91 deg C after 60 seconds.

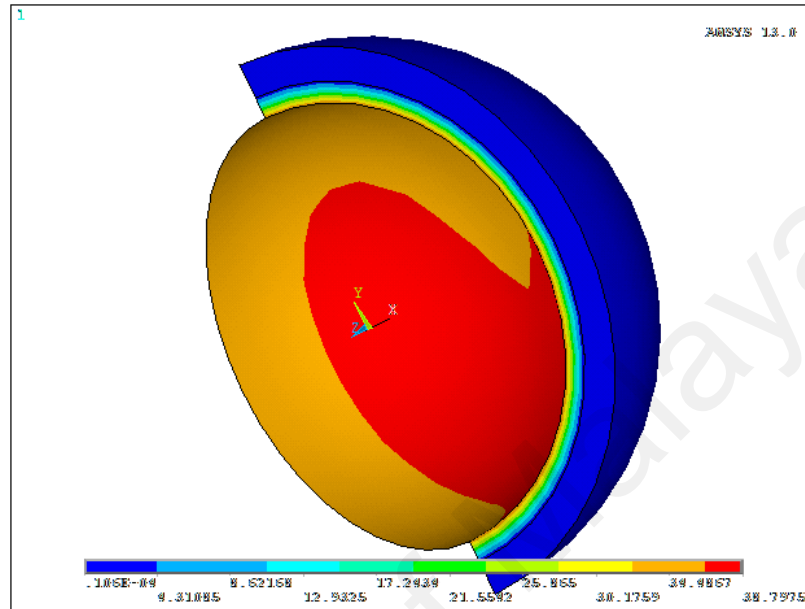


Figure 4.34: Temperature distribution after 3 seconds

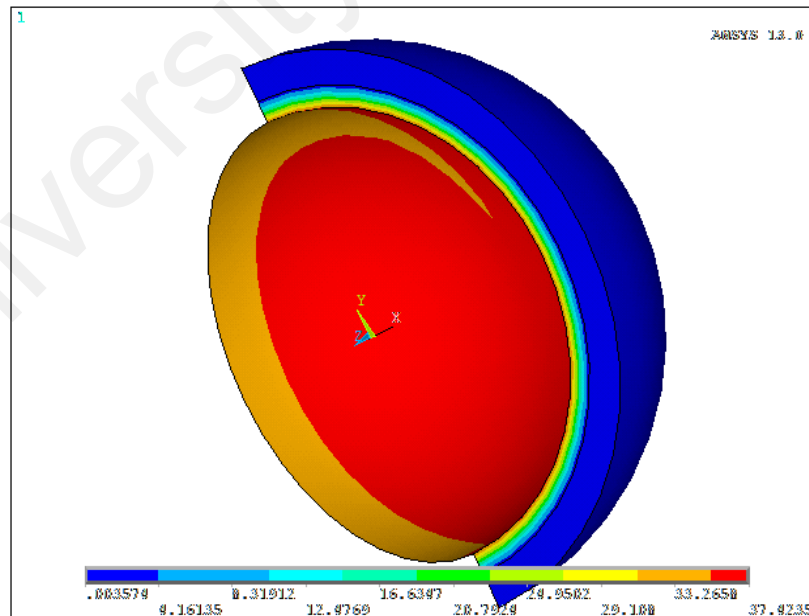


Figure 4.35: Temperature distribution after 30 seconds

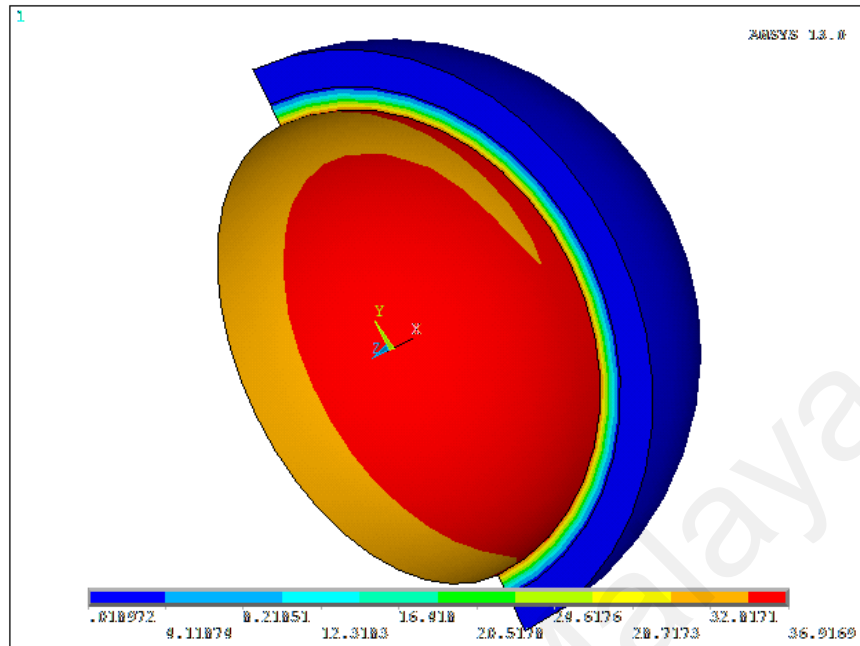


Figure 4.36: Temperature distribution after 60 seconds

Fig 4.37 to fig 4.40 illustrates the cooling after various time period. It is observed that the temperature distribution across the facial region homogenizes as the time of cooling increased. The face temperature after 1800 seconds which corresponds to 30 minutes comes down to around 22 deg C which is a bit lower side of desired temperature. By close examination of these figures one can say that the good time to cool the head is around 300 seconds which brings the temperature of head to around 30 deg C. After this period the helmet can be taken off from the head and the temperature to be observed closely. In case the temperature increases after taking off the helmet then cooling effect should be brought back by putting the helmet on head. This would contribute until the patient is brought into the observation of doctors. It is to be noted that the helmet cooling is required until the patient brought into hospital thus it can act as a first aid to prevent the severe damage to muscles due to extremely elevated temperature.

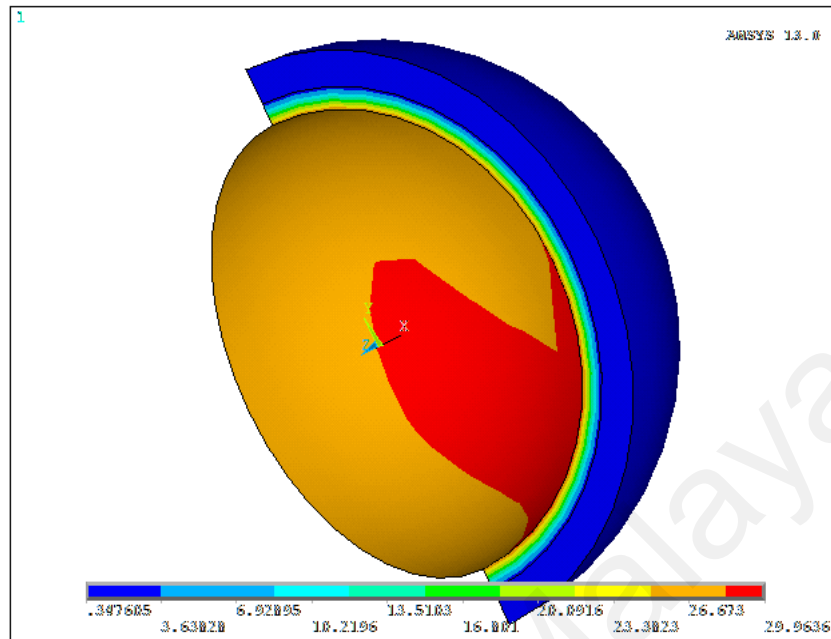


Figure 4.37: Temperature distribution after 300 seconds

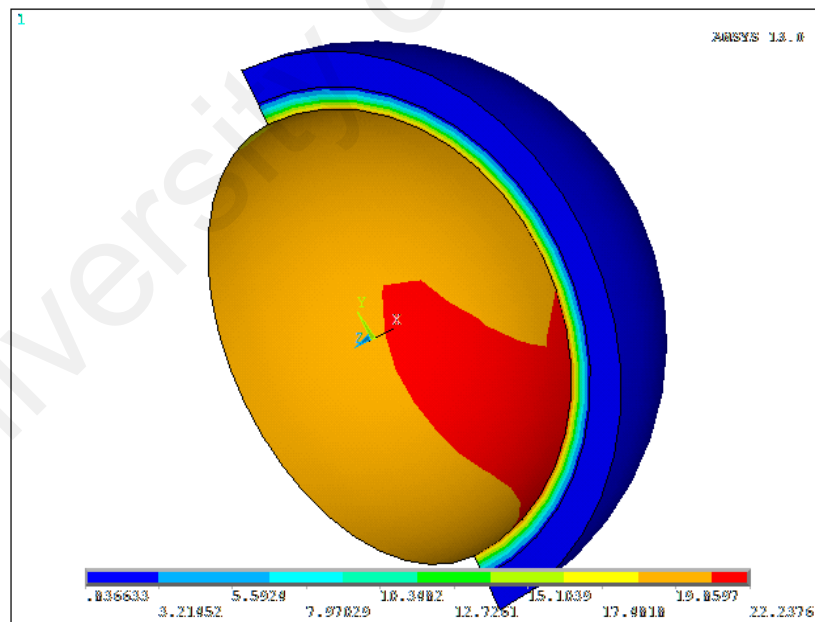


Figure 4.38: Temperature distribution after 600 seconds

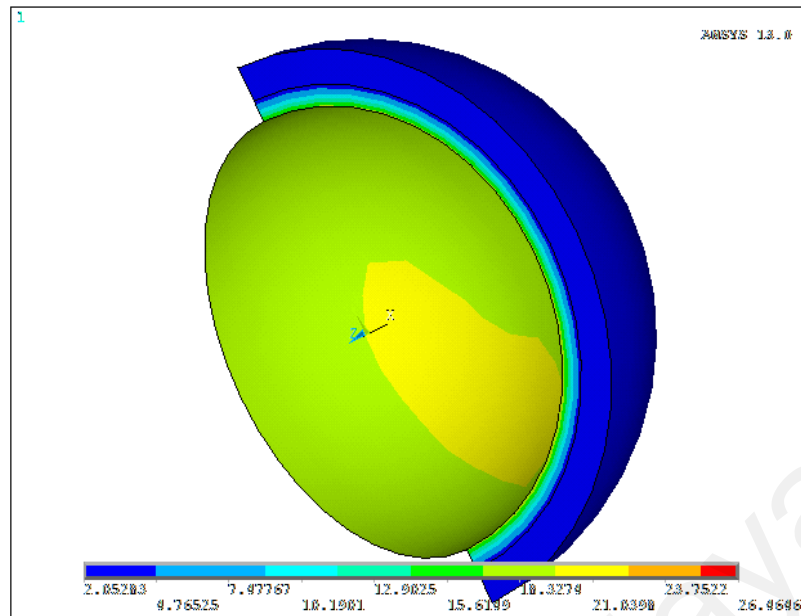


Figure 4.39: Temperature distribution after 1200 seconds

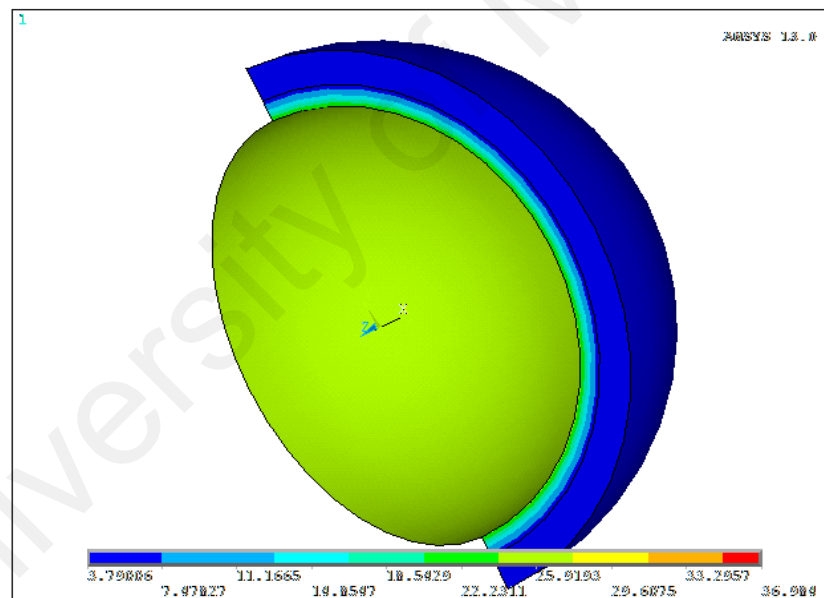


Figure 4.40: Temperature distribution after 1800 seconds

Figs 4.41a, b illustrates the temperature variations at particular points in the human head. It is observed that the helmet temperature increases continuously near the hair section with passage of time. The maximum temperature reached for helmet near the hair is around 4 deg C. The temperature at other sections of the head decreases initially until a point and then starts increasing thereafter. This is an interesting behavior that is

dictated by the properties of the cooling medium ice in this particular case. It can be said that the ice near the head absorbs heat and then starts melting. Due to change of phase, the heat absorption capacity of ice decreases that leads to increase the head temperature. The temperature around skin and fat decreases until around 900 seconds and then starts to increase. Thus it can be concluded that the ice should be replaced after 900 seconds of cooling process if the head temperature to be reduced further. The decrease of temperature at lower layers is faster than at the upper layers of the brain. This figure gives an idea until what time the helmet should be applied to reach a particular temperature level in the head.

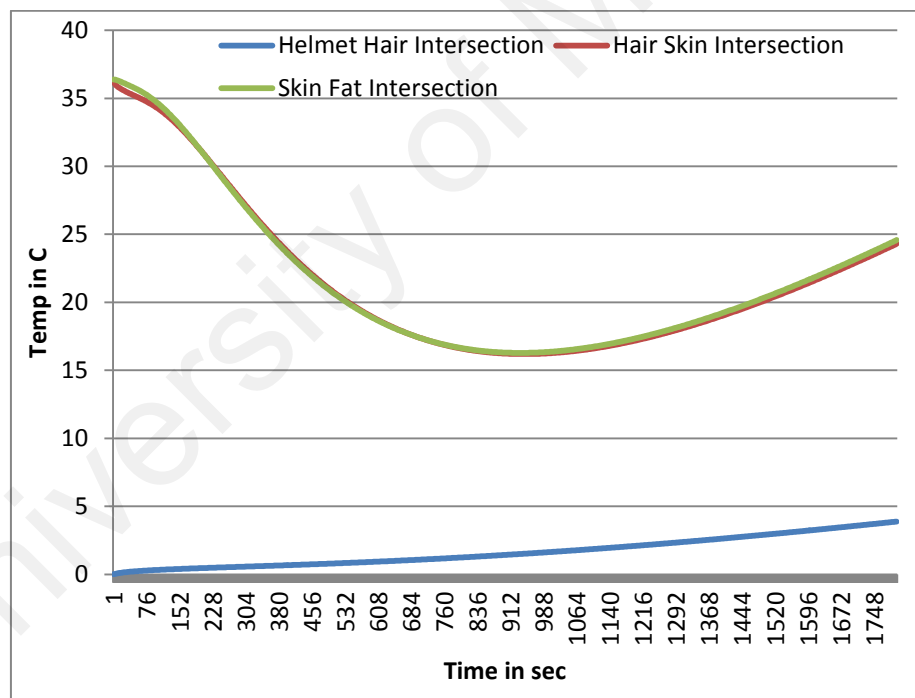


Figure 4.41a: Temperature variation with time at various points above fat layer in head

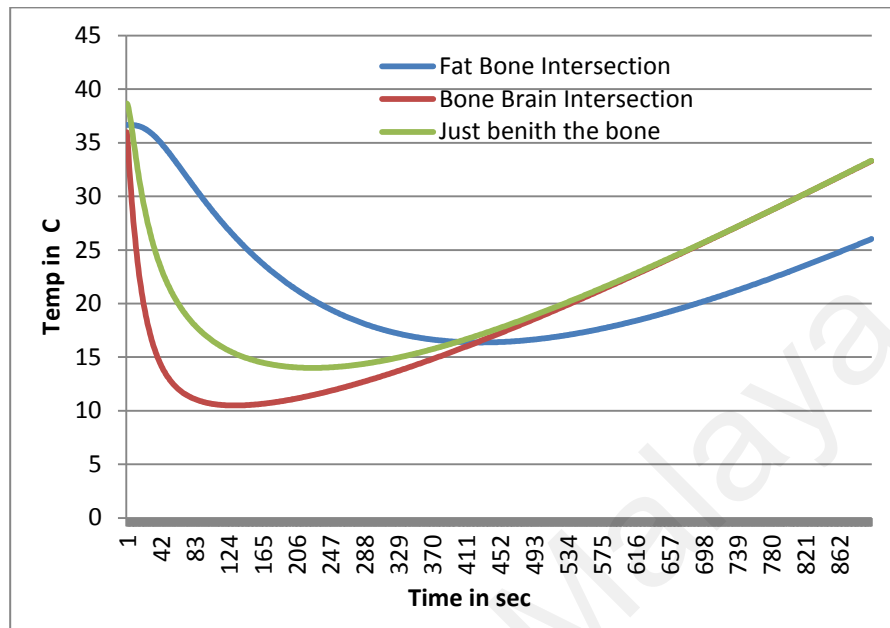


Figure 4.41b: Temperature variation with time at various points below fat layer in head

## CHAPTER 5

### 5.1 Conclusion

The current study is carried out to investigate the heat transfer behavior of human head under various environmental conditions. The study is conducted for 4 different cases such as, to

Analyze the effect of environmental conditions

Investigate the effect of thickness of different tissue layers of human head

Evaluate the heat transfer characteristics of head when exposed to sudden heated condition such as parked car

Study the cooling effect of ice helmet under severe fever condition

The following conclusions can be drawn from the study being conducted.

- It is seen that the brain temperature remains well within the controlled limit for a wide range of environmental parameters such as ambient temperature and convective heat transfer coefficient being considered in this study. For instance the temperature distribution ranges from  $37.03^{\circ}\text{C}$  to  $32.81^{\circ}\text{C}$  from brain to the skin layer when environment temperature is at  $20^{\circ}\text{C}$ .
- In general, it is seen that the skin temperature increases with increase in the ambient temperature but decreases with increase in the convective heat transfer coefficient which in turn indicates the increased wind velocity across the head. The bone and fat layers also showed decrease in the temperature with the increase in heat transfer coefficients.
- Thus it can be said that the increase in heat transfer coefficient which is strongly dependent on wind velocity is desirable to keep the skin temperature at acceptable range.

- It is observed that the skin temperature decreased from  $34.28^{\circ}\text{C}$  to  $33.87^{\circ}\text{C}$  when skin layer thickness is increased from 0.1 to 0.4 cm. It is found that the skin temperature reduced by  $1.05^{\circ}\text{C}$  when fat thickness is increased from 0.05 cm to 0.35 cm.
- Thus it can be said that the fat layer thickness plays dominant role as compared to skin layer thickness in controlling the skin temperature when all other such as environmental, physical parameters are kept constant. This happens because fat has very low thermal conductivity that makes it to act as an insulator between inner and outer layers of human head. The increase in bone layer thickness brings in similarity in heat flux profile of bone, fat and skin layer. The influence of bone thickness on skin temperature is lesser as compared to that of fat layer thickness.
- It is also observed that the brain temperature variation shows nonlinear behavior whereas the temperature varies linearly across other layers. Sharp variation of temperature is found across the hair layer.
- It is seen that the heat transfers from head to environment for ambient temperature less than  $35^{\circ}\text{C}$  and thereafter it starts reversing the process. This should force the brain to lower its activity level to reduce the heat generation inside the head thus making the human feel tired at higher ambient temperature.
- It is found that the temperature inside a car parked in open sunlight can raise upto  $75^{\circ}\text{C}$  or above in the Malaysian conditions.
- It is observed that the temperature at most of the places on human face inside the car at elevated temperature, increases exponentially with respect to time. The maximum temperature was found on the skin surface which is directly exposed to hot conditions. Its temperature rises to  $41.75^{\circ}\text{C}$  in 30 min that could produce some disastrous effects on the skin. The rise in temperature is very sharp for the

first 10 minute of entry into car and it reaches almost  $40.5^{\circ}\text{C}$  and then the subsequent rise in temperature is gradual. The rise of temperature below the bone layer is not as savior as that of above the bone layer.

- For the case of cooling of head under severe fever condition, the temperature distribution across the facial region homogenizes as the time of cooling increased. By close examination, it was found that the good time to cool the head is around 300 seconds which brings the temperature of head to around  $30^{\circ}\text{C}$ .

University of Malaya

## REFERENCES

- 1) Burton, A.C. *The application of the theory of heat flow to the study of energy metabolism*. Journal of Nutrition, 1934. **7**: p. 497-533.
- 2) Bazett, H. C. and McGlone, B. *Temperature gradients in the tissue in man*. Am. J. Physiol, 1927. **82**: p. 415-451.
- 3) Pennes, H. H. *Analysis of tissue and arterial blood temperatures in the resting human forearm*. J. Appl. Physiol, 1948**1**: p. 93–122.
- 4) Stolwijk, J. A. J. *A mathematical model of physiological temperature regulation in man*. Washington, DC: National Aeronautics and Space Administration, 1971 (NASA contractor report, NASA CR-1855).
- 5) Ferreira, M. S. and Yanagihara, J. I. *A transient three-dimensional heat transfer model of the human body*. International communications in Heat and Mass transfer, 2009. **36**(7): p.718-724.
- 6) Yildirim, E, D, and Ozerdem, B. *A numerical simulation study for human passive thermal system*. Energy and Buildings, 2008. **40**: p. 1117-1123.
- 7) Kilic, M. Kaynakli, O. and Yamankaradeniz, R. *Determination of required core temperature for thermal comfort with steady-state energy balance method*. International communication in Heat and Mass Transfer, 2006. **33**:p. 199-210.
- 8) Muhsin, k. and Gökhan S. *Modelling airflow, heat transfer and moisture transport around a Standing human body by computational fluid dynamics*. International communication in Heat and Mass Transfer, 2008. **35**: p.1159-1164.
- 9) Sørensen D. N. and Voigt, L. K. *Modelling flow and heat transfer around a seated human body by Computational fluid dynamics*. Building and Environment, 2003. **38** (6): p. 753-762.
- 10) Huizenga, C. Zhang, H. and Arens, E. *A model of human physiology and comfort for assessing complex thermal environments*. Building and Environment, 2001. **36**: p.691–699.
- 11) Murakami S, Zeng, J. and Hayashi T. *CFD analysis of wind environment around a human body*. Journal of Wind Engineering and Industrial Aerodynamics. 1999. **83**: p. 393–408.
- 12) Murakami S, Kato, S. and Zeng, J. *Combined simulation of airflow and moisture transport for heat release from a human body*, Building and Environment. 2000. **35**. p. 489-500.
- 13) Sevilgen, G and Kilic, M. *Numerical analysis of airflow, heat transfer, moisture transport and thermal comfort in a room heated by two panel radiators*. Building and Environment, 2011. **43**: p. 137-146.
- 14) Kang, Z. J. Xue, H. and Bong, T. Y. *Modeling of thermal environment and human response in a crowded space for tropical climate*. Building and Environment, 2001. **36**: p.511-525.
- 15) Miyanaga, T. Urabe, W and Nakano, Y. *Simplified human body model for evaluating thermal radiant environment in a radiant cooled space*. Building and Environment, 2001. **36**: p. 801-808.
- 16) Zolfaghari, A and Maerefat, M. *A new simplified thermoregulatory bio-heat model for evaluating thermal response of the human body to transient environments*. Building and Environment, 2010. **45**: p. 2068-2076.
- 17) Zolfaghari, A and Maerefat, M. *A new predictive index for evaluating both thermal sensation and thermal response of the human body*. Building and Environment, 2011. **46**: p.855-862.
- 18) Ring, J. W, de Dear R. *Temperature transients: A model for heat diffusion through the skin, thermo receptor response and thermal sensation*. Indoor Air 1991. **1**(4): p.448-56.

- 19) Al-Othmani, M. Ghadder, N. and Ghali, k. *A multi-segmented human bio-heat model for transient and asymmetric radiative environments*. International journal of Heat and Mass Transfer, 2008. **51**(23-24): p. 5522-5533.
- 20) Min, K. Son, Y. Kim, C. Lee, Y. and Hong, K. *Heat and moisture transfer from skin to environment through fabrics: A mathematical model*. International Journal of Heat and Mass Transfer, 2007. **50**: p. 5292-5304.
- 21) Fiala, D. Lomas, K. J. and Stohrer, M. *A computer model of human thermoregulation for a wide range of environmental conditions: the passive system*. Journal of Applied Physiology, 1999. **87**(5): p.1957–1972.
- 22) Atmaca, I. Kaynakli, O. and Yigit, A. *Effect of radiant temperature on thermal comfort*. Building and Environmet, 2007. **42**: p. 3210-3220.
- 23) Kaynakli, O. Unver, U and Kilic, M. *Evaluating thermal environments for sitting and standing posture*. International communication in Heat and Mass Transfer, 2003. **30** (8): p. 1179-1188.
- 24) Tanabe, S. Narita, C. Ozeki, Y and Konishi, *Effective radiation area of human body calculated by numerical simulation*, Energy and Buildings. 2000. **32**. p. 205-215.
- 25) Tanabe, S. Kobayashi, K. Nakano, J. Ozeki, Y and Konishi, M. *Evaluation of thermal comfort using combined multi-node thermoregulation (65MN) and radiation models and computational fluid dynamics (CFD)*. Energy and Buildings, 2002. **34**: p. 637-346.
- 26) Foda, E. Almesri, L. Awbi, H. B. and Siren, K. *Models of human thermoregulation and the predictions of local and overall thermal sensations*. Building and Environment, 2011. **46**: p. 2023-2032.
- 27) Karaa, S. Zhang, J. and Yang, F. *A numerical study of a 3D bioheat transfer problem with different spatial heating*, Mathematics and Computers in Simulation. 2005. **68**. p. 375-388.
- 28) Prek, M. *Thermodynamic analysis of human heat and mass transfer and their impact on thermal comfort*, International Journal of Heat and Mass Transfer. 2005. **48**. p. 731–739.
- 29) Prek, M. *Thermodynamic analysis of human thermal comfort*, Energy. 2006. **31**. p. 732-743.
- 30) Prek, M. and Butala, V. *Principles of exergy analysis of human heat and mass exchange with the indoor environment*, International Journal of Heat and Mass Transfer. 2010. **53**. p. 5806-5814.
- 31) Mady, C. E. K. Ferreira, M. S. Yanagihara, J. I. Saldiva, P. H. N. and de Oliveira Junior, S. *Modeling the exergy behavior of human body*, Energy. 2012. **45**. p. 546-553.
- 32) Wu, X. Zhao, J. Olesen, B. W. and Fang, L. *A novel human body exergy consumption formula to determine indoor thermal conditions for optimal human performance in office buildings*, Energy and Buildings. 2013. **56**. p. 48-55.
- 33) Nilsson, H. O. *Thermal comfort evaluation with virtual manikin method*, Building and Environments. 2007. **42**. P. 4000-4005.
- 34) Yi, L. Fengzhi, L. Yingxi, L and Zhongxuan, L. *An integrated model for simulating interactive thermal processes in human-clothing system*, Journal of Thermal Biology. 2004. **29**. p. 567-575.
- 35) Afrin, N. Zhang, Y. and Chen, J. K. *Thermal lagging in living biological tissue based on non-equilibrium heat transfer between tissue, arterial and venous blood*, International Journal of Heat and Mass Transfer. 2011. **54**. p. 2419-2426.
- 36) Dongmei, P. Mingyin, C. Shiming, D. and Minglu, Q. *A four-node thermoregulation model for predicting thermal physiological responses of a sleeping person*, Building and Environment. 2012. **52**. p. 88-97.

- 37) Salloum, M. Ghaddar, N. and Ghali, K. *A new transient bioheat model of the human body and its integratioto clothing models*, International Journal of Thermal Sciences. 2007. **46**.p. 371–384.
- 38) Wan, X. and Fan, J. *A transient thermal model of the human body–clothing–environment system*, Journal of Thermal Biology. 2008. **33**. p. 87–97.
- 39) Min, K. Son, Y. Kim, C. Lee, Y. and Hong, K. *Heat and moisture transfer from skin to environment through fabrics: A mathematical model*, International Journal of Heat and Mass Transfer. 2007. **50**. p. 5292–5304.
- 40) Wu, H. and Fan, J. *Study of heat and moisture transfer within multi-layer clothing assemblies consisting of different types of battings*, International Journal of Thermal Sciences. 2008. **47**. p. 641–647.
- 41) Xu, X. Tikuisis, P. Gonzalez, R. and Giesbrecht, G. *Thermoregulatory model for prediction of long-term cold exposure*, Computers in Biology and Medicine. 2005. **35**. p. 287-298.
- 42) Zhang, H. Huizenga, C. Arens, E. and Yu, T. *Considering individual physiological differences in a human thermal model*, Journal of Thermal Biology. 2001. **26**. p. 401-408.
- 43) Pardasani, K. R. and Adlakha, N. *Coaxial Circular Sector Element to Study Two-Dimensional Heat Distribution Problem in Dermal Regions of Human Limbs*, Mathl. Comput. Modelling. 1995. **22**(9). p. 127-140.
- 44) Agrwal, M. Adlakha, N and Pardasani, K. R *Three dimensional finite element model to study heat flow in dermal regions of elliptical and tapered shape human limbs*. Applied Mathematics and Computation, 2010. **217**: p. 4129-4140.
- 45) Ferreira, M. S and Yanagihara, J. I. *A heat transfer model of the human upper limbs*. International Communication in Heat and Mass Transfer, 2011. **39**: p.196-203.
- 46) Trobec, R. and Depolli, M. *Simulated temperature distribution of the proximal forearm*.Computers in Biology and Medicine, 2011. **4**(1): p. 971-979.
- 47) He, Y. Liu, H. Himeno, R. Sunaga, J. Kakusho, N. and Yokota, H. *Finite element analysis of blood flow and heat transfer in an image based human finger*. Computers in Biology and Medicine, 2008. **38**: p. 555-562.
- 48) Gan, Y. Cheng, L. Ding, X. and Pan, N. *Blood flow fluctuation underneath human forearm skin caused by local thermal stimuli of different fabrics*. Journal of Thermal Biology,2010. **35**: p. 372-37.
- 49) Upreti, S. R. and Jeje, A. A. *A noninvasive technique to determine peripheral blood flow and heat generation in a human limb*, Chemical Engineering Science, 2004. **59**: p. 4415-4423.
- 50) Zhang, H. D. He, Y. Wang, X. Shao, H. W. Mu, L. Z. and Zhang, J. *Dynamic infrared imaging for analysis of fingertip temperature after cold water stimulation and neurothermal modeling study*, Computers in Biology and Medicine. 2010. **40** p. 650-656.
- 51) Scott, J. A. *A finite element model of heat transport in the human eye*. Phys. Med. Biol, 1988. **33** (2): p. 227–241.
- 52) Amaran, E. H. *Numerical investigations on thermal effects of laser-ocular media interaction*. International Journal of Heat and Mass Transfer, 1995. **38**: p. 2479-2488.
- 53) Chua, K. J. Ho, J. C. Chou, S. K. Islam, M. R. *On the study of the temperature distribution within a human eye subjected to a laser source*. International Communications in Heat and Mass Transfer, 2005. **32**: p. 1057–1065.
- 54) Avtar, R. and Srivastava, R. *Modelling the flow of aqueous humor in anterior chamber of the eye*, Applied Mathematics and Computation. 2006. **181**. p. 1336-1348.

- 55) Ng, E. Y. K. and Ooi, E. H. *FEM simulation of the eye structure with bio-heat analysis*. Comput. Meth. Progr. Biomed, 2006. **82**(3): p. 268–276.
- 56) Ng, E. Y. K. and Ooi, E. H. *Ocular surface temperature: A 3D FEM prediction using bio-heat equation*. Computers in Biology and Medicine, 2007. **37**: p. 829-835.
- 57) Ng, E. Y. K. Ooi, E. H. and Archarya, U. R. *A comparative study between the two dimensional and three dimensional human eye models*, Mathematical and Computer Modelling. 2008. **48**. P. 712-720.
- 58) Ooi, E. H. and Ng, E. Y. K. *Simulation of aqueous humor hydrodynamics in human eye heat transfer*. Computers in Biology and Medicine, 2008. **38**: p. 252-262.
- 59) Ooi E. H. Ang, W. T. and Ng, E. Y. K. *A boundary element model for investigating the effects of eye tumor on the temperature distribution inside the human eye*, Computers in Biology and Medicine. 2009. **39**: p. 667-677.
- 60) Narasimhan, A. Jha, K. K. and Gopal, L. *Transient simulation of heat transfer in human eye undergoing laser surgery*. International Journal of Heat and Mass Transfer. 2010. **53**: p. 482-490.
- 61) Jha, K. K. and Narasimhan, A. *Three dimensional bio-heat transfer simulation of sequential and simultaneous retinal laser irradiation*, International Journal of Thermal Sciences. 2011. **50**. p. 1191-1198.
- 62) Kunter, F. C. and Seker, S. S. *3D web-spline solution to human eye heat distribution using bioheat equation*, *Engineering Analysis with Boundary Elements*. 2011. **35**. p. 639-646.
- 63) Ley, O. and Bayazitoblu, Y. *Effect of physiology on the temperature distribution of a layered head with external convection*. International Journal of Heat and Mass Transfer, 2003. **46**: p. 3233-3241.
- 64) Sukstanskii, A. L. and Yablonskiy, D. A. *An analytical model of temperature regulation in human head*. Journal of Thermal Biology, 2004. **29**: p. 583-587.
- 65) Sukstanskii, A. L. and Yablonskiy, D. A. *Theoretical limits on brain cooling by external head cooling devices*, Eur. J. Appl. Physiol. 2007. **101**: p. 41-49.
- 66) Khanday, M. A and Saxena, V. P. *Finite Element Approach for the Study of Thermoregulation in Human Head Exposed to Cold Environment*, AIP conference proceedings. 2009.
- 67) Janssen, F. E. M. Van Leeuwen, G. M. J. and Van Steenhoven, A. A. *Modeling of temperature and perfusion during scalp cooling*. Phys. Med. Biol, 2005. **50**: p. 4065–4073.
- 68) Xiao, J. He, Z. Yang, Y. Chen, B. Deng, Z. and Liu, J. *Investigation on three-dimensional temperature field of human knee considering anatomical structure*. International Journal of Heat and Mass Transfer, 2011. **54**: p. 1851-186.
- 69) Trobec, R. sterk, M. AlMawed, S and Veselko, M. *Computer simulation of topical Knee cooling*. Computers in biology and medicine, 2008. **38**: p. 1076-1083.
- 70) Kai, Z. Yan, Z. Ruiqiu, C. Yufeng, Z. Zhihao, J. Boli, Z. and Yi, W. *Heat transfer modeling of the tongue*. Journal of Thermal Biology, 2007. **32**: p. 97-101.
- 71) Van Marken Lichtenbelt, W. D. Frijns, A. J. H. Fiala, D. Janssen, F. E. M. van Ooijen, A. M. J. and van Steenhoven, A. A. *Effect of individual characteristics on a mathematical model of human thermoregulation*. Journal of Thermal Biology, 2004. **29**: p. 577-581.
- 72) Ishigaki, H. Horikoshi, T. Uematsu, T. Sahashi, M. Tsuchikawa, T. Mochida, T. Hieda, T. Isoda, N. and Kubo, H. *Experimental study on convective heat transfer coefficient of the human body*. J. therm. Biol, 1993. **18**: no, 5/6. p. 455-458.

- 73) de Dear, R. J. Arens, E. Hui, Z. and Oguro, M. *Convective and radiative heat transfer coefficients for individual human body segments*. Int. J Biometeorol. 1997. **40**: p. 141-156.
- 74) Kurazumi, Y. Tsuchikawa, T. Matsubara, N. and Horikoshi, T. *Convective heat transfers area of the human body*, European Journal of Applied Physiology, 2004. **93**: p. 273-285.
- 75) Kurazumi, Y. Tsuchikawa, T. Matsubara, N. and Horikoshi, T. *Effect of posture on the heat transfer areas of the human body*, Building and Environment, 2008. **43**: p. 1555-1565.
- 76) Kurazumi, Y. Tsuchikawa, T. Ishii, J. Fukagawa, K. Yamato, Y. Matsubara, N. *Radiative and convective heat transfer coefficients of the human body in natural convection*, Building and Environments, 2008. **43**: p. 2142-2153.
- 77) Qian, X. and Fan, J. *Interaction of the surface heat and moisture transfer from the human body under varying climatic conditions and walking speeds*. Applied Ergonomics, 2006. **37**: p. 685-693.
- 78) Huizenga, C. Zhang, H. Arens, E. and Wang, D. *Skin and core temperature response to partial and whole-body heating and cooling*. Journal of thermal Biology, 2004. **29**: p. 549-558.
- 79) Sakoi, T. Tsuzuki, K. Kato, S. Ooka, R. Song, D. and Zhu, S. *Thermal comfort, skin temperature distribution, and sensible heat loss distribution in the sitting posture in various asymmetric radiant fields*. Building and Environment, 2007. **42**: p. 3984-3999.
- 80) Munir, A. Takada, S. and Matsushita, T. *Re-evaluation of Stolwijk's 25-node human thermal model under thermal-transient conditions: Prediction of skin temperature in low-activity conditions*. Building and Environments, 2009. **44**: p.1777-1787.
- 81) Atmaca, I and Yigit, A. *Predicting the effect of relative humidity on skin temperature and skin wittedness*, Journal of Thermal Biology. 2007. **31**: p.442-452.
- 82) Zhang, Y and Zhao, R. *Effect of local exposure on human responses*, Building and Environments. 2007. **42**: p. 2737-2745.
- 83) Ono, T. Murakami, S. Ooka, R. and Omori, T. *Numerical and experimental study on convective heat and transfer of the human body in the outdoor environment*, Journal of Wind Engineering and Industrial Aerodynamics. 2008. **96**. p. 1719-1732.
- 84) van Ooijen, A. M. J. van Marken Lichtenbelt, W. D. van Steenhoven, A. A. Westerterp, K. R. *Seasonal changes in metabolic and temperature responses to cold air in humans*, Physiology & Behavior. 2004. **82**. p. 545– 553.
- 85) Janskya, L. Vavra, V. Jansky, P. Kunc, P. Knizkova, I. Jandova, D. and Slovacek, K. *Skin temperature changes in humans induced by local peripheral cooling*, Journal of Thermal Biology. 2003. **28**. p. 429–437.
- 86) Arens, E. Zhang, H. and Huizenga, C. *Partial- and whole-body thermal sensation and comfort— Part I: Uniform environmental conditions*, Journal of Thermal Biology. 2006. **31**. p. 53–59.
- 87) Arens, E. Zhang, H. and Huizenga, C. *Partial- and whole-body thermal sensation and comfort— Part II: Non-uniform environmental conditions*, Journal of Thermal Biology. 2006. **31**.p. 60–66.
- 88) Zhang, H. Arens, E. Huizenga, C. and Han, T. *Thermal sensation and comfort models for non-uniform and transient environments, part I: Local sensation of individual body parts*, Building and Environment. 2010. **45**. p. 380–388.

- 89) Zhang, H. Arens, E. Huizenga, C. and Han, T. *Thermal sensation and comfort models for non-uniform and transient environments, part II: Local comfort of individual body parts*, Building and Environment. 2010. **45**. p. 389–398.
- 90) Zhang, H. Arens, E. Huizenga, C. and Han, T. *Thermal sensation and comfort models for non-uniform and transient environments, part III: Whole body sensation and comfort*, Building and Environment. 2010. **45**. p. 399–410.
- 91) Masayuki, O. Edward, A. de Dear, R. J. Zhang, H. and Katayama, T. *Convective heat transfer coefficients and clothing insulations for parts of the clothed human body under airflow conditions*, J. Archit. Plann. Environ. Eng., AIJ, 2002. no **561**. p. 21-29.
- 92) Takada, S. Kobayashi, H. Matsushita, T. *Thermal model of human body fitted with individual characteristics of body temperature regulation*, Building and Environment. 2009. **44**. p. 463-470.
- 93) Takada, S. Sakiyama, T. Matsushita, T. *Validity of the two-node model for predicting steady-state skin temperature*, Building and Environment. 2011. **46**. p. 597-604.
- 94) Lee, J. Y. and Choi, J. W. *Influences of clothing types on metabolic, thermal and subjective responses in a cool environment*, Journal of Thermal Biology. 2004. **29**. p. 221–229.
- 95) Jin, Q. Li, X. Duanmu, L. Shu, H. Sun, Y. and Ding, Q. *Predictive model of local and overall thermal sensations for non-uniform environments*, Building and environment. 2012. **51**. 330-344.
- 96) Foda, E. and Siren, K. *A new approach using the Pierce two-node model for different body parts*, Int. J. Biometeorol. 2011. **55**: p. 519–532.
- 97) Choi, J. H. and Loftness, V. L. *Investigation of human body skin temperature as a bio-signal to indicate overall thermal sensations*, Building and Environment. 2012. **58**. p. 258-269.
- 98) Chen, C. P. Hwang, R. L. Chang, S. Y. and Lu, Y. T. *Effects of temperature steps on human skin physiology and thermal sensation response*, Building and Environment. 2011. **46**. 2387-2397.
- 99) Clough, R.W. *The Finite Element Method in Plane Stress Analysis*. in *2nd ASCE Conference on Electronic Computation*. 1960. Pittsburgh.
- 100) Zienkiewicz, O.C. and C.J. Parekh, *Transient field problems: Two-dimensional and three-dimensional analysis by isoparametric finite elements*. International Journal for Numerical Methods in Engineering, 1970. **2**(1): p. 61–71.